Laser and Particle Guiding in Plasmas at I-LUCE (INFN Laser indUCEd radiation production)

Dr GA Pablo Cirrone
Istituto Nazionale di Fisica Nucleare
Laboratori Nazionali del Sud (Italy)

Carmen Altana, Sahar Arjmand, Danilo Bonanno, Antonio Caruso, Roberto Catalano, Giacomo Cuttone, Serena Fattori, Alma Kurmanova, Mariacristina Guarrera, Demetrio Oliva, Alfio Pappalardo, Giada Petringa, Josè Suarez, Salvatore Tudisco

The 10th International Conference Charged & Neutral Particles Channeling Phenomena
8-13 September 2024 Riccione (Rimini), Italy

CHANNELING 2024

Outline

High power lasers and radiation production

Protons and electrons acceleration: status and perspectives

The upcoming INFN **I-LUCE** high-power laser facility

Istituto Nazionale di Fisica Nucleare

lasers and radiation production: what we need?

The main ingredients for radiation productions

A pulsed laser

- High power (TW - PW)
- Short pulse duration (ps - fs)
- Intensity > 10^{16} W/cm^2

A Target:

- Thin/thick solid/liquid/gassous

…

Other useful things

- High contrast laser
- High quality target fabrication
- High quality wave front-end
- …..

1960

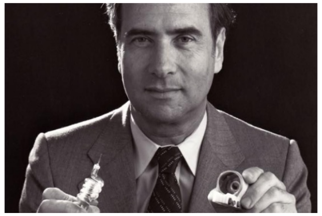

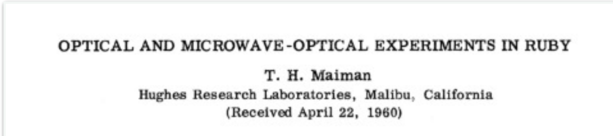

OPTICAL AND MICROWAVE-OPTICAL EXPERIMENTS IN RUBY

T. H. Maiman

Hughes Research Laboratories, Malibu, California

(Received April 22, 1960)

Ruby Laser (solid state) – 694 nm, ~1 ms

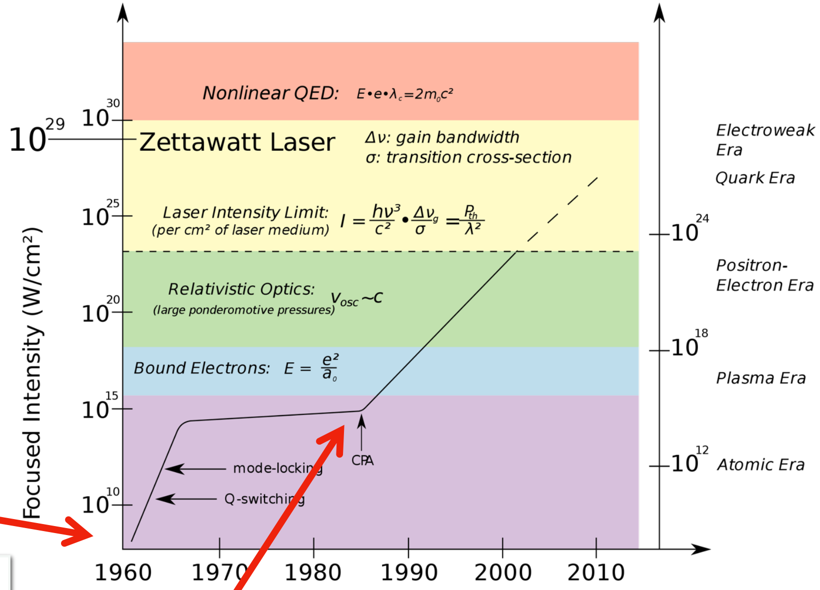

1985

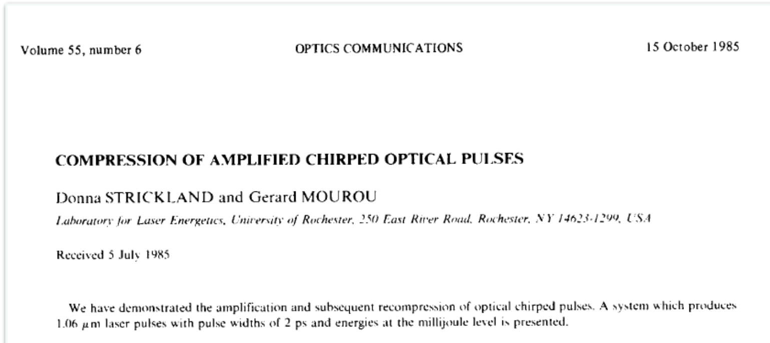

Volume 55, number 6 OPTICS COMMUNICATIONS 15 October 1985

COMPRESSION OF AMPLIFIED CHIRPED OPTICAL PULSES

Donna STRICKLAND and Gerard MOUROU

Laboratory for Laser Energetics, University of Rochester, 250 East River Road, Rochester, NY 14623-1299, USA

Received 5 July 1985

We have demonstrated the amplification and subsequent recompression of optical chirped pulses. A system which produces 1.06 μm laser pulses with pulse widths of 2 ps and energies at the millijoule level is presented.

The laser: femtosecond and power explained

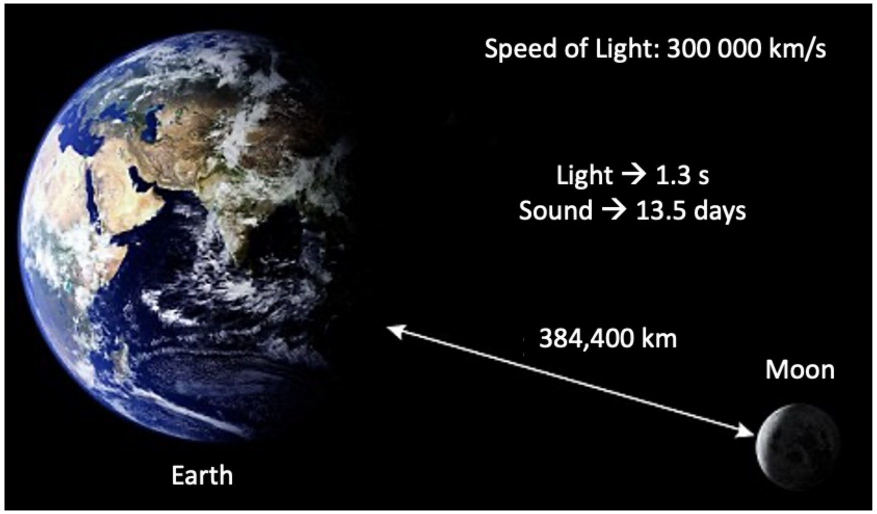

$$1\ \text{fs} = 10^{-15}\ \text{s} = \frac{1}{1000000000000000} = 0.000000000000001$$

$$1\ \text{PW} = 10^{15}\ \text{W} = 1000000000000000$$

$$\text{POWER} = \frac{\text{ENERGY}}{\text{TIME}}\ [\text{W} = \text{J/s}]$$

Surface= 4 μm^2

Power pressure = $10^{15}/10^{-8}$ cm^2 =10^{23} W/cm2

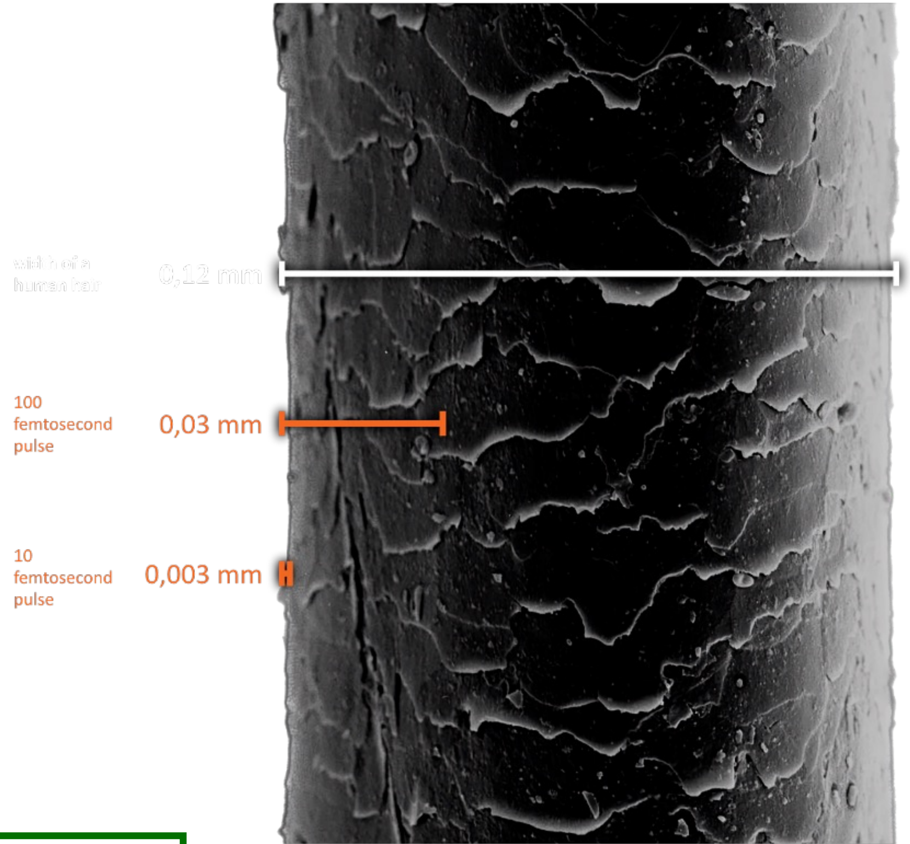

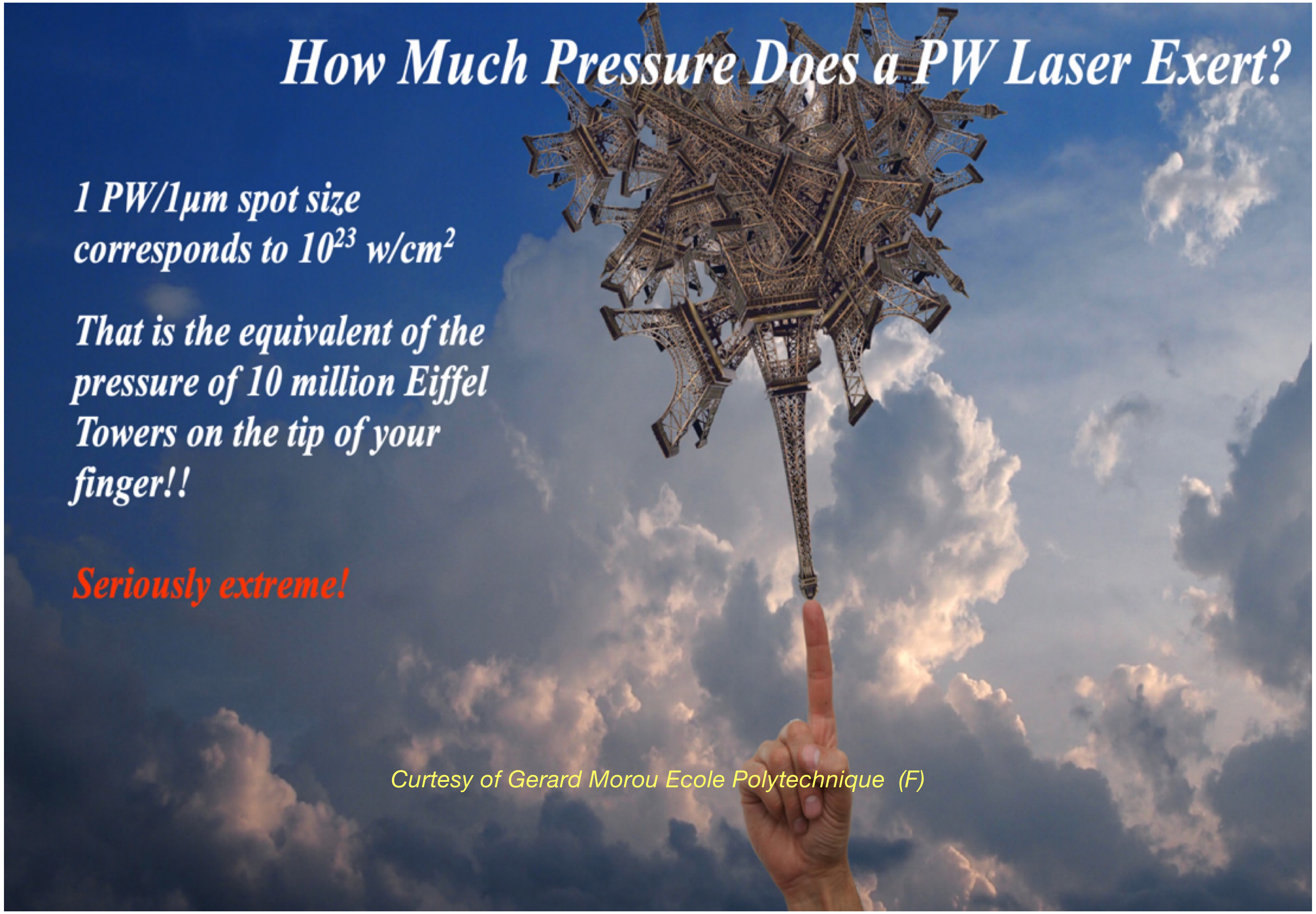
How Much Pressure Does a PW Laser Exert?
1 PW/1μm spot size
corresponds to 10^23 w/cm^2
That is the equivalent of the pressure of 10 million Eiffel Towers on the tip of your finger!!
Seriously extreme!
Curtesy of Gerard Morou Ecole Polytechnique (F)

Laser plasma ion-acceleration

current facilities

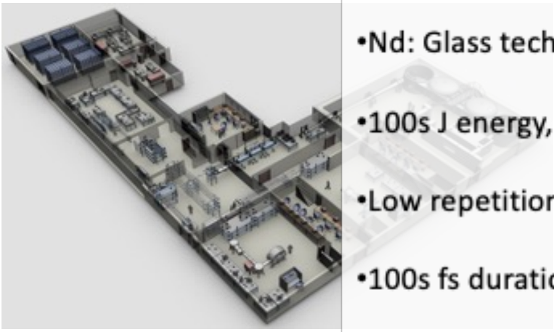

High energy CPA systems

- Nd: Glass technology
- 100s J energy, up to 1 PW power
- Low repetition rate (1shot/30min)
- 100s fs duration
- I_{max}~ 10^{21} Wcm^2

I_{max}~ 10^{21} W/cm^2

VULCAN, RAL (UK)
Phelix, GSI (De)
Texas PW (US)
...
ATON-L4 (ELI Beamlines)
10 PW (1.5kJ/150fs)

E_{max}~ 100 MeV

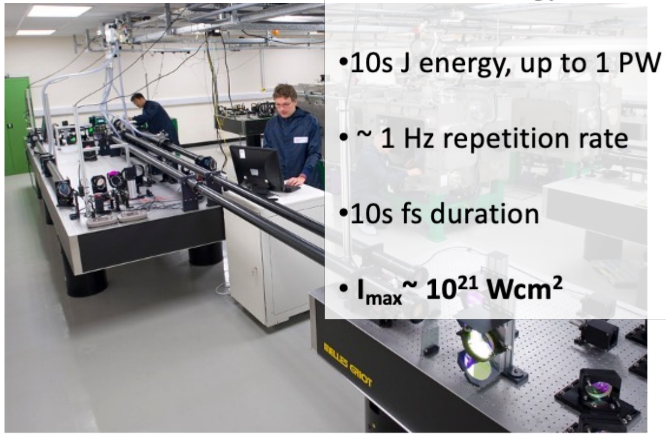

Ultrashort CPA systems

- Ti:Sa technology
- 10s J energy, up to 1 PW power
- ~ 1 Hz repetition rate
- 10s fs duration
- I_{max}~ 10^{21} Wcm^2

I_{max}~ 10^{21} W/cm^2

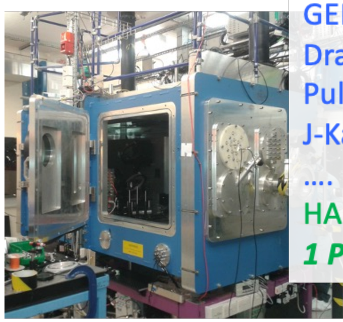

GEMINI, RAL (UK)
Draco, HZDR (De)
Pulser I, APRI (Kr)
J-Karen, JAEA (J)
....
HAPLS-L3, (ELI Beamlines)
1 PW (30J/30fs/10Hz)

E_{max}~ 70-110 MeV

2020 world lasers facilities

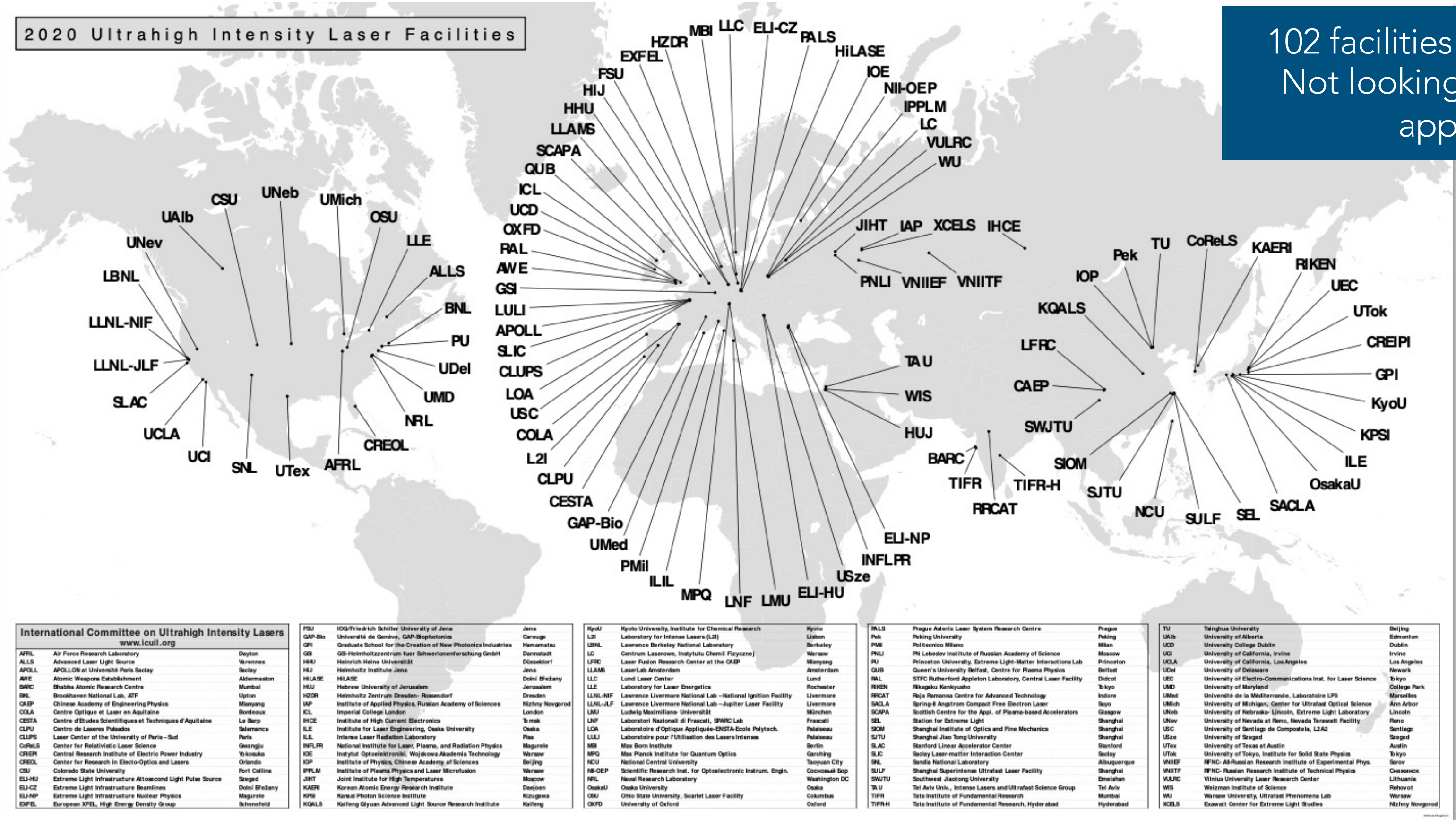

102 facilities (approx > 1TW)
Not looking to the specific application

From ICUIL (International Committee on Ultra-High Intensity Lasers) https://www.icuil.org/

Targets: for ions, electrons, gamma, …

Ions acceleration

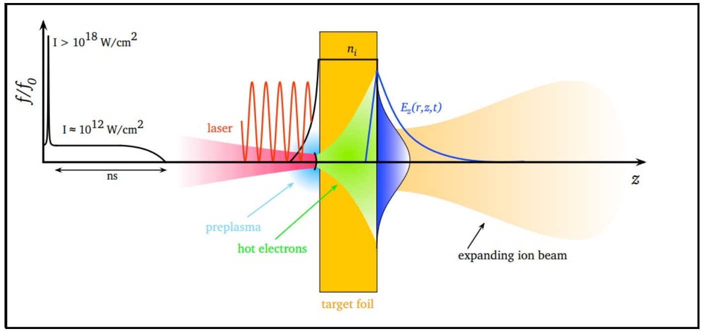

$$E(0) = \frac{KT_h}{e\lambda_D} = \sqrt{\frac{n_h K T_h}{\varepsilon_0}}$$

$$E(0) = \frac{10^6 V}{10^{-6} m} \sim TV/m$$

Typical values are:
$\lambda_D \sim 1\ \mu m$
$T_h \sim$ MeV

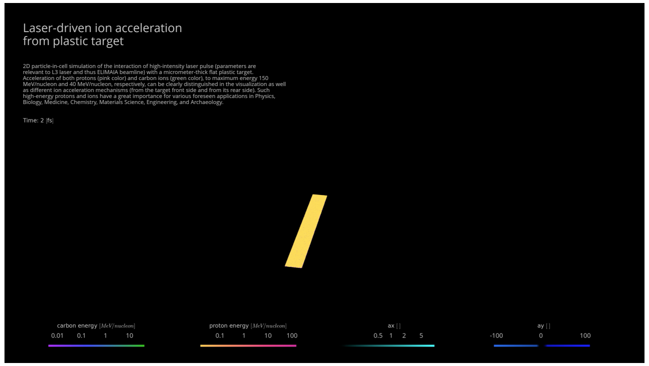

Ponderomotive force on electrons energy gain

$$f_p = -m_e c^2 \nabla \sqrt{(1 + < a >^2)}$$

Electrons acceleration

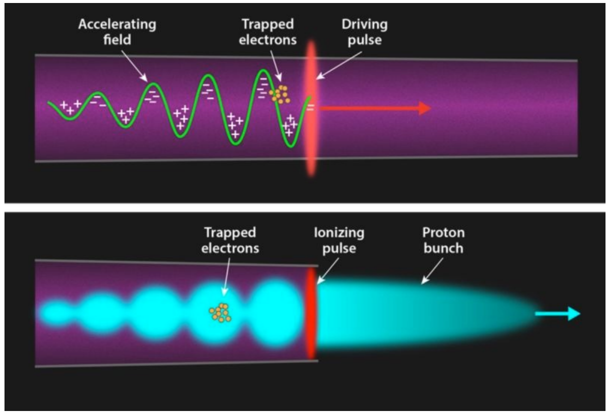

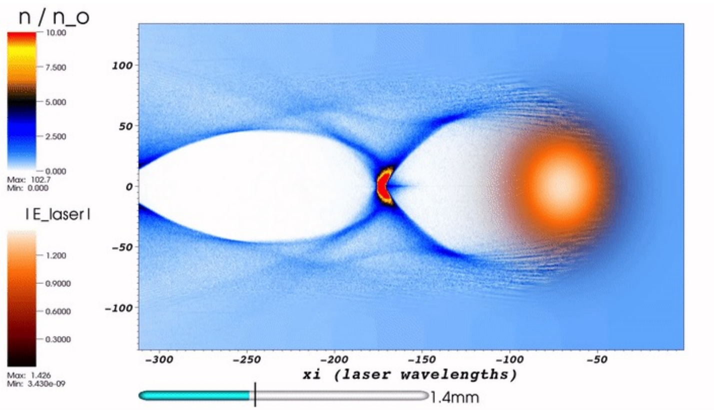

See talks by **Dr Sahar Arjmand**

Journal of Instrumentation

SISSA

TECHNICAL REPORT

Linear colliders based on laser-plasma accelerators

To cite this article: C.B. Schroeder *et al* 2023 *JINST* **18** T06001

View the article online for updates and enhancements.

You may also like

- On the possibility of accelerating charged particles in the low-pressure acoustoplasma and plasma bunches in the air
A.S. Abrahamyan, R.Yu. Chilingaryan, S.A. Mkhitaryan et al.
- Considerations for a TeV collider based on dielectric laser accelerators
R.J. England, U. Niedermayer, L. Schächter et al.
- The science case for an intermediate energy advanced and novel accelerator linear collider facility
S.S. Bulanov, C.A. Aidala, C. Benedetti et al.

PHYSICAL REVIEW LETTERS **122,** 084801 (2019)

Editors' Suggestion | Featured in Physics

Petawatt Laser Guiding and Electron Beam Acceleration to 8 GeV in a Laser-Heated Capillary Discharge Waveguide

A. J. Gonsalves,[1,*] K. Nakamura,[1] J. Daniels,[1] C. Benedetti,[1] C. Pieronek,[1,2] T. C. H. de Raadt,[1] S. Steinke,[1] J. H. Bin,[1] S. S. Bulanov,[1] J. van Tilborg,[1] C. G. R. Geddes,[1] C. B. Schroeder,[1,2] Cs. Tóth,[1] E. Esarey,[1] K. Swanson,[1,2] L. Fan-Chiang,[1,2] G. Bagdasarov,[3,4] N. Bobrova,[3,5] V. Gasilov,[3,4] G. Korn,[6] P. Sasorov,[3,6] and W. P. Leemans[1,2,†]
[1]*Lawrence Berkeley National Laboratory, Berkeley, California 94720, USA*
[2]*University of California, Berkeley, California 94720, USA*
[3]*Keldysh Institute of Applied Mathematics RAS, Moscow 125047, Russia*
[4]*National Research Nuclear University MEPhI (Moscow Engineering Physics Institute), Moscow 115409, Russia*
[5]*Faculty of Nuclear Science and Physical Engineering, CTU in Prague, Brehova 7, Prague 1, Czech Republic*
[6]*Institute of Physics ASCR, v.v.i. (FZU), ELI-Beamlines Project, 182 21 Prague, Czech Republic*

(Received 7 December 2018; revised manuscript received 30 January 2019; published 25 February 2019)

So far LPAs have demonstrated the production of high-quality electron beams with HEPrelevant parameters, such as relative energy spreads as low as ∼ 1% [31, 32], normalized emittances of ∼ 0.1 µm [33, 34], and high charge (100s of pC) [35, 36],

TUPAB110 Proceedings of IPAC2017, Copenhagen, Denmark

POSSIBLE LIMITS OF PLASMA LINEAR COLLIDERS*

F. Zimmermann[†], CERN, Geneva, Switzerland

Abstract the plasma density and the beta function greater than [10]

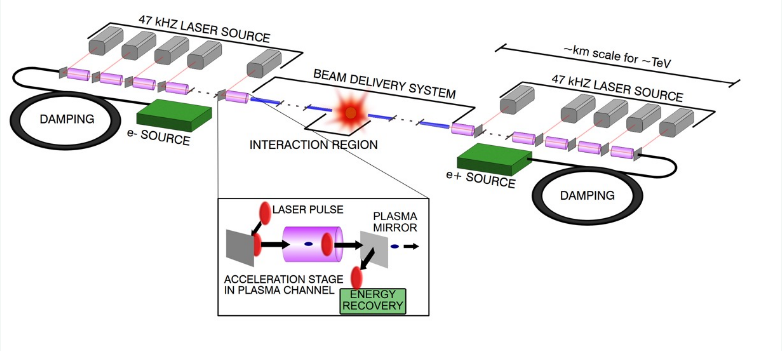

Figure 1. Schematic of an LPA-based linear collider.

Electrons acceleration

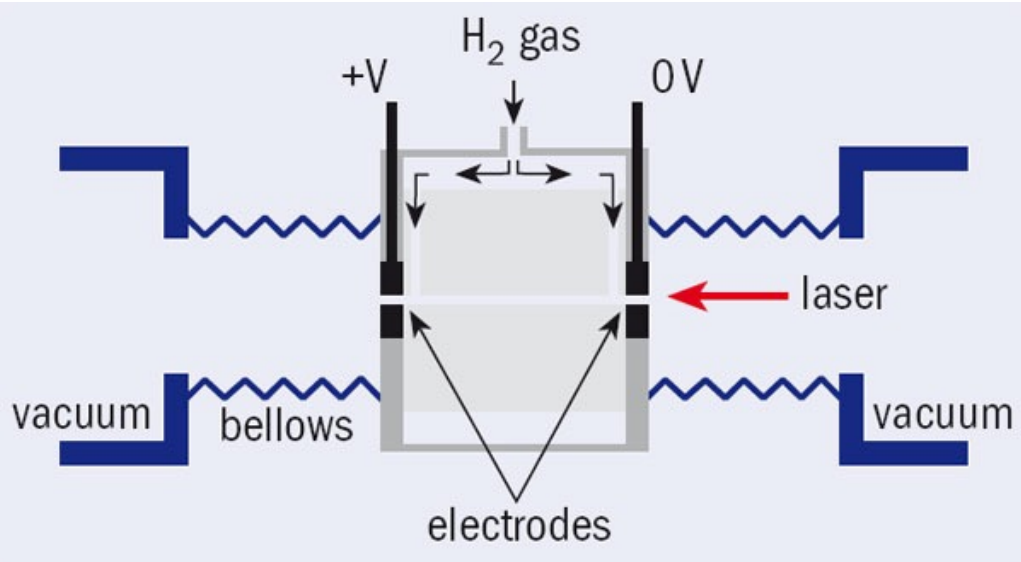

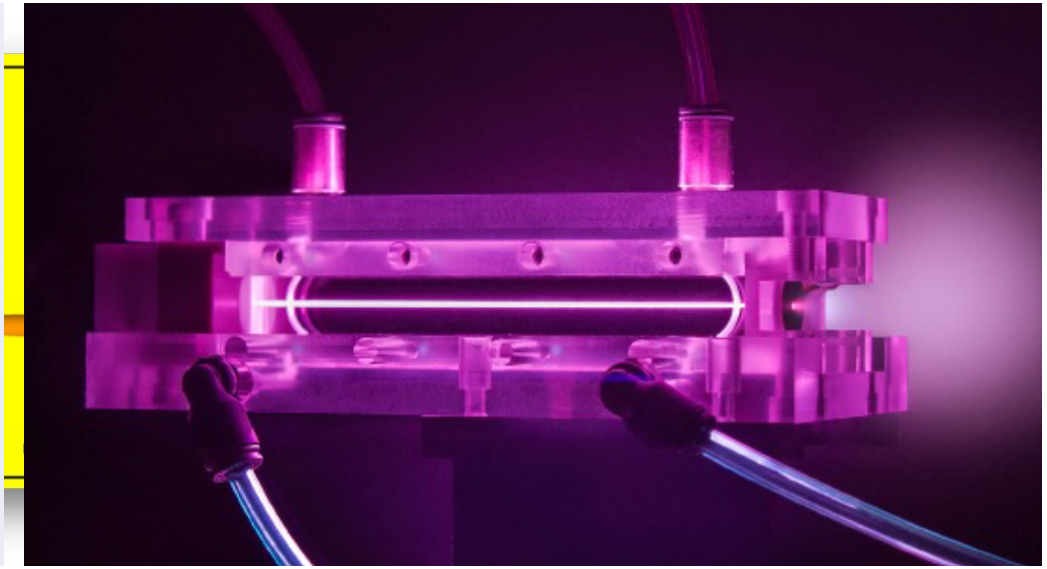

Courtesy of Massimo Ferrario, INFN-LNF

Pablo Cirrone, PhD - pablo.cirrone@lns.infn.it

INFN

Istituto Nazionale di Fisica Nucleare

I LUCE

Let's concentrate on ion acceleration

Laser plasma ion-acceleration

principal motivation

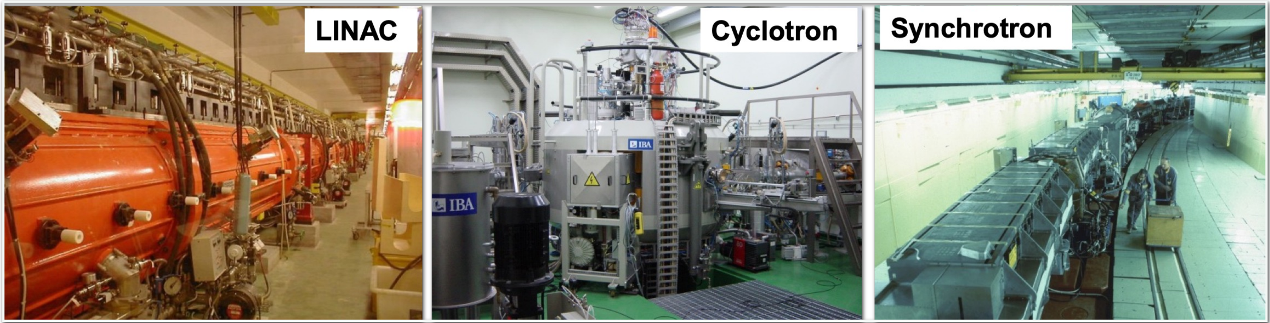

E_{max} ~ 50 MV/m

L_{acc} ~ 1-10 m

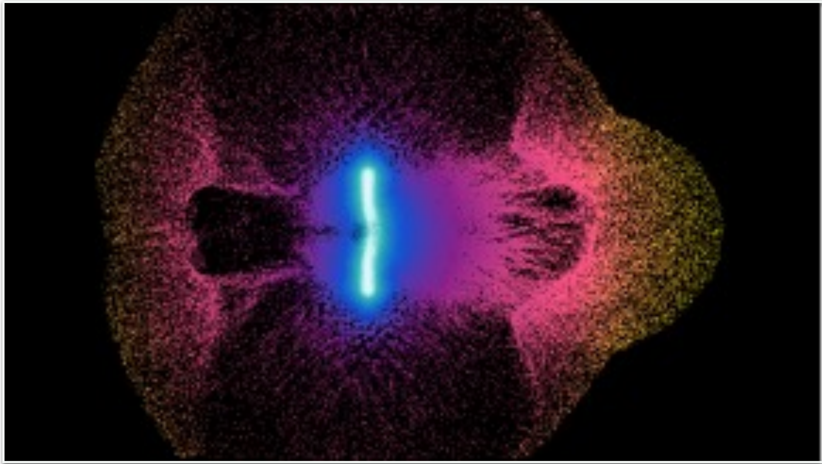

E_{max} ~ 1 TV/m

L_{acc} ~ 1 μm

→ **10,000 smaller!!!**

BUT...

Laser plasma ion-acceleration

physical picture

Target Normal Sheath Acceleration

0.1-10 μm long

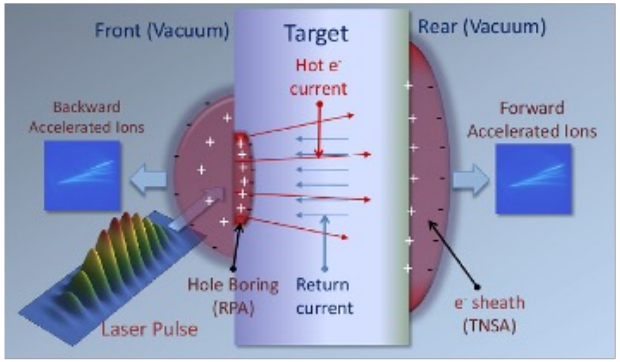

REVIEW PAPERS:

- *Macchi, Borghesi, Passoni, Rev. Mod. Phys. 85 (2013) 751*
- *Borghesi et al, Springer Proc. Phys. 231 (2019) 143*

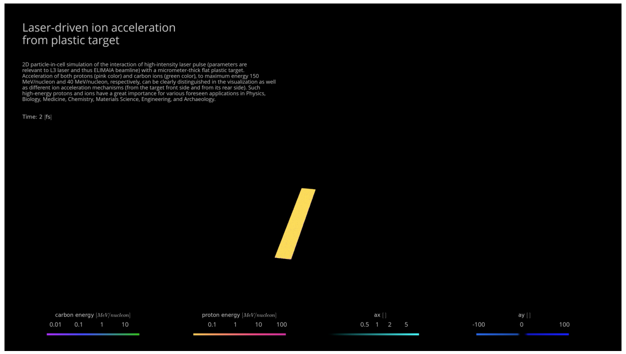

I_L (laser intensity) = E/τ/S = **10^{21} W/cm²**

Direct Laser interaction:

- $E \sim I_L^{1/2}\lambda = 10^{14}$ V/m
- $B = E/c = 3\times10^{5}$ T
- $P_{rad} = I_L/c = 3\times10^{10}$ J/cm³ = 300 Gbar

Laser-Plasma interaction:

- Debye Length

$$\lambda_D = 2.4\,\mu m \cdot \sqrt{\frac{T_{hot}}{1MeV}} \cdot \sqrt{\frac{10^{19}\,cm^{-3}}{N_{hot}}} \Longrightarrow \sim \mu m!$$

- Acceleration time

$$\tau = \sqrt{\frac{\lambda_D^2 m_{ion}}{T_{hot}}} = 0.24\,ps \sqrt{\frac{\lambda_D^2 n_{hot}}{10^{19}}} \Longrightarrow \sim ps!$$

- Electric Field

$$E = \frac{T_{hot}}{e\lambda_D} \approx \frac{MV}{\mu m} \Longrightarrow \sim TV/m!$$

Energy Gain: 100 MeV/um (in a plasma medium)!!!

Characteristics of the laser-driven protons

Energy spectra

Boltzman-like (from zero to a given cut-off)

100% energy spread for a pure-TNSA

Selection procedures are adopted

Angular divergency

30°/40° degree (FWHM)

Temporal features

10^8 - 10^9 selected 20 ns - 200 ns bunches

1 Hz - 10 Hz - …..

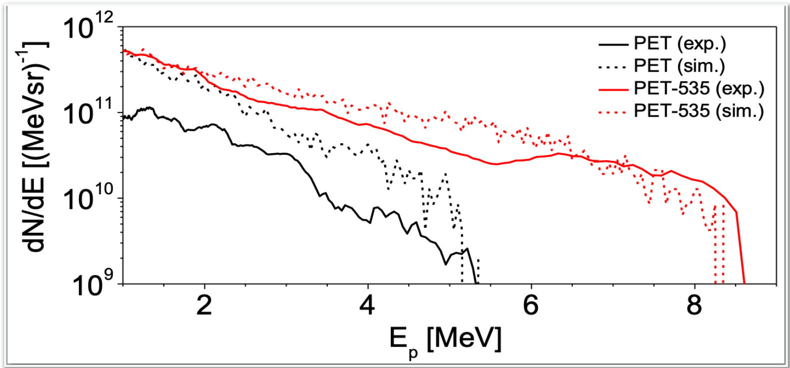

70 TW laser

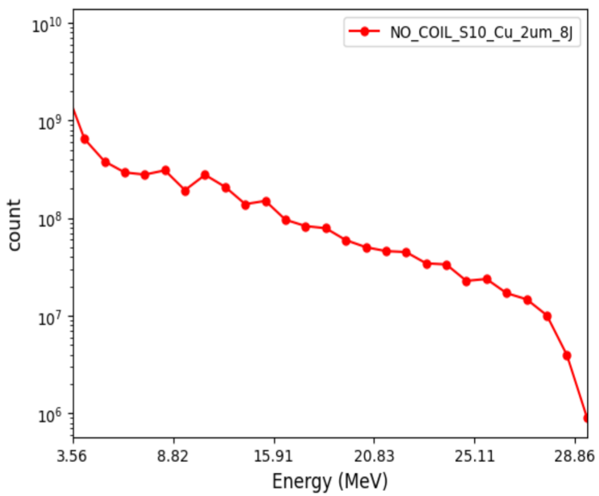

250 TW laser

Beam shape at source

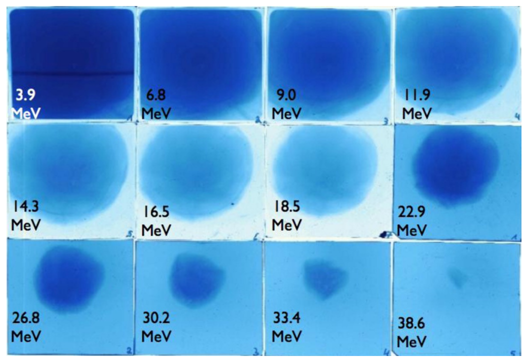

Maximum proton energy

experimental scaling laws (TNSA)

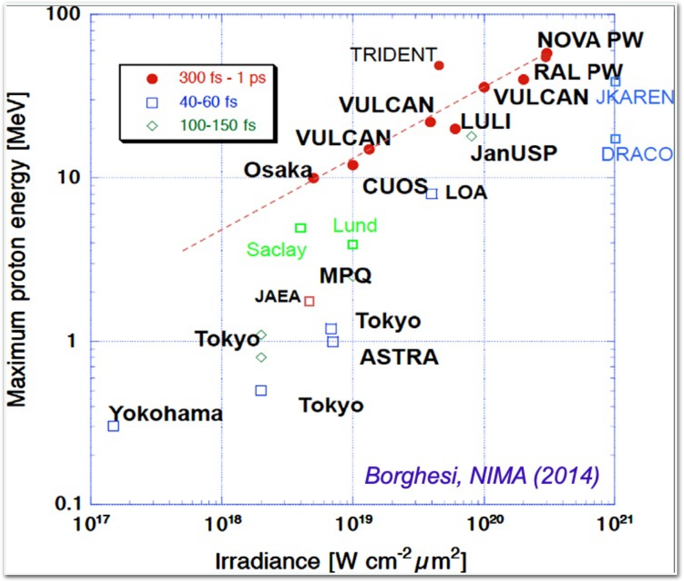

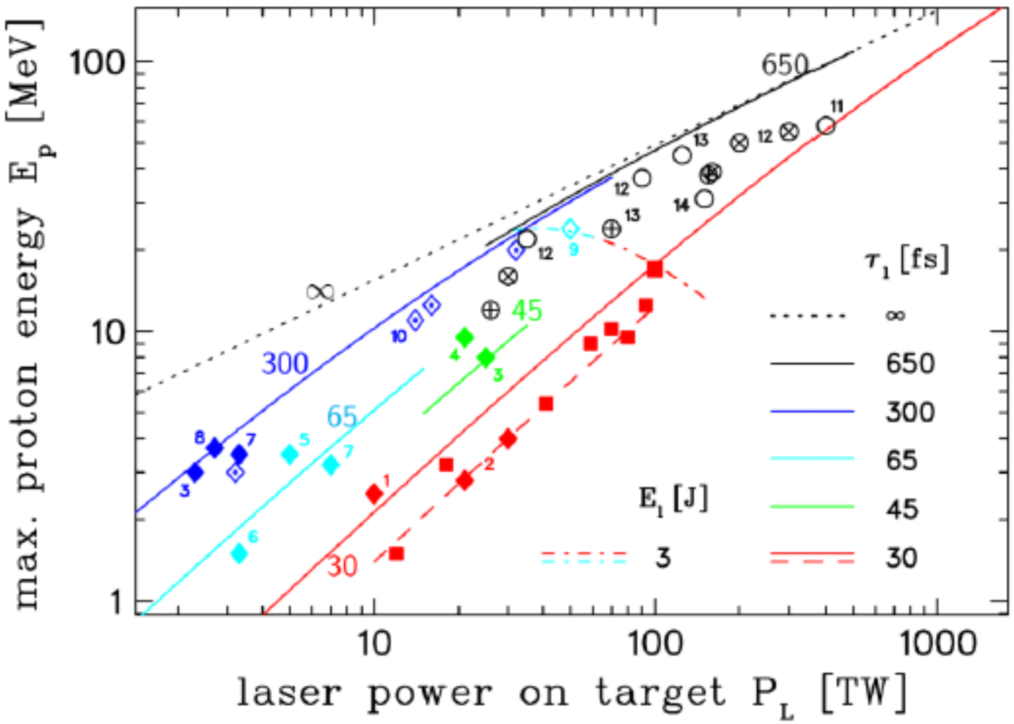

$E \sim I_L^{1/2}$

$$I \propto \frac{E_p}{\tau A}$$

Intensity W/cm^2

proton energy

pulse lenght

spot surface on target

The scaling of proton energies in ultrashort pulse laser plasma acceleration
K Zeil et al 2010 New J. Phys. 12 045015

Laser-driven ion acceleration mechanisms

laser intensity vs target density

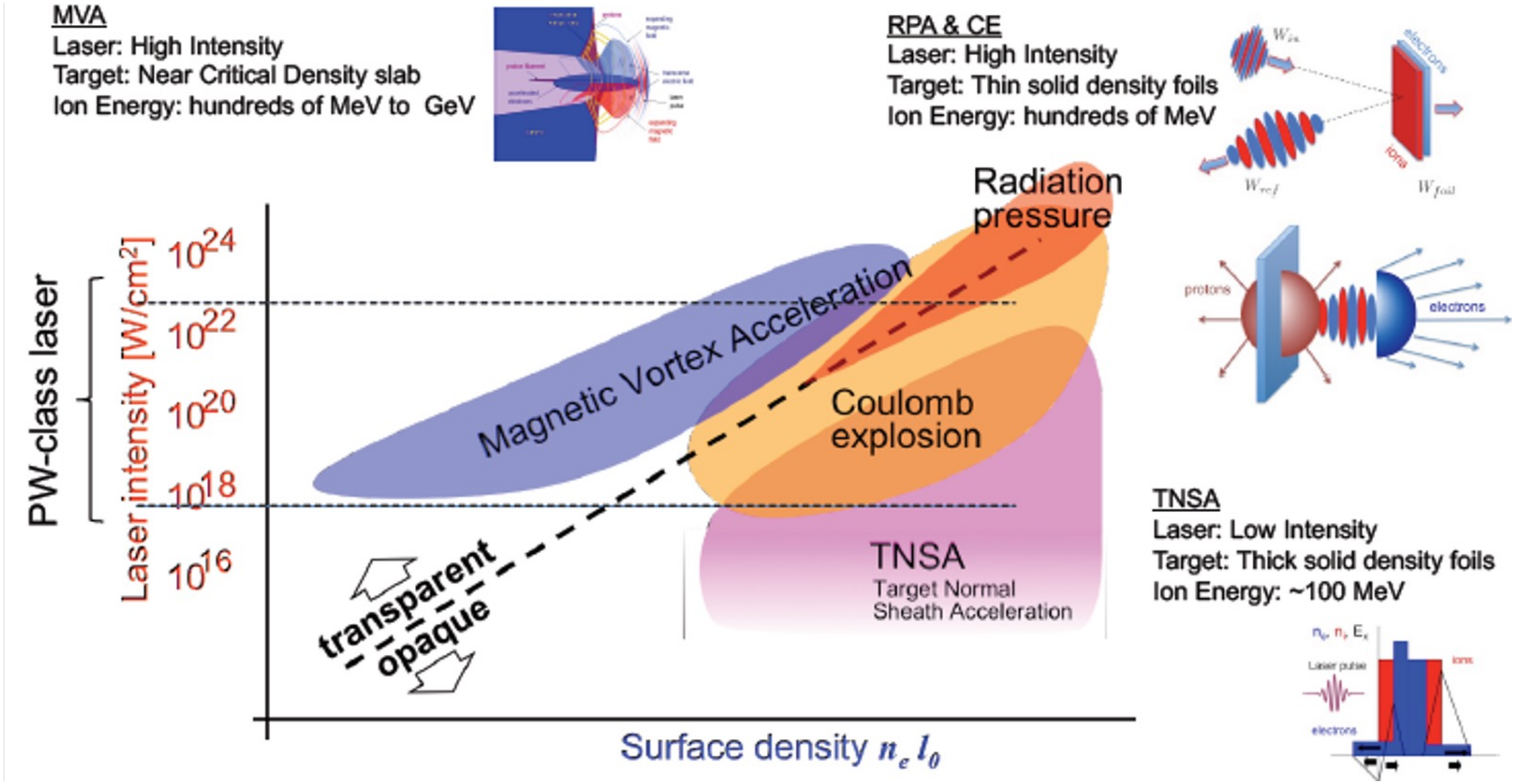

Curtesy of S. Bulanov (ELI-Beamlines)

Energy world record

nature physics

Article https://doi.org/10.1038/s41567-024-02505-0

Laser-driven high-energy proton beams from cascaded acceleration regimes

Received: 7 August 2023

Accepted: 5 April 2024

Published online: 13 May 2024

Check for updates

Tim Ziegler[1,2], Ilja Göthel[1,2], Stefan Assenbaum[1,2], Constantin Bernert[1,2], Florian-Emanuel Brack[1,2], Thomas E. Cowan[1,2], Nicholas P. Dover[3,4], Lennart Gaus[1,2], Thomas Kluge[1], Stephan Kraft[1], Florian Kroll[1], Josefine Metzkes-Ng[1], Mamiko Nishiuchi[3], Irene Prencipe[1], Thomas Püschel[1], Martin Rehwald[1,2], Marvin Reimold[1,2], Hans-Peter Schlenvoigt[1], Marvin E. P. Umlandt[1,2], Milenko Vescovi[1], Ulrich Schramm[1,2] & Karl Zeil[1]

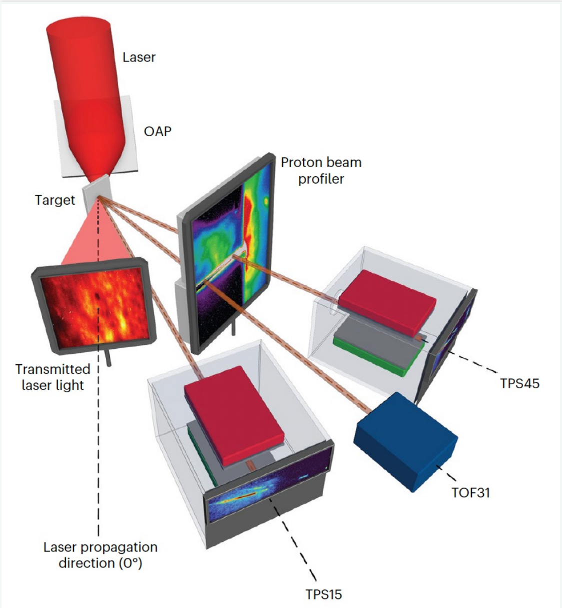

2024

DRACO-PW laser systemem (Dresden, D)

Intensity = ~ 6.5E21Wcm^{-2}

Pulses of p-polarised, **1.053 µm-wavelength**

Pulse duration τ = 30 fs

Energy after the plasma mirror: 22.4 J

Target: thin planar plastic foil with thickness 250 nm

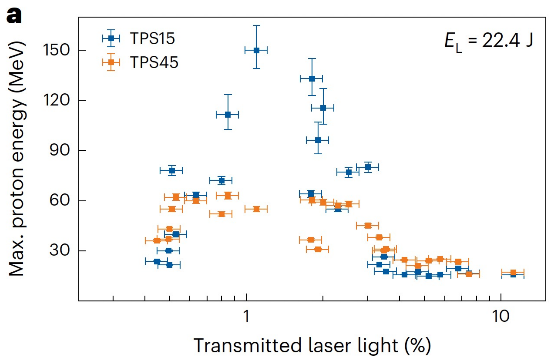

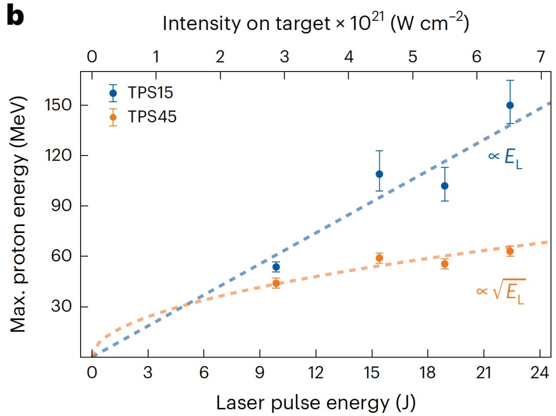

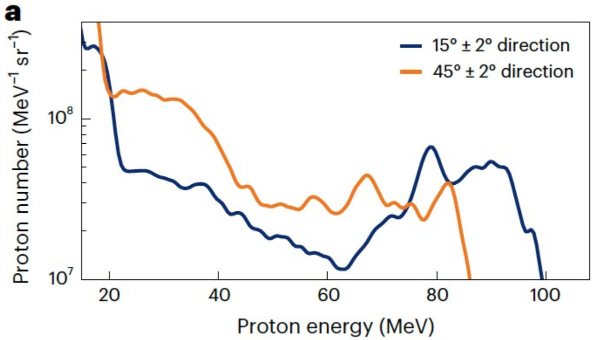

Hybrid TNSA and RPA mechanisms

- Hole-boring RPA
- Relativistic transparency front RPA
- Collisionless shock acceleration

INFN

Istituto Nazionale di Fisica Nucleare

I LUCE

I-LUCE at INFN-LNS

INFN Laser indUCEd
radiation production

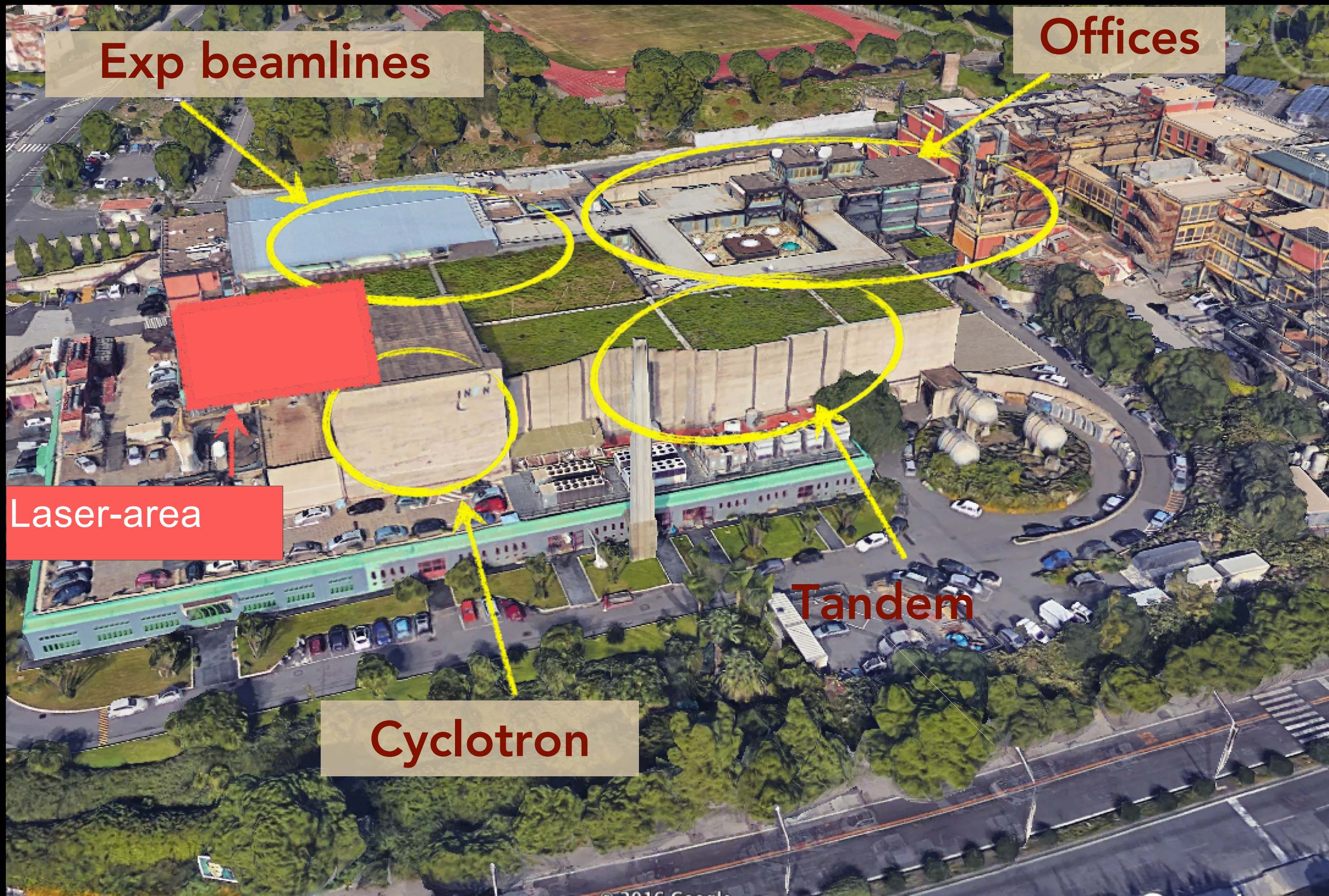

Exp beamlines
Offices
Laser-area
Tandem
Cyclotron

I-LUCE current status

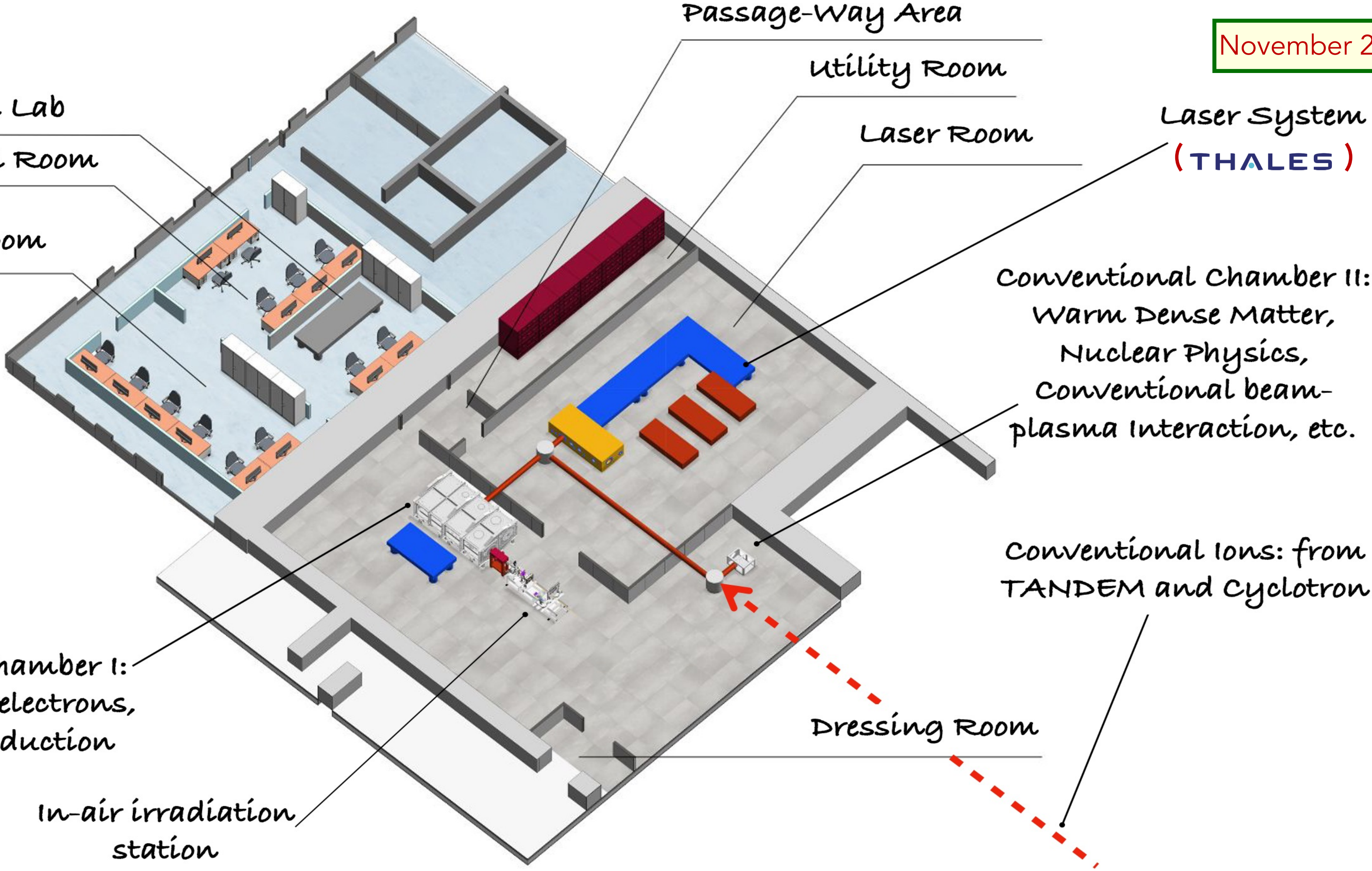

Two laser outputs

1J+/23fs/45TW

7J+/23fs/320TW

I-LUCE first phase

Two interaction chambers

1) **Interaction Chamber n.1:** Radiation production (protons/ions, electrons, neutrons, gamma, etc.)
   - One in-air irradiation station for multidisciplinary studies

2) **Interaction Chamber n.2:** Warm Dense Matter studies (WDM)
   - Nuclear physics in plasma
   - Interaction of conventional ion beams with laser-generated plasma
   - Nuclear physics fusion studies in plasma
   - ……

Two working modalities

1) Low power: 50 TW/23fs/10Hz
2) High power: 350 TW/23fs/1Hz

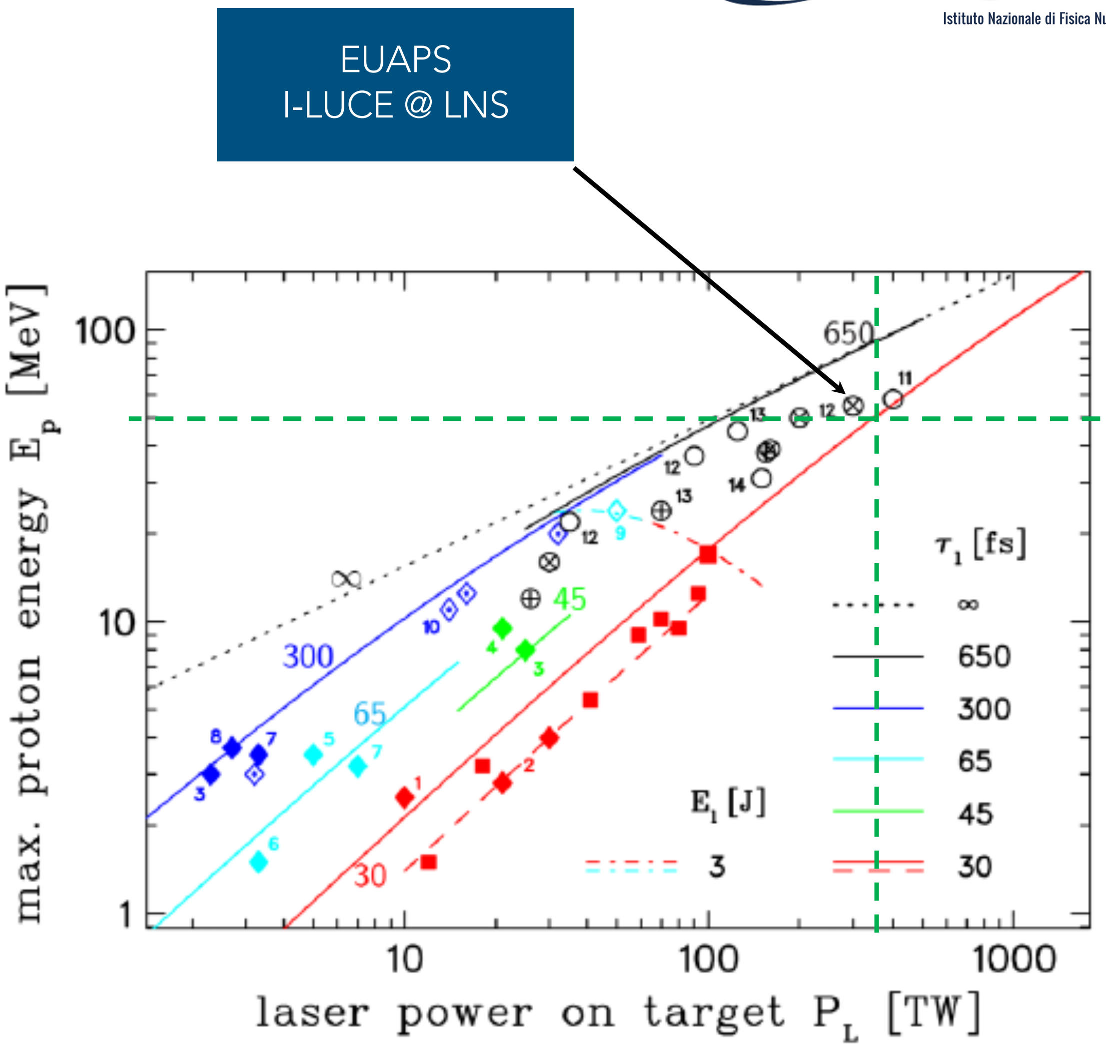

Low power modality: 45 TW

Laser Power		≥ 50 TW
Energy per pulse		≥ 1 J
Pulse duration		≤ 23 fs
Focusing surface		36 μm^2
Max power density (at the target)		$1.21\cdot10^{20}$
$I*\lambda^2$		$7.72\cdot10^{19}$
Contrast ratio @100 ps (ASE)		> 10^{10}
Repetition rate		≥ 10 Hz
Protons Ions	Max energy	4 MeV
	Particle per pulse (at 2 MeV)	10^{11} MeV^{-1} Sr^{-1}
	Energy spread	100%
	Beam divergency (max)	±20°
Eletrons	Max energy	0.1 GeV
	Particles per pulse	10^9
	Beam divergency (max)	± 20 mad
Neutrons	Max energy	TBD
	Particles per pulse	
	Energy spread	
	Beam divergency	
Gamma X-beams	Synchrotron radiation of the electrons inside the plasma or breemsstrahlung	
	Energy	up to 20 MeV
	Beam divergency	Directionality in the beam propabgation direction

Fusion studies,
nuclear studies,
radioisotopes production,
…..

Acting on the compression procedure, the pulse duration can be increased up to 1/10 ps:

==> $2.78\cdot10^{18}\ W/cm^2$
$2.78\cdot10^{17}\ W/cm^2$
==> $i\lambda^2 = 1.77\,.10^{18}$
$i\lambda^2 = 1.77\,.10^{17}$

Longer plasma expansion times:
— Decay studies
— Stopping powers studies
— WDM characterisation

Power densities can be improved reducing the focusing spot:
— shorter focusing parabola
— but issues related to the: target degree, back reflection, …

High-power modality: 320 TW

Laser Power		350 TW
Energy per pulse		>7 J
Pulse duration		≤ 25 fs
Focusing surface		36 µm² or better
Max power density (at the target)		8.82·10²⁰
I*λ²		5.64·10²⁰
Contrast ratio @100 ps (ASE)		> 10¹⁰
Repetition rate		1 Hz
Protons Ions	Max energy	50 MeV
	Particle per pulse (at 30 MeV)	10^{11} MeV^{-1} Sr^{-1}
	Energy spread	100%
	Beam divergency (max)	±20°
Eletrons	Max energy	3 GeV
	Particles per pulse	10^{9}
	Beam divergency (max)	± 20 mad
Neutrons	Max energy	20 MeV
	Particles per pulse	10^{10}
	Energy spread	100
	Beam divergency	Isotropic
Gamma X-beams	Synchrotron radiation of the electrons inside the plasma or breemsstrahlung	
	Energy	up to 80 MeV
	Beam divergency	Directionality in the beam ropagbation direction

Protons spectra from A. Higginson et al. "Near-100 MeV protons via a laser-driven transparency-enhanced hybrid acceleration scheme", NATURE COMMUNICATIONS | (2018) 9:724

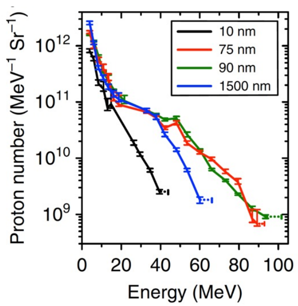

Electrons spectra from X. Wang et al. "Quasi-monoenergetic laser-plasma acceleration of electrons to 2 GeV", NATURE COMMUNICATIONS, 4:1988 2018 DOI: 10.1038/ncomms2988

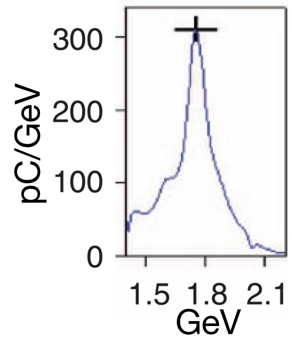

Neutrons spectra from A.Yogo et al. "Single shot radiography by a bright source of laser-driven thermal neutrons and x-rays", Applied Physics Express 14, 106001 (2021)

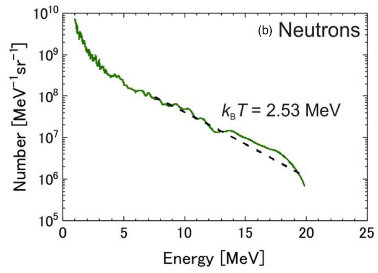

Gamma spectra from M. M. Günther et al "Forward-looking insights in laser-generated ultraintense γ-ray and neutron sources for nuclear application and science" NATURE COMMUNICATIONS | (2022) 13:170

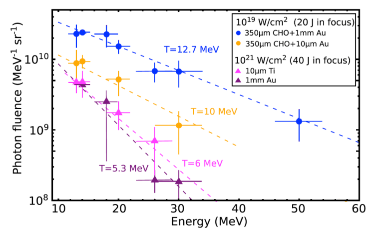

I-LUCE first phase

Available secondary sources – endstation

Protons acceleration up to 15 MeV with solid target (up to 50 MeV)

Electrons acceleration up to 300 MeV with capillary and gas-jet system

Neutron beam

Irradiations stations for both protons and electrons for medical and multidisciplinary applications

- Radiobiology
- FLASH radiotherapy applications
- Material science

Interaction of conventional ion beams with laser-generated plasmas

Physics cases

Chapter 6.2 Laser applications

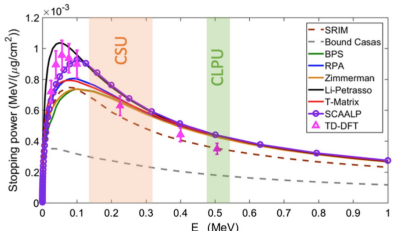

Stopping power in plasma

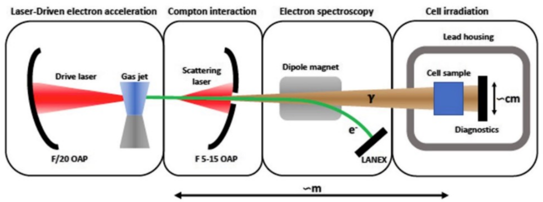

Positrons generation

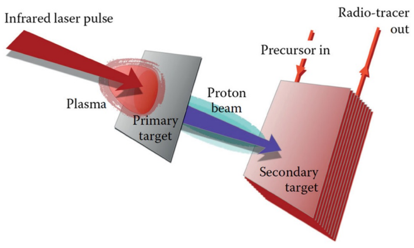

Radioisotopes

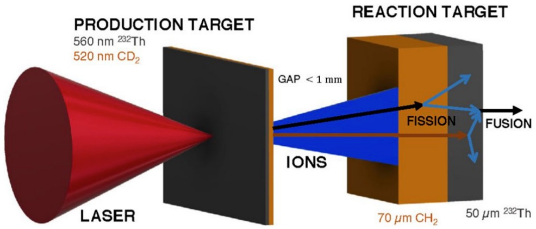

Nuclear reaction schemes

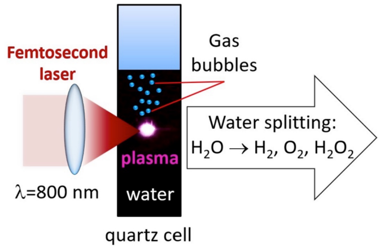

Hydrogen generation

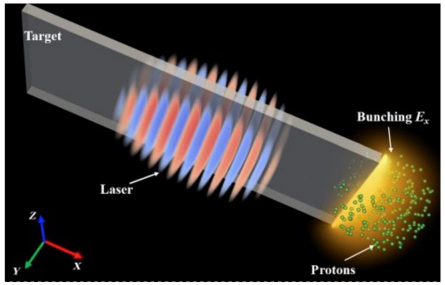

Protons and electrons generation

Eur. Phys. J. Plus (2023) 138:1038
https://doi.org/10.1140/epjp/s13360-023-04358-7

THE EUROPEAN PHYSICAL JOURNAL PLUS

Regular Article

Check for updates

Nuclear physics midterm plan at LNS

C. Agodi[1], F. Cappuzzello[1,2], G. Cardella[3], G. A. P. Cirrone[1], E. De Filippo[3], A. Di Pietro[1], A. Gargano[4], M. La Cognata[1,a], D. Mascali[1], G. Milluzzo[1], R. Nania[5], G. Petringa[1], A. Pidatella[1], S. Pirrone[3], R. G. Pizzone[1], G. G. Rapisarda[1,2,b], M. L. Sergi[1,2], S. Tudisco[1], J. J. Valiente-Dobón[7], E. Vardaci[4,8], H. Abramczyk[9], L. Acosta[10], P. Adsley[11], S. Amaducci[1], T. Banerjee[4], D. Batani[12], J. Bellone[1,2], C. Bertulani[11,13], S. Biri[14], A. Bogachev[15], A. Bonanno[1,16], A. Bonasera[1,11], C. Borcea[17], M. Borghesi[18], S. Bortolussi[19,20], D. Boscolo[14], G. A. Brischetto[1,2], S. Burrello[1,21,22], M. Busso[23,24], S. Calabrese[1], S. Calinescu[17], D. Calvo[25], V. Capirossi[25,26], D. Carbone[1], A. Cardinali[27], G. Casini[28], R. Catalano[1], M. Cavallaro[1], S. Ceccuzzi[29], L. Celona[1], S. Cherubini[1,2], A. Chieffi[24,30], I. Ciraldo[1,2], G. Ciullo[31,32], M. Colonna[1], L. Cosentino[1], G. Cuttone[1], G. D'Agata[1,2], G. De Gregorio[4,33], S. Degl'Innocenti[34], F. Delaunay[1,2,35], L. Di Donato[1,36], A. Di Nitto[4,8], T. Dickel[37,38], D. Doria[17,39], J. E. Ducret[40], M. Durante[14], J. Esposito[7], F. Farrokhi[1], J. P. Fernandez Garcia[21], P. Figuera[1], M. Fisichella[1], Z. Fulop[14], A. Galatá[6], D. Galaviz Redondo[41], D. Gambacurta[1], S. Gammino[1], E. Geraci[2,3], L. Gizzi[42], B. Gnoffo[2,3], F. Groppi[26,27], G. L. Guardo[1], M. Guarrera[1], S. Hayakawa[43], F. Horst[14], S. Q. Hou[44], A. Jarota[8], J. José[45], S. Kar[18,46], A. Karpov[15], H. Kierzkowska-Pawlak[9], G. G. Kiss[14], G. Knyazheva[15], H. Koivisto[47], B. Koop[72], E. Kozulin[14], D. Kumar[37,38], A. Kurmanova[1], G. La Rana[4,8], L. Labate[42], L. Lamia[1,2], E. G. Lanza[3], J. A. Lay[48,49], D. Lattuada[1,6], H. Lenske[50], M. Limongi[24,30,51], M. Lipoglavsek[52], I. Lombardo[2,3], A. Mairani[72], S. Manetti[26,27], M. Marafini[71], L. Marcucci[34], D. Margarone[53], N. S. Martorana[1,3], L. Maunoury[40], G. S. Mauro[1], M. Mazzaglia[1], S. Mein[72], A. Mengoni[5,54], M. Milin[55], B. Mishra[1], L. Mou[7], J. Mrazek[56], P. Nadtochy[57], E. Naselli[1], P. Nicolai[12], K. Novikov[15], A. A. Oliva[1], A. Pagano[3], E. V. Pagano[1], S. Palmerini[23,24], M. Papa[3], K. Parodi[73], V. Patera[58], J. Pellumaj[7,31], C. Petrone[24], S. Piantelli[28], D. Pierroutsakou[4], F. Pinna[25], G. Politi[2,3], I. Postuma[19,20], P. Prajapati[1,59], P. G. Prada Moroni[35], G. Pupillo[7], D. Raffestin[12], R. Racz[14], C.-A. Reidel[14], D. Rifuggiato[1], F. Risitano[3,60], F. Rizzo[2,3], X. Roca Maza[61,62], S. Romano[1,2], L. Roso[63], F. Rotaru[17], A. D. Russo[1], P. Russotto[1], V. Saiko[15], D. Santonocito[1], E. Santopinto[64], G. Sarri[46], D. Sartirana[25], C. Schuy[14], O. Sgouros[1], S. Simonucci[65], G. Sorbello[1,36], V. Soukeras[1], R. Spartá[1], A. Spatafora[1,2], M. Stanoiu[17], S. Taioli[66,67,68], T. Tessonnier[72], P. Thirolf[73], E. Tognelli[34], D. Torresi[1], G. Torrisi[1], L. Trache[17], G. Traini[70], M. Trimarchi[3,60], S. Tsikata[69], A. Tumino[1,6], J. Tyczkowski[9], H. Yamaguchi[43], V. Vercesi[19,20], I. Vidana[3], L. Volpe[63], U. Weber[14]

[1] Laboratori Nazionali del Sud, Istituto Nazionale di Fisica Nucleare, 95123 Catania, Italy
[2] Dipartimento di Fisica e Astronomia "Ettore Majorana", University of Catania, 95123 Catania, Italy
[3] Sezione di Catania, Istituto Nazionale di Fisica Nucleare, 95123 Catania, Italy
[4] Sezione di Napoli, Istituto Nazionale di Fisica Nucleare, 80126 Napoli, Italy
[5] Sezione di Bologna, Istituto Nazionale di Fisica Nucleare, 40127 Bologna, Italy
[6] Facoltà di Ingegneria e Architettura, Università degli Studi di Enna "Kore", 94100 Enna, Italy
[7] Laboratori Nazionali di Legnaro, Istituto Nazionale di Fisica Nucleare, 35020 Legnaro, Italy
[8] Dipartimento di Fisica "Ettore Pancini", Università di Napoli Federico II, 80126 Napoli, Italy
[9] Department of Molecular Engineering, Faculty of Process and Environmental Engineering, Lodz University of Technology, 93-005 Lodz, Poland
[10] Instituto de Fisica, Universidad Nacional Autonoma de Mexico, 04510 Mexico City, Mexico
[11] Cyclotron Institute, Texas A &M University, College Station, TX 77840, USA
[12] Centre Lasers Intenses et Applications (CELIA), University of Bordeaux, 33400 Talence, Bordeaux, France
[13] Department of Physics and Astronomy, Texas A &M University-Commerce, Commerce, TX 75429-3011, USA
[14] Atomki, Institute of Nuclear Research, 4026 Debrecen, Hungary
[15] Flerov Laboratory of Nuclear Reactions, Joint Institute for Nuclear Research, Dubna, Russia 141980
[16] Osservatorio Astrofisico di Catania, INAF, via S.Sofia 78, 95123 Catania, Italy
[17] IFIN-HH "Horia Hulubei", National Institute of Physics and Nuclear Engineering, 077125 Magurele, Romania
[18] School of Mathematics and Physics, Centre for Plasma Physics, Queen's University, Belfast, Northern Ireland BT7 1NN, UK
[19] Dipartimento di Fisica, Università degli Studi di Pavia, Via Agostino Bassi, 6, 27100 Pavia, Italy
[20] Sezione di Pavia, Istituto Nazionale di Fisica Nucleare (INFN), Via Agostino Bassi, 6, 27100 Pavia, Italy
[21] Departamento de Física Atómica Molecular y Nuclear, University of Seville, 41012 Sevilla, Spain
[22] Fachbereich Physik, Institut für Kernphysik, Technische Universität Darmstadt, 610101 Darmstadt, Germany
[23] Dipartimento di Fisica e Geologia, Università di Perugia, 06125 Perugia, Italy
[24] Sezione di Perugia, Istituto Nazionale di Fisica Nucleare, 06125 Perugia, Italy
[25] Sezione di Torino, Istituto Nazionale di Fisica Nucleare, 10125 Torino, Italy
[26] DISAT, Politecnico di Torino, 10129 Torino, Italy
[27] FSN Department, ENEA, DTT S.C.a r.l., 00044 Frascati, Italy
[28] Sezione di Firenze, Istituto Nazionale di Fisica Nucleare, 50019 Sesto Fiorentino (Fi), Italy
[29] ENEA, DTT S.C.a r.l., 00044 Frascati, Italy

C Agodi et al., Eur. Phys. J. Plus (2023) 138:1038

Thanks for listening

The basic ingredients: an high-power, short-pulse laser

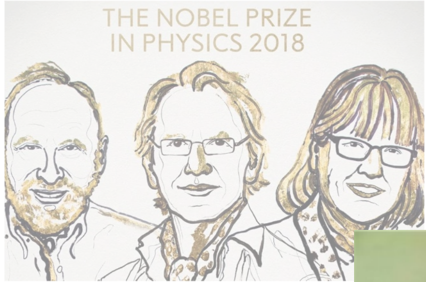

Center for Relativistic Laser Science

Explore the interaction between ultra-intense light and matter

South Korea

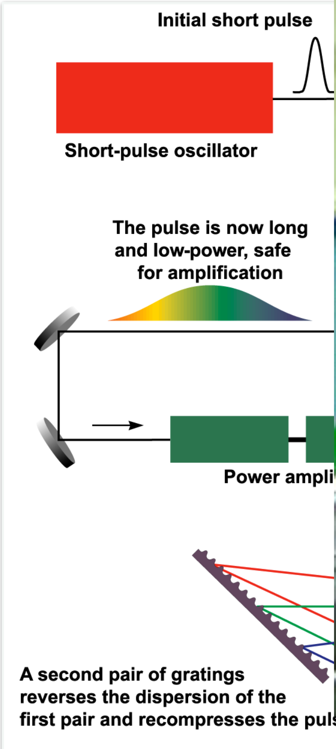

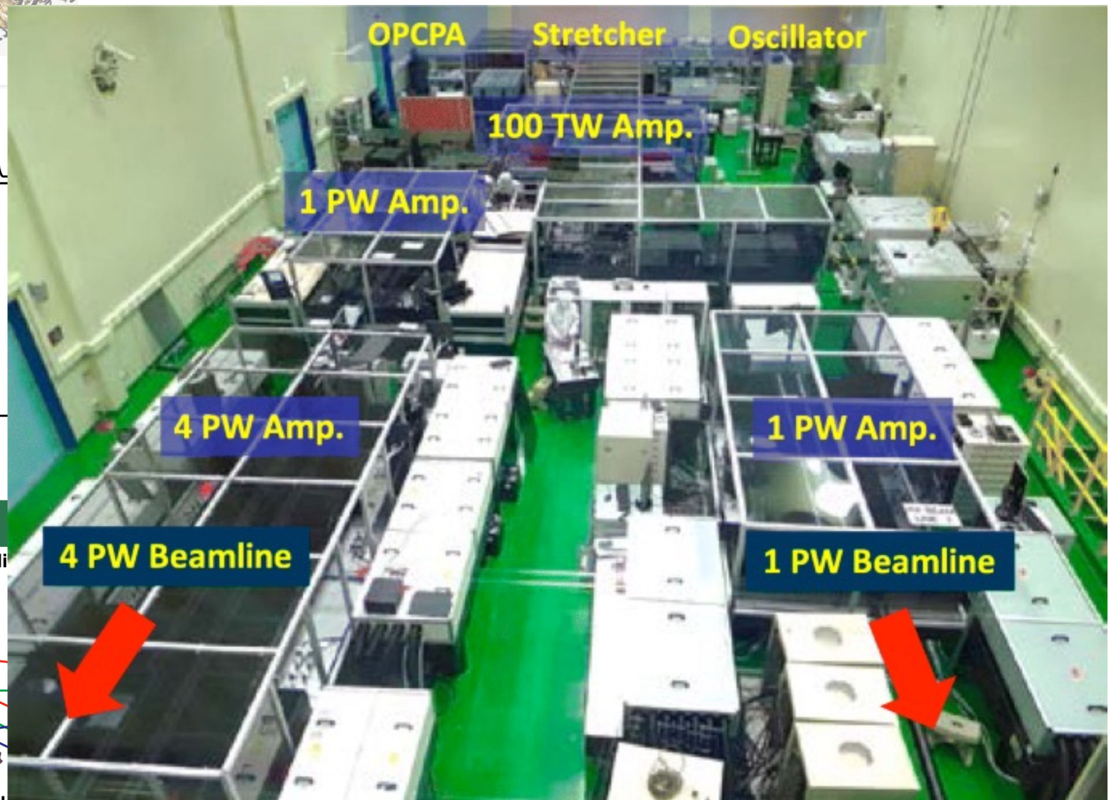

ARTICLE

DOI: 10.1038/s41467-018-03063-9 OPEN

Near-100 MeV protons via a laser-driven transparency-enhanced hybrid acceleration scheme

A. Higginson[1], R.J. Gray[1], M. King[1], R.J. Dance[1], S.D.R. Williamson[1], N.M.H. Butler[1], R. Wilson[1], R. Capdessus[1], C. Armstrong[1,2], J.S. Green[2], S.J. Hawkes[1,2], P. Martin[3], W.Q. Wei[4], S.R. Mirfayzi[3], X.H. Yuan[4], S. Kar[2,3], M. Borghesi[3], R.J. Clarke[2], D. Neely[1,2] & P. McKenna[1]

2018

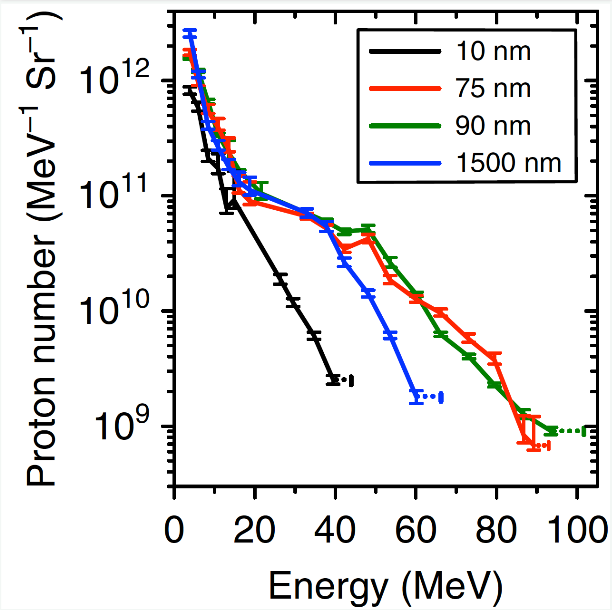

Vulcan laser at the Rutherford Appleton Laboratory (UK)

Intensity = ~ 10^{20}Wcm^{-2}

Pulses of p-polarised, **1.053 µm-wavelength**

Pulse duration τ = (0.9 ± 0.1) ps (FWHM)
Energy after the plasma mirror: (210 ± 40) J

Target: thin planar plastic foil with thickness in the range 10 nm-1.5 um

Laser room implementation proposal and timeline

Control room and optical laboratory, December 2024

Laser and interaction areas July 2026

Laser system, November 2026

THALES

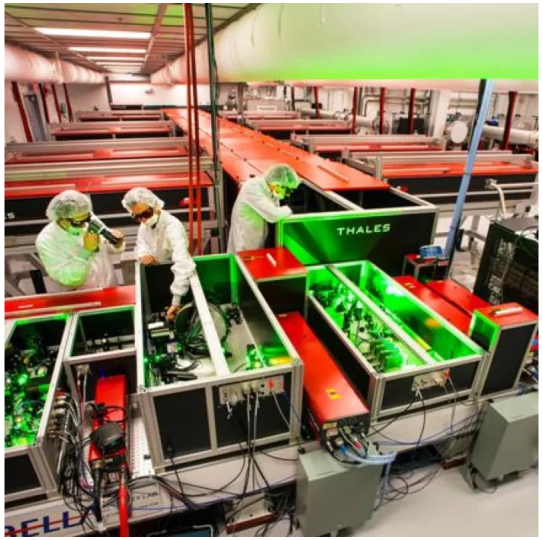

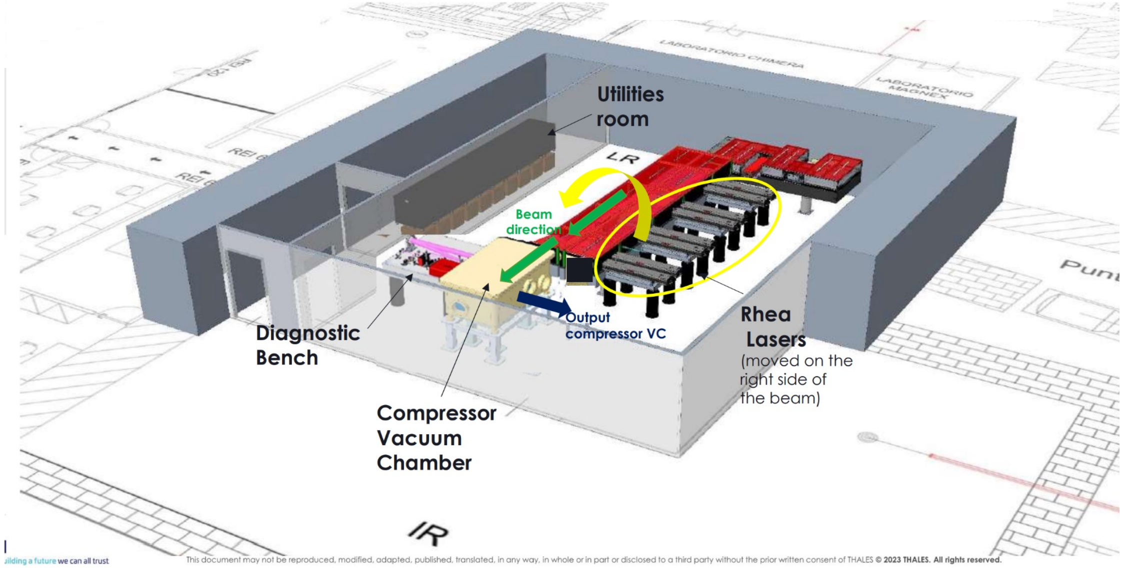

I-LUCE current status

THALES

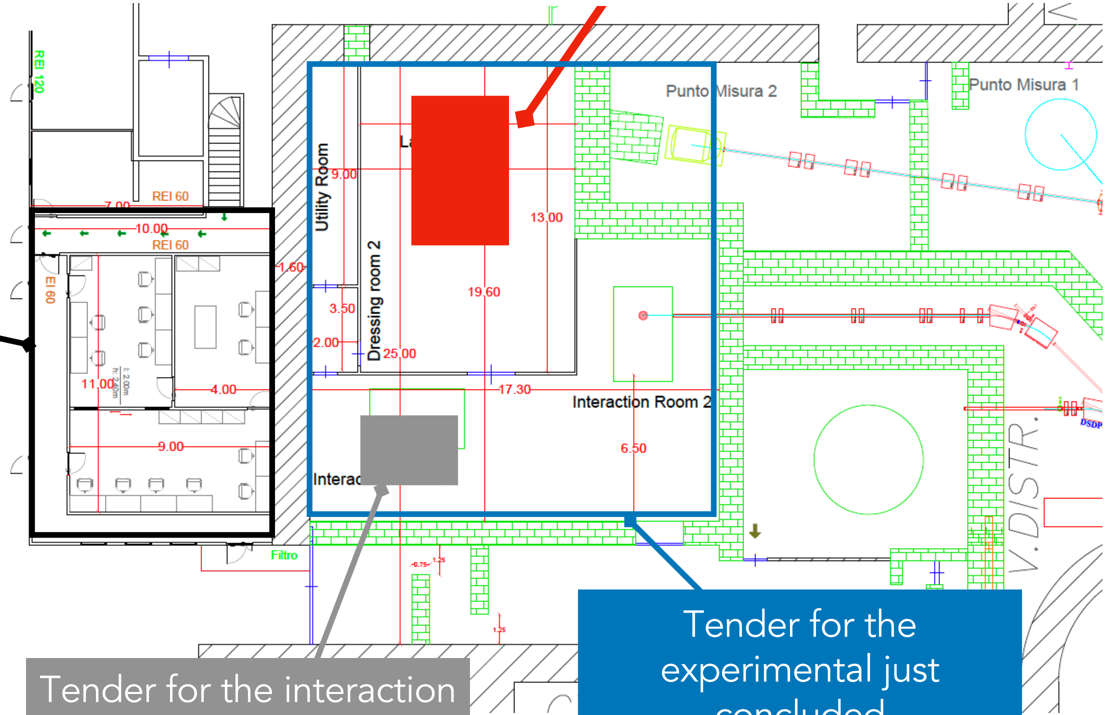

Tender for the interaction chamber just concluded

Tender for the experimental just concluded

Physics cases at I-LUCE

What we will have at disposal?

An high power laser: 8J/23fs/1Hz

A plasma generated by the laser:

Temperature: 2 eV - 200 eV

$$T \approx \left(\frac{I}{1.37\times10^{16}\ \mathrm{W/cm^2}} \right)^{1/2}$$

Density: 10^{25} m^{-3}

$$n \approx \frac{I}{e^2 T}$$

Ion beams in a wide Z range up to 70 AMeV

$$n \approx \frac{\varepsilon_0 m_e \omega_p^2}{e^2}$$

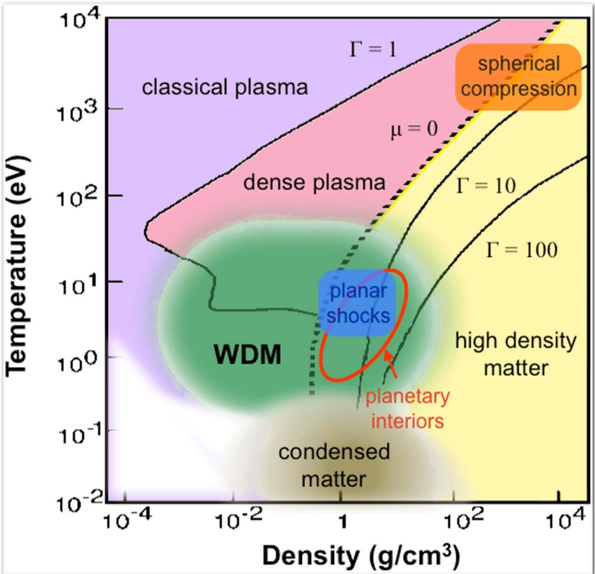

Medical and interdisciplinary applications

Use of ions/electrons beams for radiobiology studies

....for radioisotope production

... for hydrogen production

....for cultural heritage applications

... for inertial confinement studies

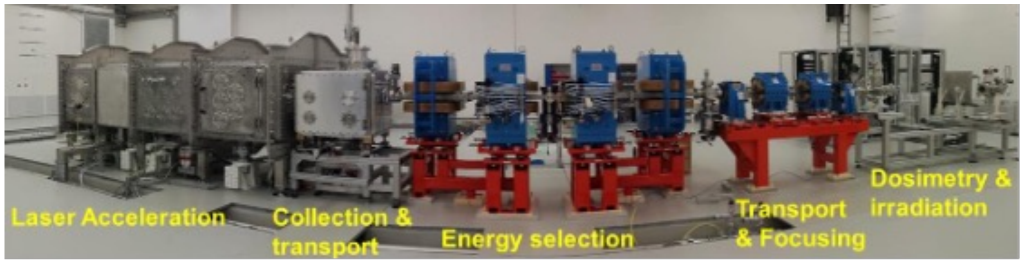

ELIMED/LIMAIA beamline th ELI-Beamlies facility (CZ)


quantum beam science

MDPI

Review

ELIMAIA: A Laser-Driven Ion Accelerator for Multidisciplinary Applications

Daniele Margarone [1,*], G. A. Pablo Cirrone [1,2], Giacomo Cuttone [2], Antonio Amico [2], Lucio Andò [2], Marco Borghesi [3], Stepan S. Bulanov [4], Sergei V. Bulanov [1], Denis Chatain [5], Antonín Fajstavr [1], Lorenzo Giuffrida [1], Filip Grepl [1], Satyabrata Kar [3], Josef Krasa [1], Daniel Kramer [1], Giuseppina Larosa [2], Renata Leanza [2], Tadzio Levato [1], Mario Maggiore [6], Lorenzo Manti [7], Guliana Milluzzo [2,3], Boris Odlozilik [1], Veronika Olsovcova [1], Jean-Paul Perin [5], Jan Pipek [2], Jan Psikal [1], Giada Petringa [2], Jan Ridky [1], Francesco Romano [2,8], Bedřich Rus [1], Antonio Russo [2], Francesco Schillaci [1,2], Valentina Scuderi [1,2], Andriy Velyhan [1], Roberto Versaci [1], Tuomas Wiste [1], Martina Zakova [1] and Georg Korn [1]

Nuclear astrophysics

The AsFiN laser collaboration:

A.Bonasera, G.L. Guardo, M. La Cognata, L. Lamia, D. Lattuada, A.A. Oliva, R.G. Pizzone, G.G. Rapisarda, S. Romano, D. Santonocito, A. Tumino

THE COULOMB EXPLOSION PARADIGMA

The interaction of ultra-short laser pulses with an expanding gas mixture at controlled temperature and pressure inside a vacuum chamber causes the formation of **plasmas with multi-keV temperature**. These energies overlap with the typical temperatures of stellar environments **where thermonuclear reactions occur**, thus making this paradigm a perfect scenario for nuclear astrophysics research.

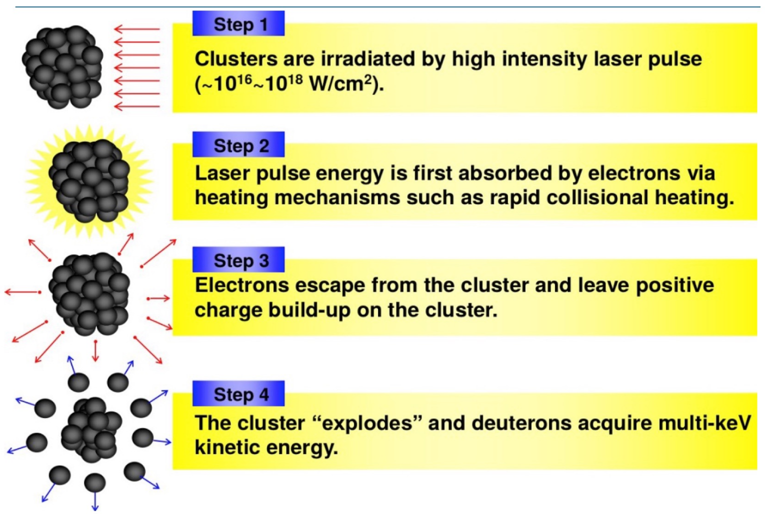

Example: deuterium-deuterium fusion

$$d + d \rightarrow {}^3\text{He}(0.82MeV) + n(2.45MeV)$$

$$d + d \rightarrow p(3.02MeV) + t(1.01MeV)$$

$$d + {}^3\text{He} \rightarrow p(14.7MeV) + {}^4\text{He}(3.6MeV)$$

Nuclear fusion from laser-cluster interaction

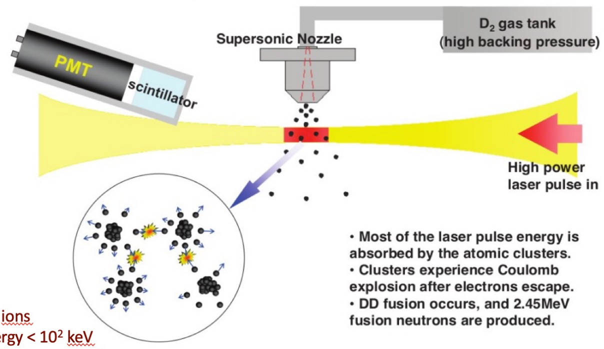

deuterium ions
Kinetic Energy < 10^2 keV
Density ~ 10^{18} atoms/cm^3
10^5-10^7neutrons per shot

Nuclear astrophysics: dd fusion

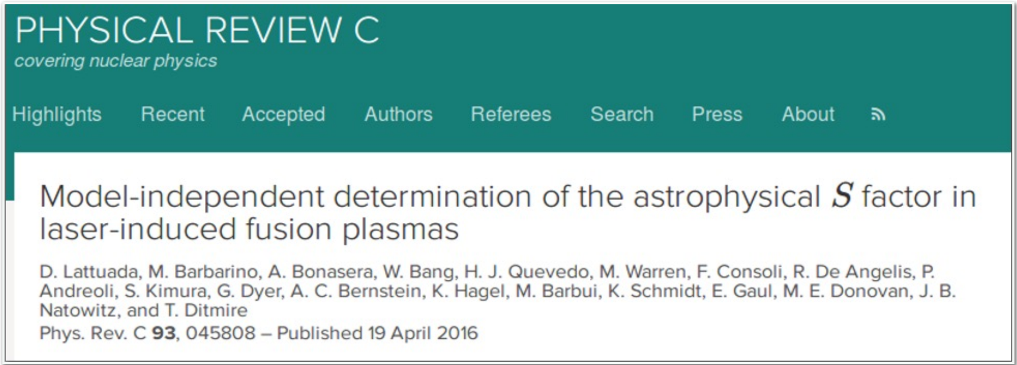
PHYSICAL REVIEW C
covering nuclear physics
Highlights Recent Accepted Authors Referees Search Press About

Model-independent determination of the astrophysical S factor in laser-induced fusion plasmas

D. Lattuada, M. Barbarino, A. Bonasera, W. Bang, H. J. Quevedo, M. Warren, F. Consoli, R. De Angelis, P. Andreoli, S. Kimura, G. Dyer, A. C. Bernstein, K. Hagel, M. Barbui, K. Schmidt, E. Gaul, M. E. Donovan, J. B. Natowitz, and T. Ditmire

Phys. Rev. C **93**, 045808 – Published 19 April 2016

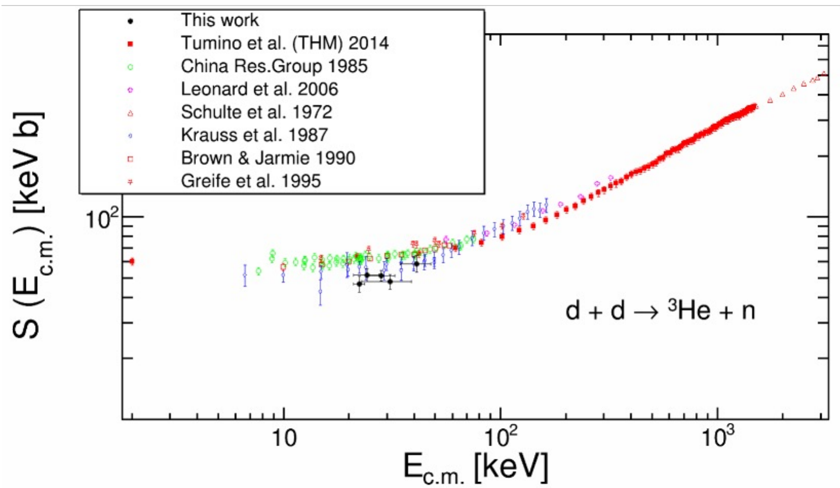

This method will open the way for a new approach to study nuclear astrophysics reactions such as:

-deuterium- deuterium

-deuterium-^{3}He

-proton-lithium

-proton-boron

-^{12}C-^{12}C

-^{16}O-^{16}O

-and much more….

Stopping powers in plasma

Stopping power of ions in plasma is a process of fundamental importance in many applications:

- Inertial Confinement Fusion
- Astrophysics and Nuclear Astrophysics
- High-energy Density Physics
- Plasma strippers
- Solid State Physics

Characterization of ions stopping power in plasma at I-LUCE facility

Collaboration: C. Altana, G. Castro, S. Cavallaro, C. Ciampi, G.A.P. Cirrone, R. De Angelis, S. De Luca, G. Lanzalone, L. Malferrari, F. Odorici, L. Palladino, G. Pasquali, A. Russo, A. Trifirò and S. Tudisco

Partecipating INFN sections: Catania, LNS, LNGS, Bologna, Firenze

Stopping powers in plasma

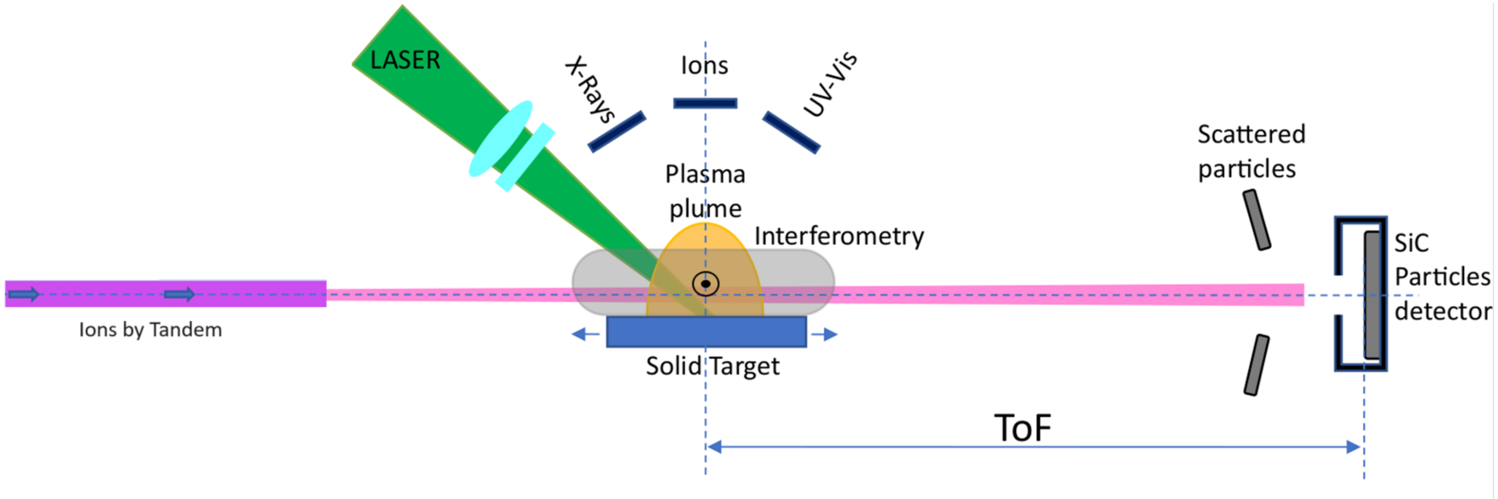

LNS has the only possibility, together with GSI, to deliver a beam with low energy by Tandem accelerator that cross a plasma plume generated under vacuum by a laser beam interacting with a solid target.

Nuclear physics mid-term plan

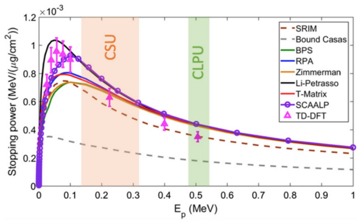

Stopping power in plasma

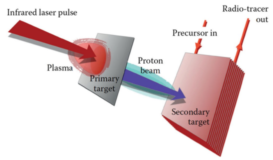

Radioisotopes

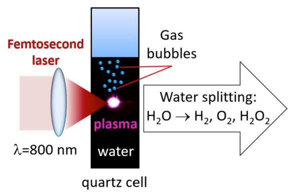

Hydrogen generation

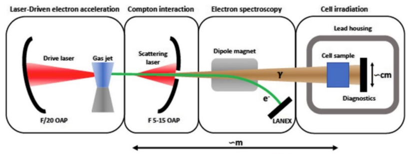

Fig. 48 Setup for the high-brilliance γ production via inverse Compton-scattering (from Sarri et al. [371])

Positrons generation

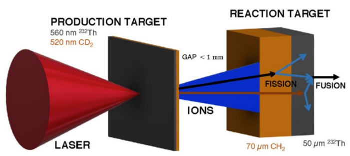

Nuclear reaction schemes

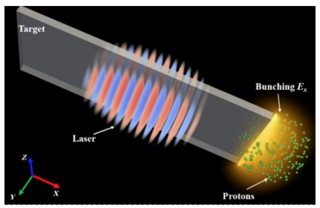

Protons and electrons generation

Chapter 6.2 Laser applications

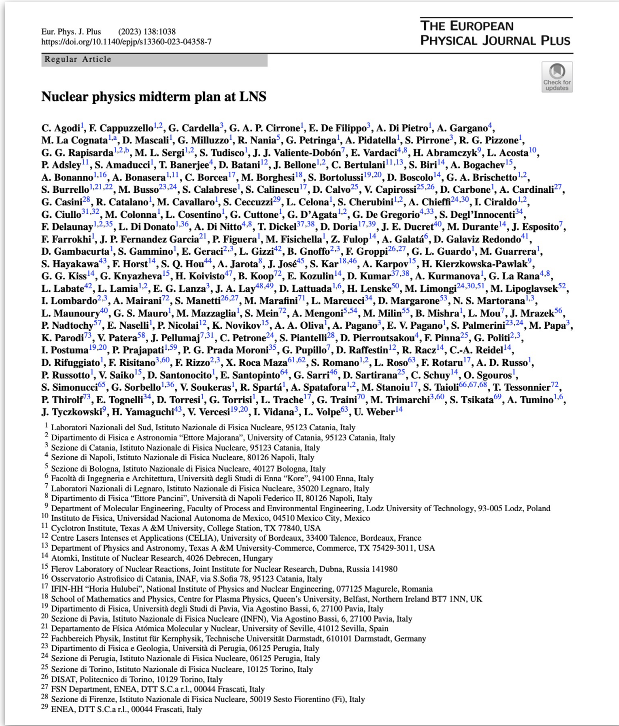

Eur. Phys. J. Plus (2023) 138:1038
https://doi.org/10.1140/epjp/s13360-023-04358-7
THE EUROPEAN PHYSICAL JOURNAL PLUS
Regular Article

Check for updates

Nuclear physics midterm plan at LNS

C. Agodi[1], F. Cappuzzello[1,2], G. Cardella[3], G. A. P. Cirrone[1], E. De Filippo[3], A. Di Pietro[1], A. Gargano[4], M. La Cognata[1,a], D. Mascali[1], G. Milluzzo[1], R. Nania[5], G. Petringa[1], A. Pidatella[1], S. Pirrone[3], R. G. Pizzone[1], G. G. Rapisarda[1,2,b], M. L. Sergi[1,2], S. Tudisco[1], J. J. Valiente-Dobón[7], E. Vardaci[4,8], H. Abramczyk[9], L. Acosta[10], P. Adsley[11], S. Amaducci[1], T. Banerjee[4], D. Batani[12], J. Bellone[1,2], C. Bertulani[11,13], S. Biri[14], A. Bogachev[15], A. Bonanno[1,16], A. Bonasera[1,11], C. Borcea[17], M. Borghesi[18], S. Bortolussi[19,20], D. Boscolo[14], G. A. Brischetto[1,2], S. Burrello[1,21,22], M. Busso[23,24], S. Calabrese[1], S. Calinescu[17], D. Calvo[25], V. Capirossi[25,26], D. Carbone[1], A. Cardinali[27], G. Casini[28], R. Catalano[1], M. Cavallaro[1], S. Ceccuzzi[29], L. Celona[1], S. Cherubini[1,2], A. Chieffi[24,30], I. Ciraldo[1,2], G. Ciullo[31,32], M. Colonna[1], L. Cosentino[1], G. Cuttone[1], G. D'Agata[1,2], G. De Gregorio[4,33], S. Degl'Innocenti[34], F. Delaunay[1,2,35], L. Di Donato[1,36], A. Di Nitto[4,8], T. Dickel[37,38], D. Doria[17,39], J. E. Ducret[40], M. Durante[14], J. Esposito[7], F. Farrokhi[1], J. P. Fernandez Garcia[21], P. Figuera[1], M. Fisichella[1], Z. Fulop[14], A. Galatá[6], D. Galaviz Redondo[41], D. Gambacurta[1], S. Gammino[1], E. Geraci[2,3], L. Gizzi[42], B. Gnoffo[2,3], F. Groppi[26,27], G. L. Guardo[1], M. Guarrera[1], S. Hayakawa[43], F. Horst[14], S. Q. Hou[44], A. Jarota[8], J. José[45], S. Kar[18,46], A. Karpov[15], H. Kierzkowska-Pawlak[9], G. G. Kiss[14], G. Knyazheva[15], H. Koivisto[47], B. Koop[72], E. Kozulin[14], D. Kumar[37,38], A. Kurmanova[1], G. La Rana[4,8], L. Labate[42], L. Lamia[1,2], E. G. Lanza[3], J. A. Lay[48,49], D. Lattuada[1,6], H. Lenske[50], M. Limongi[24,30,51], M. Lipoglavsek[52], I. Lombardo[2,3], A. Mairani[72], S. Manetti[26,27], M. Marafini[71], L. Marcucci[34], D. Margarone[53], N. S. Martorana[1,3], L. Maunoury[40], G. S. Mauro[1], M. Mazzaglia[1], S. Mein[72], A. Mengoni[5,54], M. Milin[55], B. Mishra[1], L. Mou[7], J. Mrazek[56], P. Nadtochy[57], E. Naselli[1], P. Nicolai[12], K. Novikov[15], A. A. Oliva[1], A. Pagano[3], E. V. Pagano[1], S. Palmerini[23,24], M. Papa[3], K. Parodi[73], V. Patera[58], J. Pellumaj[7,31], C. Petrone[24], S. Piantelli[28], D. Pierroutsakou[4], F. Pinna[25], G. Politi[2,3], I. Postuma[19,20], P. Prajapati[1,59], P. G. Prada Moroni[35], G. Pupillo[7], D. Raffestin[12], R. Racz[14], C.-A. Reidel[14], D. Rifuggiato[1], F. Risitano[3,60], F. Rizzo[2,3], X. Roca Maza[61,62], S. Romano[1,2], L. Roso[63], F. Rotaru[17], A. D. Russo[1], P. Russotto[1], V. Saiko[15], D. Santonocito[1], E. Santopinto[64], G. Sarri[46], D. Sartirana[25], C. Schuy[14], O. Sgouros[1], S. Simonucci[65], G. Sorbello[1,36], V. Soukeras[1], R. Spartá[1], A. Spatafora[1,2], M. Stanoiu[17], S. Taioli[66,67,68], T. Tessonnier[72], P. Thirolf[73], E. Tognelli[34], D. Torresi[1], G. Torrisi[1], L. Trache[17], G. Traini[70], M. Trimarchi[3,60], S. Tsikata[69], A. Tumino[1,6], J. Tyczkowski[9], H. Yamaguchi[43], V. Vercesi[19,20], I. Vidana[3], L. Volpe[63], U. Weber[14]

1 Laboratori Nazionali del Sud, Istituto Nazionale di Fisica Nucleare, 95123 Catania, Italy
2 Dipartimento di Fisica e Astronomia "Ettore Majorana", University of Catania, 95123 Catania, Italy
3 Sezione di Catania, Istituto Nazionale di Fisica Nucleare, 95123 Catania, Italy
4 Sezione di Napoli, Istituto Nazionale di Fisica Nucleare, 80126 Napoli, Italy
5 Sezione di Bologna, Istituto Nazionale di Fisica Nucleare, 40127 Bologna, Italy
6 Facoltà di Ingegneria e Architettura, Università degli Studi di Enna "Kore", 94100 Enna, Italy
7 Laboratori Nazionali di Legnaro, Istituto Nazionale di Fisica Nucleare, 35020 Legnaro, Italy
8 Dipartimento di Fisica "Ettore Pancini", Università di Napoli Federico II, 80126 Napoli, Italy
9 Department of Molecular Engineering, Faculty of Process and Environmental Engineering, Lodz University of Technology, 93-005 Lodz, Poland
10 Instituto de Fisica, Universidad Nacional Autonoma de Mexico, 04510 Mexico City, Mexico
11 Cyclotron Institute, Texas A &M University, College Station, TX 77840, USA
12 Centre Lasers Intenses et Applications (CELIA), University of Bordeaux, 33400 Talence, Bordeaux, France
13 Department of Physics and Astronomy, Texas A &M University-Commerce, Commerce, TX 75429-3011, USA
14 Atomki, Institute of Nuclear Research, 4026 Debrecen, Hungary
15 Flerov Laboratory of Nuclear Reactions, Joint Institute for Nuclear Research, Dubna, Russia 141980
16 Osservatorio Astrofisico di Catania, INAF, via S.Sofia 78, 95123 Catania, Italy
17 IFIN-HH "Horia Hulubei", National Institute of Physics and Nuclear Engineering, 077125 Magurele, Romania
18 School of Mathematics and Physics, Centre for Plasma Physics, Queen's University, Belfast, Northern Ireland BT7 1NN, UK
19 Dipartimento di Fisica, Università degli Studi di Pavia, Via Agostino Bassi, 6, 27100 Pavia, Italy
20 Sezione di Pavia, Istituto Nazionale di Fisica Nucleare (INFN), Via Agostino Bassi, 6, 27100 Pavia, Italy
21 Departamento de Física Atómica Molecular y Nuclear, University of Seville, 41012 Sevilla, Spain
22 Fachbereich Physik, Institut für Kernphysik, Technische Universität Darmstadt, 610101 Darmstadt, Germany
23 Dipartimento di Fisica e Geologia, Università di Perugia, 06125 Perugia, Italy
24 Sezione di Perugia, Istituto Nazionale di Fisica Nucleare, 06125 Perugia, Italy
25 Sezione di Torino, Istituto Nazionale di Fisica Nucleare, 10125 Torino, Italy
26 DISAT, Politecnico di Torino, 10129 Torino, Italy
27 FSN Department, ENEA, DTT S.C.a r.l., 00044 Frascati, Italy
28 Sezione di Firenze, Istituto Nazionale di Fisica Nucleare, 50019 Sesto Fiorentino (Fi), Italy
29 ENEA, DTT S.C.a r.l., 00044 Frascati, Italy

Take-to-home message

New radiation beams, complementary to the existing ones

New basic physics and multidisciplinary studies (also complementary to other apparata in realisation, i.e PANDORA)

A new European facility with unique features

Thanks to everyone

Thanks for listening

Laser-plama Ion acceleration: some physical quantities

I_L (Laser intensity) = 10^{21} W/cm^2

Direct laser interaction

- $E \backsim I_L^{1/2}\lambda = 10^{14}$ V/m
- $B = E/c = 3 \cdot 10^5$ T
- $P_{rad} = I_L/c = 3 \cdot 10^{10}$ J/cm^3 = 300 Gbar

Laser-plasma interaction

Debye Length: ⟹ $\lambda_D = 2.4\,\mu m \cdot \sqrt{\frac{T_{hot}}{1MeV}} \cdot \sqrt{\frac{10^{19}\,cm^{-3}}{N_{hot}}}$ ⟹ **~ µm!**

Acceleration time: ⟹ $\tau = \sqrt{\frac{\lambda_D^2 m_{ion}}{T_{hot}}} = 0.24\,ps\sqrt{\frac{\lambda_D^2 n_{hot}}{10^{19}}}$ ⟹ **~ ps!**

Electric Field: ⟹ $\tau = \frac{T_{hot}}{e\lambda_D} \approx \frac{MV}{\mu m}$ ⟹ **~ TV/m!**

Introduction

Concept of the "coherent acceleration"

The accelerating field on each particle is proportional to the number of particles being accelerated

(Veksler, V., 1957, At. Energ. 2, 525.)

Use of intense laser pulses on a target

In this case the energy transferred to the target produce a **displacement of a large number of electrons**; this produce a strong **electric field able to accelerate ions** until the neutrality is again reached.

Introduction

Observation of fast ions in a laser plasma

Yu. A. Zakharenkov, O. N. Krokhin, G. V. Sklizkov, and A. S. Shikanov

P. N. Lebedev Physics Institute, USSR Academy of Sciences

(Submitted March 18, 1977)
Pis'ma Zh. Eksp. Teor. Fiz. **25**, No. 9, 415–418 (5 May 1977)

Experiments on heating of spherical targets wth the high-power "Kal'mar" laser installation revealed a group of fast ions with energy $\lesssim 0.5$ MeV. The possible generation mechanisms are discussed.

PACS numbers: 52.50.Jm, 52.25.Lp

The appearance of a group of fast ions that carry away an appreciable fraction of the energy absorbed by the plasma has been reported repeatedly in recent years.[1] These ions were registered with the aid of time-of-flight corpuscular methods having a small angular aperture and in which the plasma is investigated during the later stages of the dispersal.

In our experiment, using high-speed multiframe interferometry,[2] we observed generation of fast ions in a plasma produced with the 9-channel laser setup "Kal'mar" and by irradiating solid and hollow targets of glass (SiO_2) of $\sim 100\ \mu$ diameter. At a light-beam diameter $\sim 150\ \mu$ in the target region and at an energy $E_L \approx 150$ J, the flux density was $q \sim 10^{14}$ W/cm^2.[3]

Introduction

Before the year 2000

Many experiments observed MeV ion emission from laser with **thick solid**, gas-jet and sub micrometric cluster.

Common feature of these experiments:

- isotropic ion emission
- low brilliance

In 2000

Three different experiments independently observed high-intensity, **multi MeV emission** from the high-intensity laser interaction with **micrometric-scale** targets

- Particles on the **back side of the target**
- Much more collimated

Clark, E. L., et al., 2000a, Phys. Rev. Lett. 84, 670.

Snavely, R. A., et al., 2000, Phys. Rev. Lett. 85, 2945.

Maksimchuk, A., S. Gu, K. Flippo, D. Umstadter, and V.Y. Bychenkov, 2000, Phys. Rev. Lett. 84, 4108.

Introduction

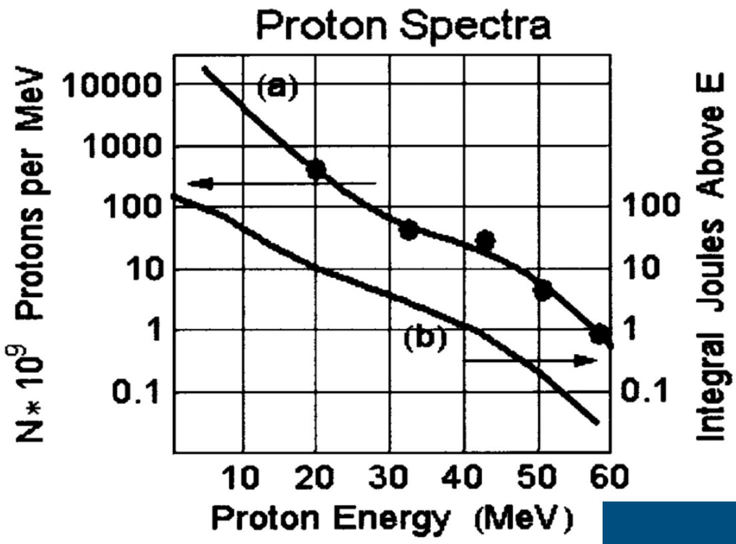

Snavely, R. A., et al., 2000, Phys. Rev. Lett. 85, 2945.

Proton spectrum from the rear side of a 100 um solid target irradiated by a 423 J, **0.5 ps** pulse at normal incidence, corresponding to an intensity of $3*10^{20}$ W/cm^2.
The integrated energy of protons indicates a conversion efficiency of 10% for protons above 10 MeV.

	Laser intensity [W cm-2]	Number of protons	Max proton energy [MeV]
Maksimchuk et al., 2000	3*E18	> 1E9	1.5
Clark et al., 2000	5E+19	1E+12	18
Snavely et al., 2000	3E+20	2E+13	58

Introduction

Emission of protons from metallic targets (not containing hydrogen) may sound surprising:

thin layer of water or hydrocarbons normally present on solids surface in standard conditions

With "long" nano-second laser protons/ions emissions were observed in the rear part of the target with a broad angular distribution)

This acceleration was interpreted in terms of **acceleration during the expansion of the hot laser-produced plasma** at the front laser irradiated side of the target

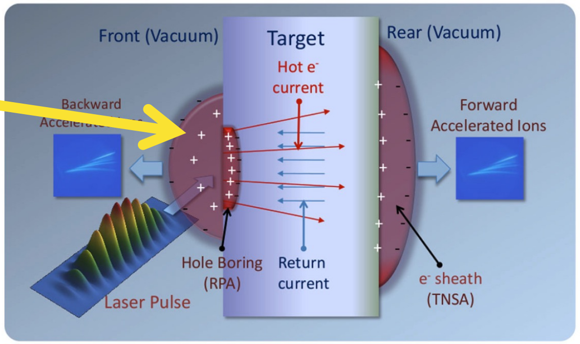

Introduction

Emission of protons from metallic targets (not containing hydrogen) may sound surprising:

thin layer of water or hydrocarbons normally present on solids surface in standard conditions

The characteristics of the forward proton emission in the new experiments, such as the **high degree of collimation** and laminarity of the beam, were much more impressive

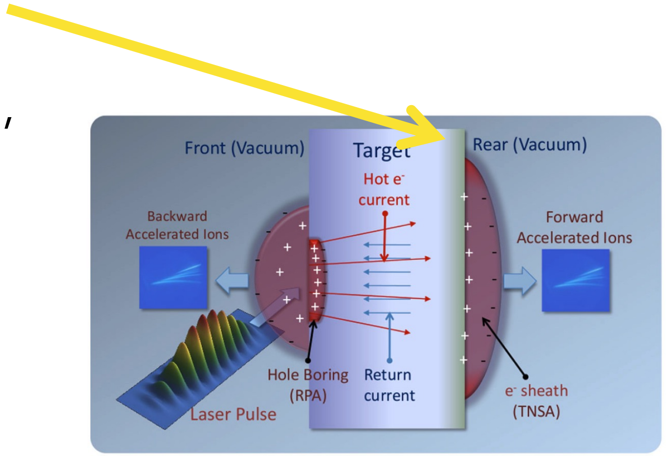

Introduction

A debated started around 2000 related to the physics mechanisms of this observed acceleration

Some authors suggested that protons were accelerated on the front side of the target and then cross the target reaching the other surface

Other authors in contrast, provided evidence that protons were accelerated at the rear side

Clark, E. L., et al., 2000a, Phys. Rev. Lett. 84, 670.

These experiments were performed at the Lawrence Livermore Petawatt facility

The TNSA (Target Normal Sheet Acceleration) mechanism was proposed

Snavely, R. A., et al., 2000, Phys. Rev. Lett. 85, 2945.

Wilks, S. C. et al, 2001, Phys. Plasmas 8, 542.

TNSA

Briefly, TNSA is driven by the space-charge field generated at the rear surface of the target **by highly energetic electrons accelerated at the front surface**, crossing the target bulk, and attempting to escape in vacuum from the rear side.

Most of the experiments investigating proton acceleration by laser interaction with solid targets have been interpreted **in terms of the TNSA framework**

At present it is not guaranteed that the ion energy **scaling observed so far will be maintained** at such extreme intensities (E22 W/cm2, today) nor that TNSA will still be effective.

TNSA: a robust and experimentally well-established mechanism

Clark, PRL (2000); Maksimchuk, PRL (2000) Snavely, PRL (2000)

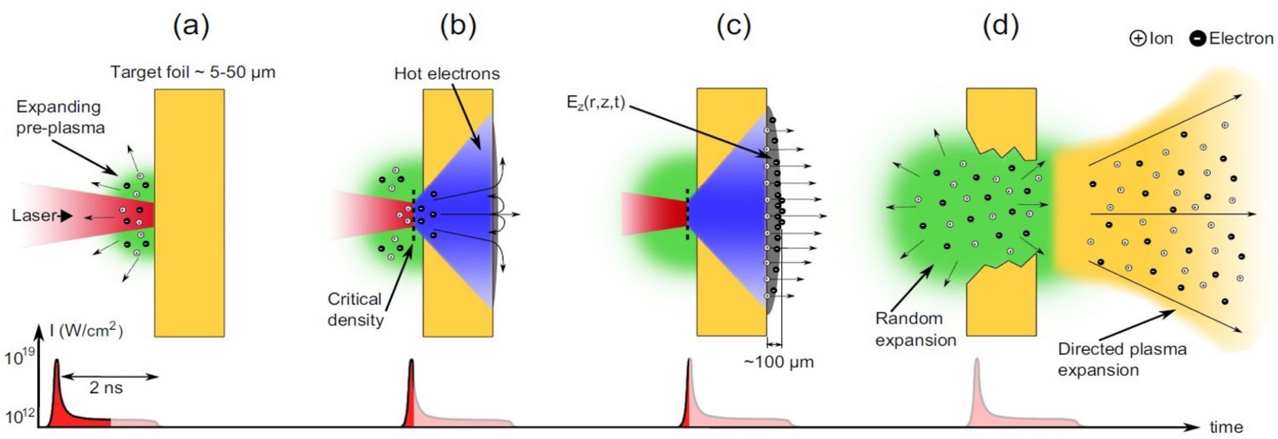

TNSA mechanism

a) Typical Laser Intensity (10^{18}-10^{20} W/cm^2)
b) Accelerated Relativistic Electrons (multi MeV) traverse the thin target (0.1÷100 mm).
c) H-ultrathin rear-side layer is ionized by the electron beam and protons are generated.
d) Fast electron cloud builds up a quasi-electrostatic field exceeding ~1 TV/m accelerating protons in the forward direction to multi-MeV energies.

TNSA features

a) Protons/ions are accelerated along the target normal
b) Ions with the highest charge-to-mass ratio (protons) dominate the acceleration, gaining the most energy (electric field screening effect)
c) Exponential ion energy distribution (large energy spread)

TNSA scaling law

Scaling of the maximum proton energy:

$(I \cdot \lambda^2)^{1/2}$ up to $I \cdot \lambda^2 = 3 \cdot 10^{20}$ W cm^{-2} µm^2

M Borghesi 2006 et al, Fusion Sci. Technol. 49, 412

$I \cdot \lambda^2$ is called "Irradiance"

λ laser wavelength

I is laser intensity as Watts on cm^2

Maximum proton energy from laser irradiated solid targets as a function of the laser irradiance and for three ranges of pulse durations, reporting experiments up to 2008. **Two trend lines are overlaid**, the shallower one corresponding to a $I^{1/2}$ dependence, and the steeper one to a scaling proportional to I

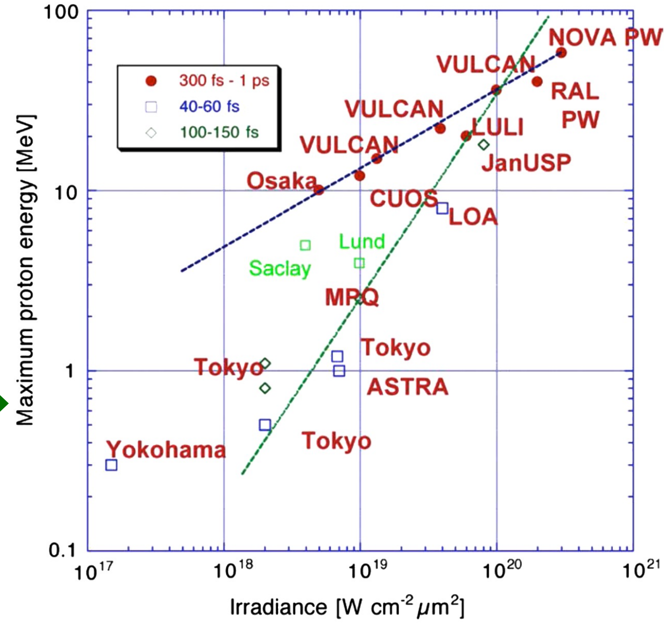

Borghesi, M., et al., 2008, Plasma Phys. Controlled Fusion 50, 124040.

Behind TNSA

Is not only the maximum proton energy an important parameter

It is also of crucial importance to establish the most relevant scaling parameters as well as to **improve or optimize beam emittance, brilliance, and monoenergeticity** for specific applications.

These issues motivate the search for other ion acceleration mechanisms

- Radiation pressure acceleration
- Collisionless shock acceleration
- Break-out afterburner

Ion acceleration

Ingredients

Solid target

High-power (TW/PW), short-pulse (20 fs - 500 fs) laser

- focused in a target 10^{19} - 10^{22} W/cm^2
- The ponderomotive force and the relativistic transparency caused by the laser-matter interaction

What is a solid target?

A solid material where the electron density **n_e** greatly exceeds the so-called critical or cutoff density **n_c**

$$n_c = \frac{m_e \omega^2}{4\pi e^2} = 1.1 \cdot 10^{21} cm^{-3} (\frac{\lambda}{\mu m})^{-1}$$

Ion acceleration

Plasma frequency

$$\omega_p = \sqrt{\frac{4\pi n_e e^2}{m_e}}$$

Laser frequency

$$\omega = \frac{2\pi c}{\lambda}$$

Linear refractive index of the plasma

$$n = \sqrt{1 - \frac{\omega_p^2}{\omega^2}} = \sqrt{1 - \frac{n_e}{n_c}}$$

Ion acceleration

Linear refractive index of the plasma

$$n = \sqrt{1 - \frac{\omega_p^2}{\omega^2}} = \sqrt{1 - \frac{n_e}{n_c}}$$

Bourdier, A., 2020, "Calculation of the refractive index for plane waves propagating in ionized gas" Results in Physics 18, 103250.

- when $n_e > n_c$ we say that we are in an "overdense" condition. In this case n assumes an imaginary valued the laser cannot propagate in the medium (**plasma mirroring)**
- All the laser plasma interaction occurs in the case of "underdense" regions $n_e < n_c$ or at the "near critical" region ($n_e \simeq n_c$)
- The condition $n_e = n_c$ is equivalent to $\omega_p = \omega$

The ponderomotive force

Before the accelerating phenomena become evident laser-electrons interactions where treated as plane waves interaction

- Plane waves: radiation whose magnitude is uniform in space and slowing varying in time

Short pulse lasers tend to violate these conditions:

- tight focusing create strong radial intensity gradients over a few wavelengths
- ==> non adiabatic treatment is required

This curious force is heuristically defined as **the gradient of the time averaged oscillation potential occurring** when laser interact with a single electron

The ponderomotive force

General definition

In physics, a **ponderomotive force** is a nonlinear force that a charged particle experiences in an inhomogeneous oscillating electromagnetic field.

It causes the particle to move towards the area of the weaker field strength, rather than oscillating around an initial point as happens in a homogeneous field.

$$F_p = \frac{e^2}{4m\omega^2}\nabla(E^2)$$

The ponderomotive force and laser penetration

In an oscillating, quasi-monochromatic electromagnetic field described by a vector potential **a**(**r**,t), the relativistic ponderomotive force is given by:

$$f_p = -m_e c^2 \nabla \sqrt{(1 + < a >^2)}$$

Action of the ponderomotive force on a solid target

- For a plane-wave interacting with an **overdense target**, the f_p acts more on the electrons (lightest particles) in the inward direction
- A laser pulse of finite width may produce a **density depression** around the propagation axis also because of the ponderomotive force pushing the electrons in the radial direction. Jointly with the relativistic effect and target expansion driven by electron heating, this mechanism may lead to a **transition to transparency as soon as the electron density drops below the cutoff value**

Role of the electron density

The hot electrons

We said that the laser pulse cannot penetrate into solid targets

But the energy is transported to the intern target mostly by the so called "**hot" or "fast" electrons** that are generated by the **laser-matter interaction** with different **mechanisms**

The energy of these electrons is of the order of the cycle-averaged oscillation energy in the laser electric field

$$\epsilon_p = m_e c^2 (\sqrt{1 + a_0^2/2} - 1)$$

$$f_p = \frac{dp^s}{dt} = -mc^2 \nabla\gamma$$

$$\gamma = \sqrt{1 + p_s^2/m^2c^2 + a_0^2)}$$

This is called the Ponderomotive energy

Hot electrons are important because

- Role in laser-driven photo nuclear physics
- Fast ignition of fusion target
- Protons/ions acceleration

Hot electrons transport in solid matter

It is of extreme importance especially in the field of Inertial Confinement Fusion processes

Freeman, R. R., D. Batani, S. Baton, M. Key, and R. Stephens, 2006, Fusion Sci. Technol. 49, 297. [http://www.new.ans.org/pubs/journals/fst/a_1150]

Most important aspects characterising this regime:

- Very high currents
- Self-generated fields

Density currents in front of the target associated to the hot electrons:

$$J_h = -en_h v_h \sim en_c c \approx 4.8 \cdot 10^{12} Acm^{-2}$$

Corresponding to a current of **around 15 MA over a spot of 10 um radius**

Summarising the TNSA

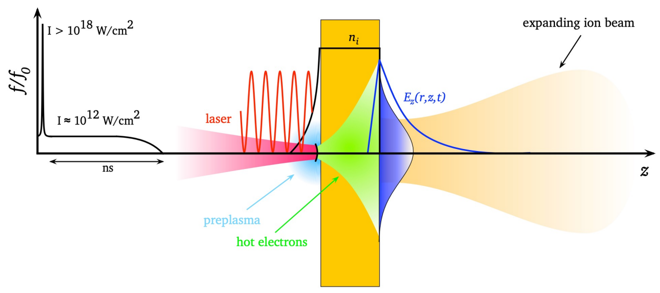

Fig. 1: Target normal sheath acceleration. A thin target foil with thickness $d = 5$–50 μm is irradiated by an intense laser pulse. The laser prepulse creates a preplasma on the target's front side. The main pulse interacts with the plasma and accelerates megaelectronvolt electrons, mainly in the forward direction. The electrons propagate through the target, where collisions with the background material can increase the divergence of the electron current. The electrons leave the rear side, resulting in a dense sheath. An electric field due to charge separation is created. The field is of the order of the laser electric field ($\sim$ TV/m), and ionizes atoms at the surface. The ions are then accelerated in this sheath field, pointing in the target normal direction.

Conversion efficiency from laser energy to hot electrons is not perfect but can reach 69% in some configuration

$$n_0 = \frac{\eta E_\mathrm{L}}{c\tau_\mathrm{L}\pi r_0^2 k_\mathrm{B} T_\mathrm{hot}} ,$$

$$\eta = 1.2 \times 10^{-15} I^{0.74} ,$$

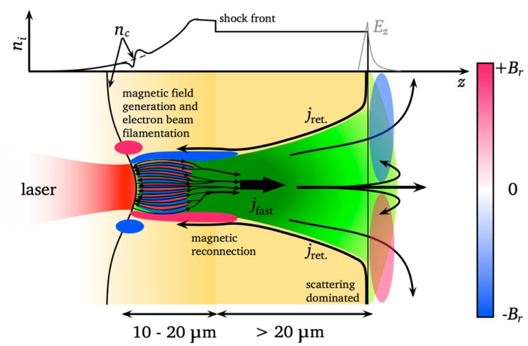

Fig. 2: Schematic of laser-generated fast-electron transport. The laser (shown in red) impinges on a preplasma with exponential density profile from the left side. The light pressure leads to profile steepening, depicted in the graph at the top of the figure. An ablation plasma creates an inward-travelling shockwave that heats, ionizes, and compresses the target. Fast electrons are created by the laser, propagating into the dense plasma towards the target's rear side. The high electron current j_fast can lead to filamentation and magnetic field generation (shown by the light red- and blue-coloured areas), as well as driving a return current j_ret. The global magnetic field tends to pinch the fast-electron current. Electrons propagating in the dense solid matter interact with the background material by binary collisions. This leads to a spatial broadening of the electron distribution, which becomes the major effect for longer distances. At the rear side, the electrons form a sheath and build up an electrostatic field E_z (grey line in graph). This can lead to refluxing (recirculation) of the electrons, heating the target even further.

Published by CERN in the Proceedings of the CAS-CERN Accelerator School: Plasma Wake Acceleration, Geneva, Switzerland, 23–29 November 2014, edited by B. Holzer, CERN-2016-001 (CERN, Geneva, 2016)

Ion Acceleration—Target Normal Sheath Acceleration*

M. Roth and M. Schollmeier
Institute for Nuclear Physics, Technische Universität Darmstadt, Darmstadt, Germany

INFN

Istituto Nazionale di Fisica Nucleare

I LUCE

Scaling laws and interaction approaches

Scaling laws

proton energy

Intensity W/cm^2 → $$I \propto \frac{E_p}{\tau A}$$

pulse lenght

spot surface on target

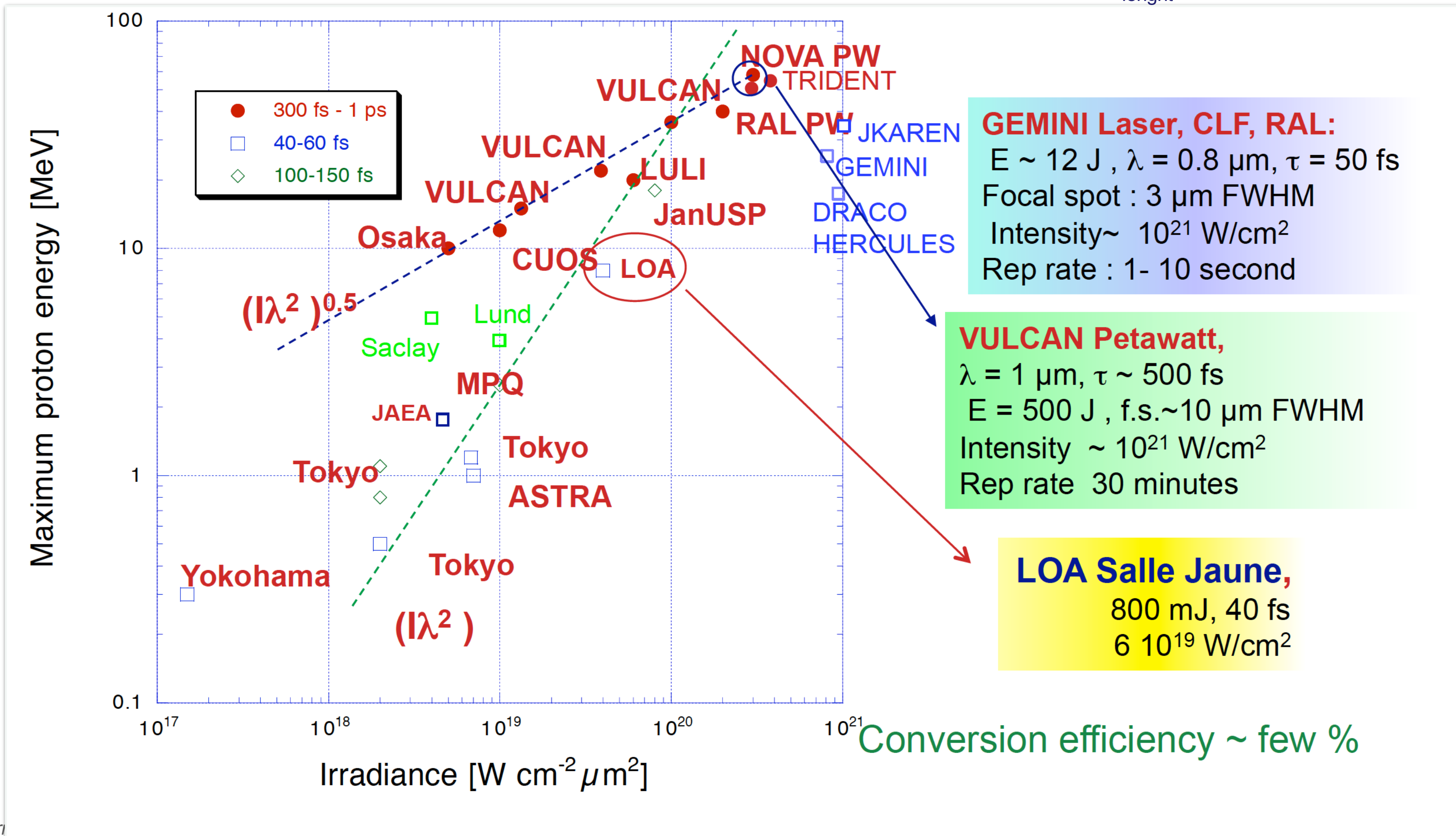

Scaling laws

$$I \propto \frac{E_p}{\tau A}$$

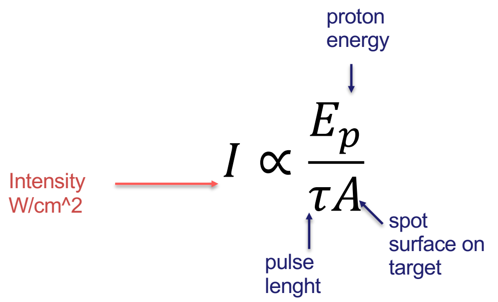

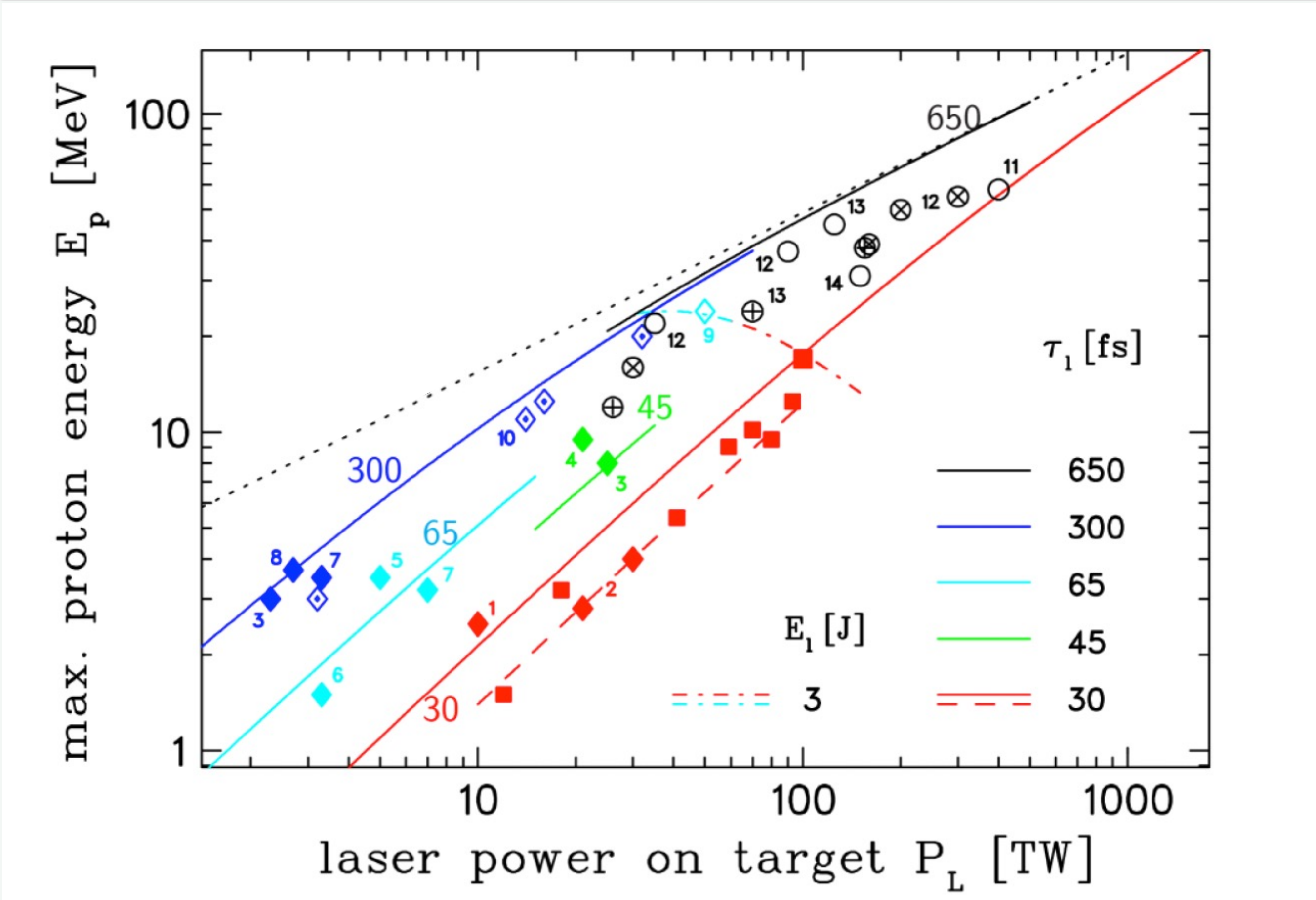

Back to the 2000

Lawrence Livermore Laboratory

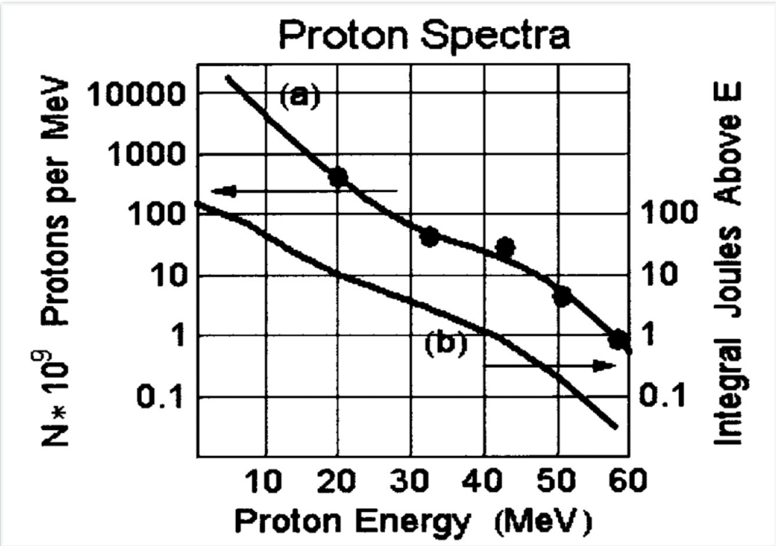

Snavely et al, *"Intense High-Energy Proton Beams from Petawatt-Laser Irradiation of Solids"* PRL, 85,2945 (2000)

Proton energy spectrum from the rear side of a 100 um solid target irradiated by a 423 J, **0.5 ps** pulse at normal incidence,
corresponding to an intensity of 3E20 W/cm2.

The integrated
energy of protons indicates a conversion efficiency of ’ 10% for protons above 10 MeV.

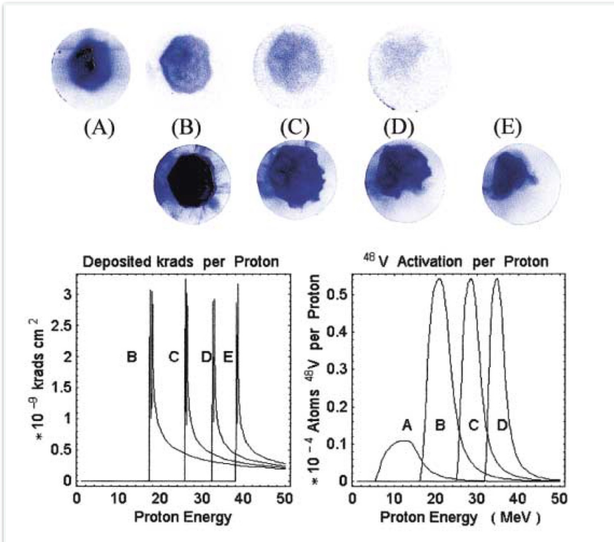

Characteristics of the laser-driven protons

Energy spectra

Boltzman-like (from zero to a given cut-off)

100% energy spread for a pure-TNSA

Selection procedures are adopted

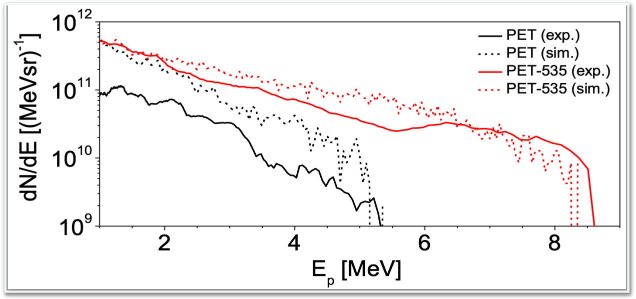

Angular divergency

30°/40° degree (FWHM)

Temporal features

10^8 - 10^9 selected 20 ns - 200 ns bunches

1 Hz - 10 Hz - …..

Proton energy scaling with short-pulse drivers

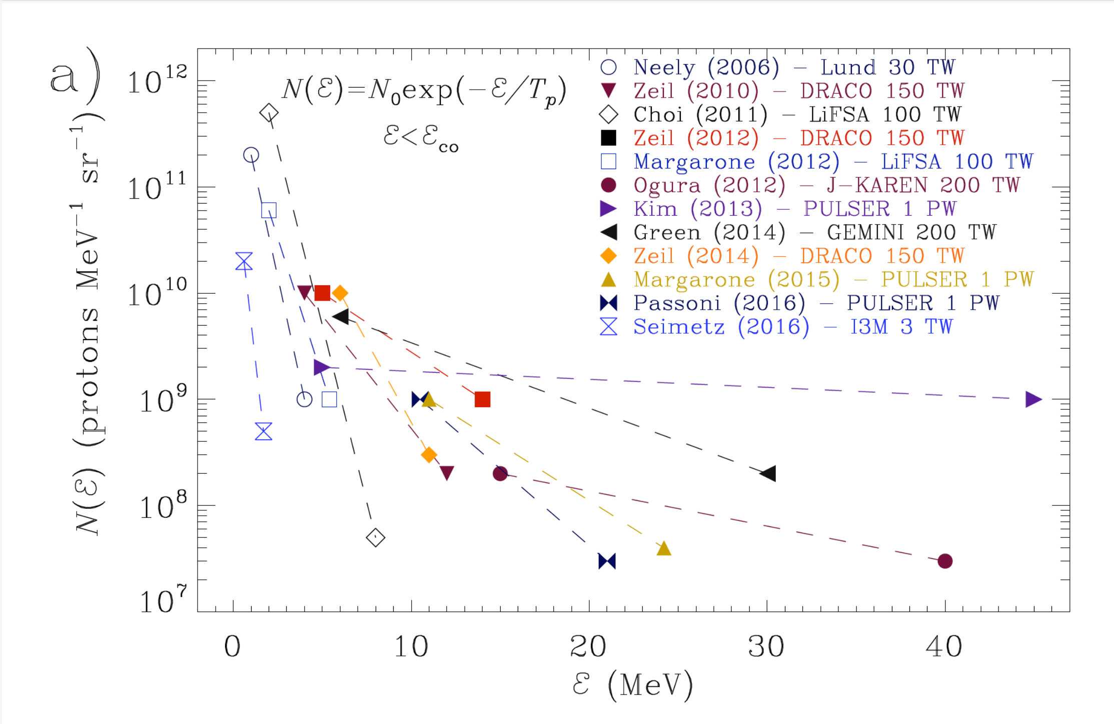

Proton energy spectra from experiments using high contrast, **sub-100 fs, sub-10 J laser** pulses and thin solid targets, shown as simple exponential interpolations (dashed lines) Np(E) = Np0 exp(–E/Tp) (with E ≤ Eco, the cut-off energy) of the high-energy tail of experimentally measured spectra.

Interaction enhancement

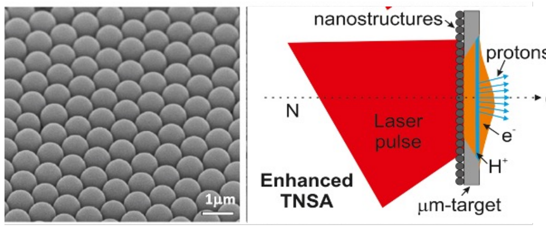

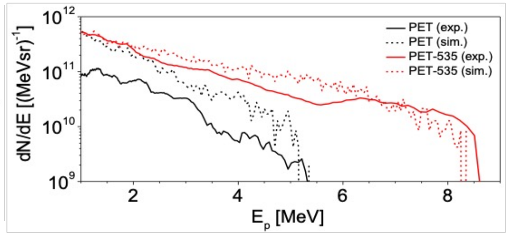

Margarone, PRL (2012)
Margarone, PRAB (2015)
Giuffrida, PRAB (2017)

Cryogenic hydrogen ribbon (ELISE)

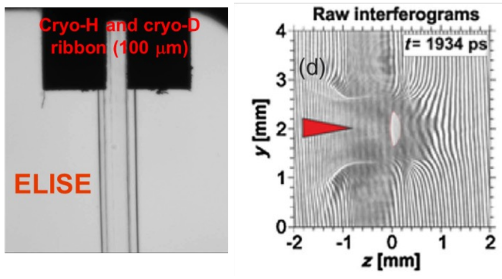

Garcia LPB (2014)
Margarone PRX (2016)

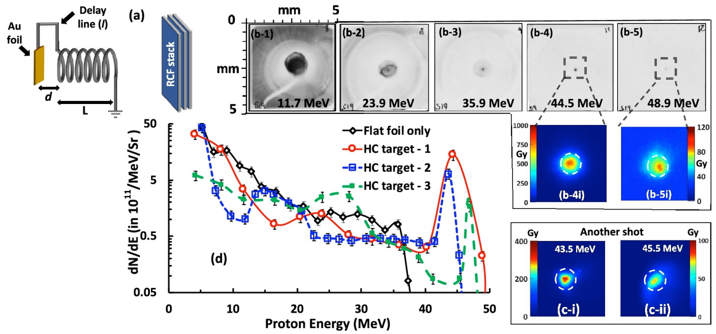

Curtesy of Prof Marco Borghesi

INFN
Istituto Nazionale di Fisica Nucleare

I-LUCE

Perspectives: Multidisciplinary applications of laser-driven ion sources

Word facilities

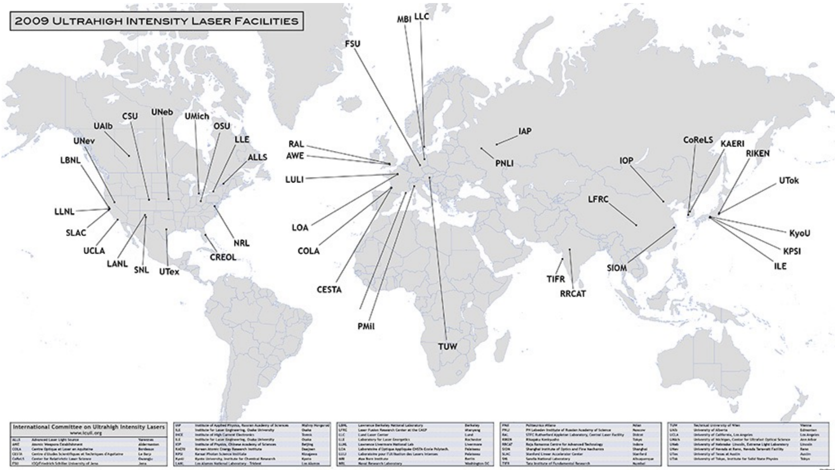

2009: 19 facilites

https://www.icuil.org/index.php

The International Committee on Ultra-High Intensity Lasers

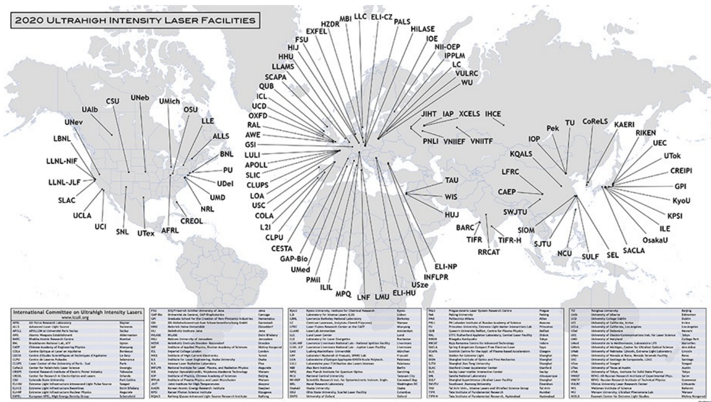

2020: 90 facilities

Pablo Cirrone, PhD - pablo.cirrone@lns.infn.it

Applications

- Diagnosis of intense interaction phenomena by **Proton Radiography**
- **Nuclear Reactions** initiated by Laser-Driven Ions (PET, fast and brilliant neutron source for radiography, ICF fast ignition with protons, proton-boron fusion, …)
- Studies of **ion stopping power** in plasmas
- Innovative approaches to **("FLASH") Radiobiology** and Hadrontherapy
- **Radiation chemistry** (pulsed radiolysis of water, management of nuclear wastes, medical therapy)
- **Mimicking space radiation** for testing electronics/detectors
- Archeology (PIXE, DPAA)

Proton radiography/deflectometry

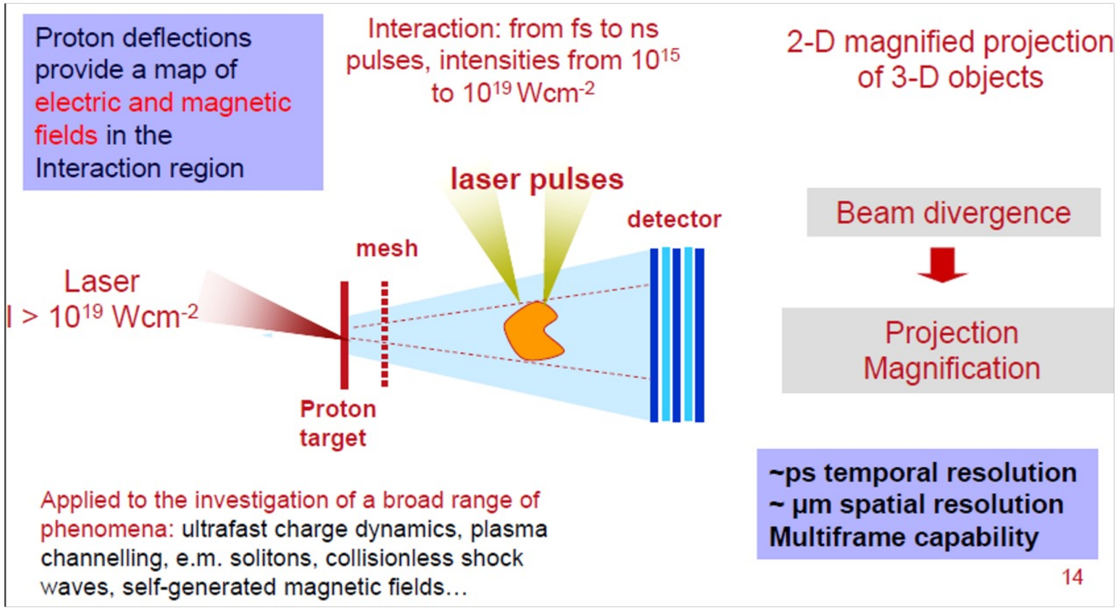

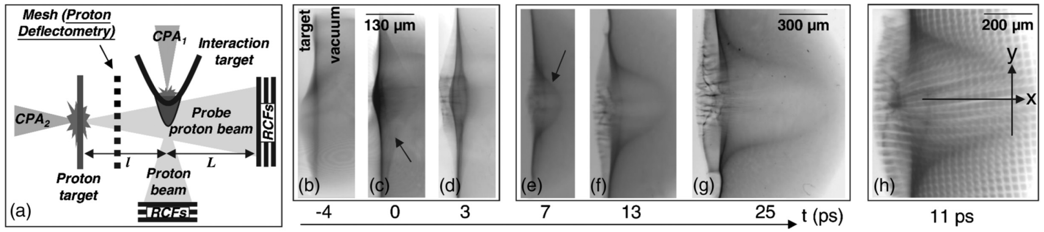

Curtesy of Prof Marco Borghesi (QUB)

FIG. 13. Proton probing of the expanding sheath at the rear surface of a laser-irradiated target. (a) Setup for the experiment. A proton beam is used as a transverse probe of the sheath. (b)–(g) Temporal series of images produced by the deflection of probe protons in the fields, in a time-of-flight arrangement. The probing times are relative to the peak of the interaction. (h) A deflectometry image where a mesh is placed between the probe and the sheath plasma for a quantitative measure of proton deflections. From Romagnani *et al.*, 2005.

Laser-based radiotherapy applications

Reduced cost/shielding

- Laser transport rather than ion transport *(vast reduction in radiation shielding)*
- Reduced size of gantry

Flexibility/modularity

- Controlling output energy and spectrum
- Possibility of varying accelerated species
- Spectral shaping for direct "painting" of tumor region *(no degrader needed)*

Novel therapeutic/diagnostic options

- Mixed fields: ions, X-rays, electrons, neutrons
- In-situ diagnosis (PET, X-rays)

Radiobiological advantages

- Short pulse radiation might reduce damage to healthy tissues
- Increase in RBE (relative biological effectiveness)?

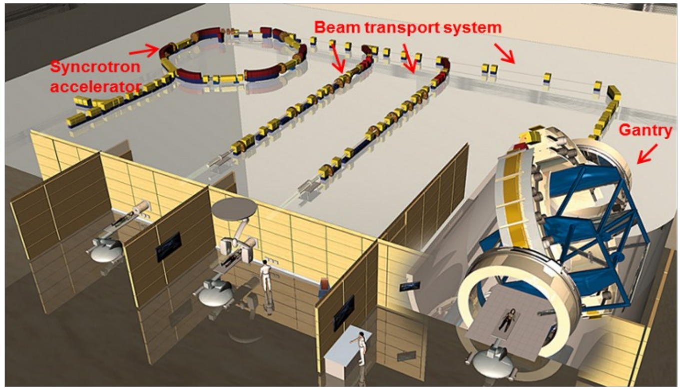

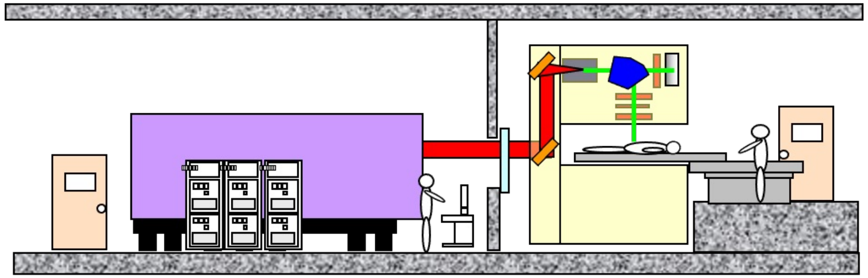

Radiobiology

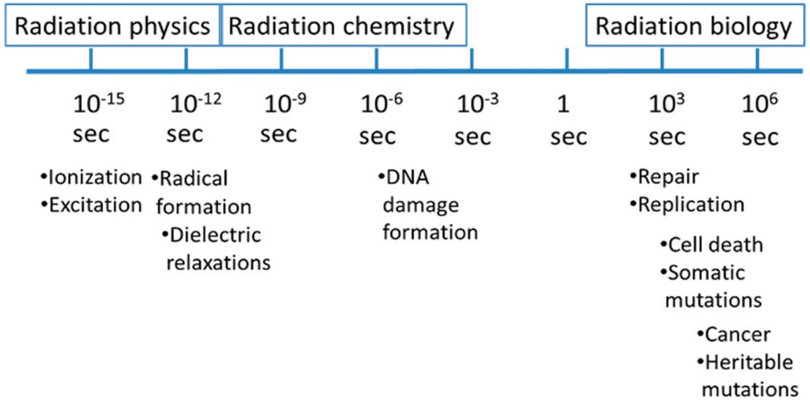

Remarks:

- ✓ Laser-driven ions are emitted at the source within a time ΔT< ps resulting in dose deposition in 100s ps - ns pulses
- ✓ **Dose rates > 10^9 Gy/s** can be achieved *(compared with Gy/min used in radiotherapy)*

Possible effects proposed in literature:

- **Spatio-temporal overlap of independent tracks** causing collective effects and enhancing LET (hence RBE)
- **Local depletion of oxygen** causing a reduction in cell radiosensitivity (healthy tissues)

Motivations:

- ➢ Development of a methodology and demonstration of viability at **ultra-high dose rate**
- ➢ Validation of laser-driven sources in view of future **therapeutic use**
- ➢ Provision of an alternative, flexible source for radiobiological studies

Radiobiology

K. Zeil et al., Appl. Phys. B (2013)

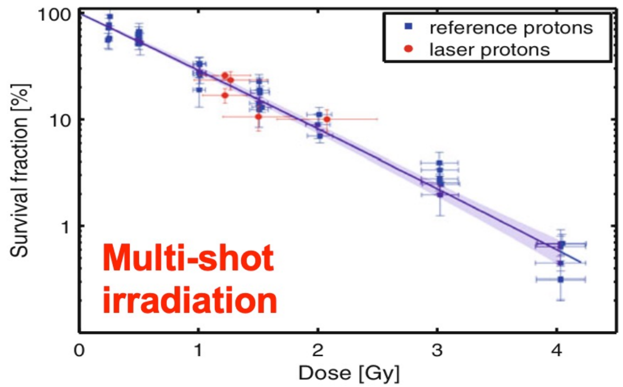

D. Doria et al., AIP Adv. 2 (2012) 011209

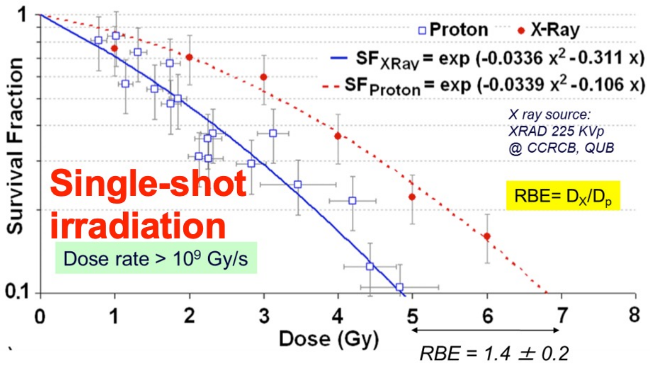

Recent results with C-ions *(courtesy of M. Borghesi)*

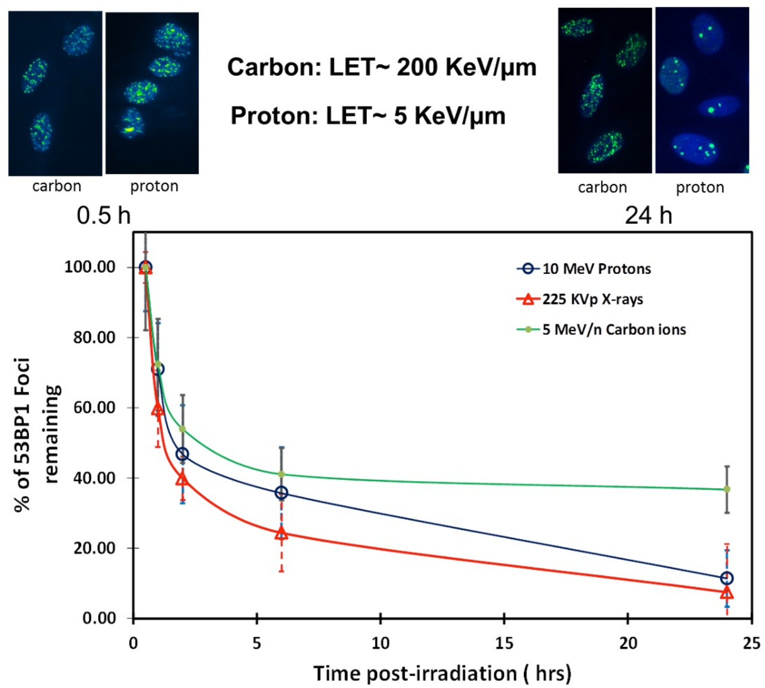

Pablo Cirrone, PhD - pablo.cirrone@lns.infn.it

Istituto Nazionale di Fisica Nucleare

Example of irradiation facilities

DRACO - Dresden (D)
ILIL - Pisa (I)
ELI-Beamlines, Dolnì Brezani (CZ)
I-LUCE facility, Catania (I)

What is done what is needed

Done

A beam sufficient energy

A beam with sufficient intensity

A reliable dosimetric diagnostic, while still room for improvement

What is needed

Increase the monochromaticity

Increase the **current** for **FLASH schemes** (do you know what is FLASH radiotherapy?)

A better control of the beam characteristics ==> **laser-target interaction level**

Stability and repeatability of the emitted particles

More **open access** facilities

Status of the art

30 MeV - 60 MeV proton beams

Focused and selected with electromagnets

Coil targets + quadrupoles and/or solenoids

Facility I: DRACO, Dresden (D)


ARTICLES
https://doi.org/10.1038/s41567-022-01520-3
nature physics
Check for updates

OPEN
Tumour irradiation in mice with a laser-accelerated proton beam

Florian Kroll[1], Florian-Emanuel Brack[1,2], Constantin Bernert[1,2], Stefan Bock[1], Elisabeth Bodenstein[3], Kerstin Brüchner[1,2,3], Thomas E. Cowan[1,2], Lennart Gaus[1,2], René Gebhardt[1], Uwe Helbig[1], Leonhard Karsch[1,3], Thomas Kluge[1], Stephan Kraft[1], Mechthild Krause[1,3,4,5,6,7], Elisabeth Lessmann[1], Umar Masood[1], Sebastian Meister[1], Josefine Metzkes-Ng[1], Alexej Nossula[1], Jörg Pawelke[1,3], Jens Pietzsch[1,2], Thomas Püschel[1], Marvin Reimold[1,2], Martin Rehwald[1,2], Christian Richter[1,3,4,5,6], Hans-Peter Schlenvoigt[1], Ulrich Schramm[1,2], Marvin E. P. Umlandt[1,2], Tim Ziegler[1,2], Karl Zeil[1] and Elke Beyreuther[1,3]

Nature Physics | VOL 18 | 316 March 2022 | 316–322 | www.nature.com/naturephysics

Helmholtz-Zentrum Dresden-Rossendorf D
18 J in 30 fs on the target.
Protons are emitted from plastic foils of ~220 nm thickness, cut-off energy of up to ~70 MeV.

ESA: Energy selection aperture: protons of higher energies have larger beam diameters because of the rising focal length of the solenoid lens with increasing particle energy

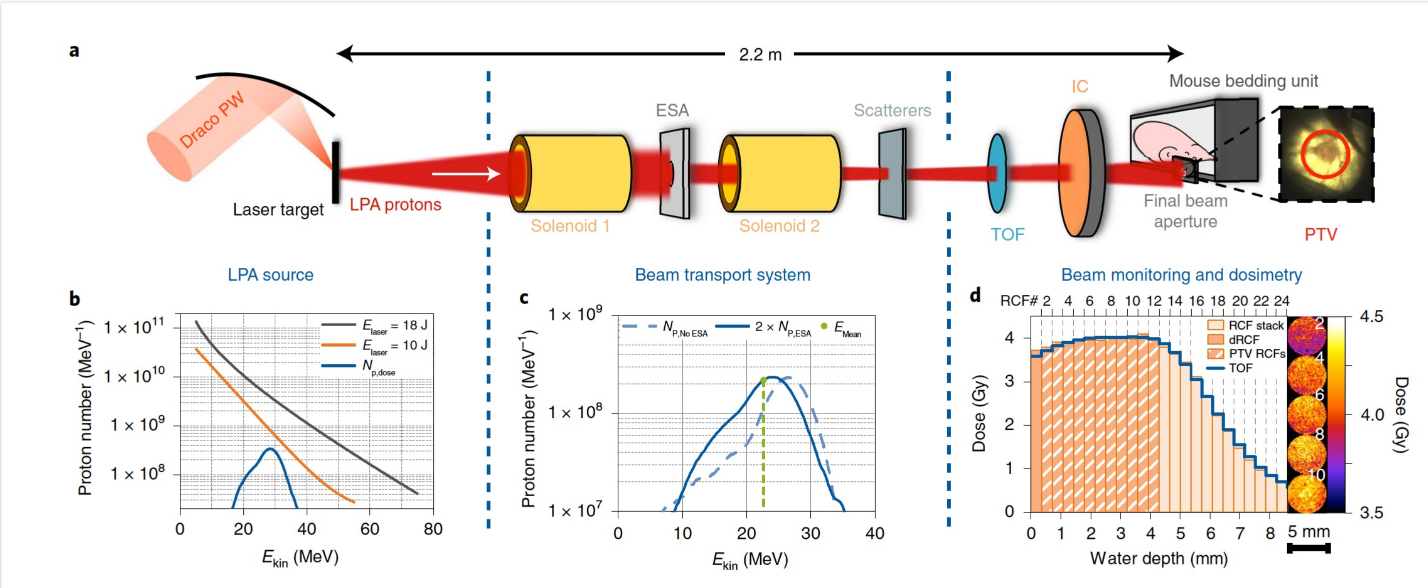

Pablo Cirrone, PhD - pablo.cirrone@lns.infn.it

Facility II: ILIL Pisa (I)

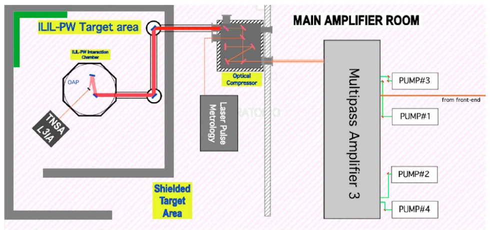

Figure 1. Schematic view of the ILIL-PW facility at INO, including the main amplifier room, the shielded target area, and the laser-driven light ions acceleration (L3IA) dedicated line. OAP: Off-Axis Parabolic.

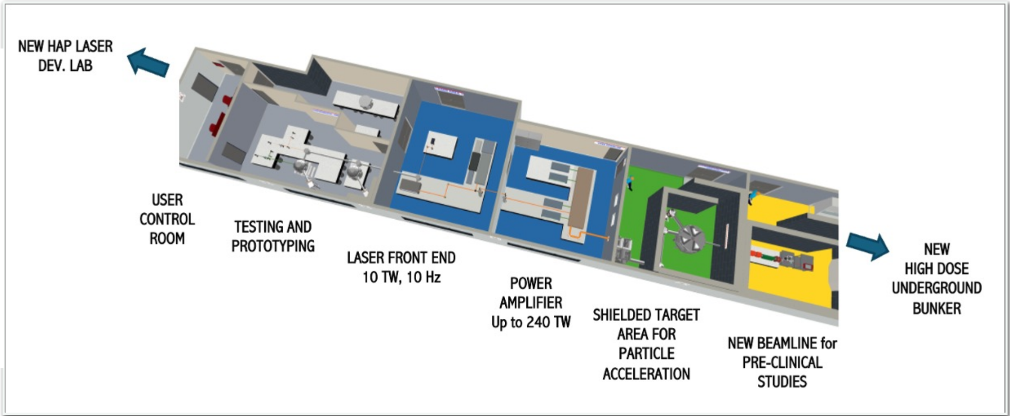

LASER CAPABILITIES:

- 240 TW, Ti:Sa, up to 5 Hz, 27 fs;
- 1kHz, >20 mJ, Ti:Sa + OPA
- 100 Hz, >1J, TiSA (procurement in progress)

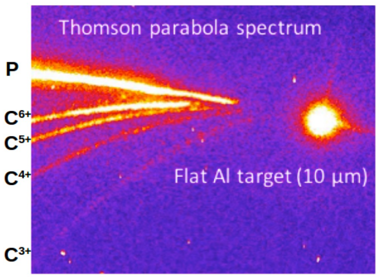

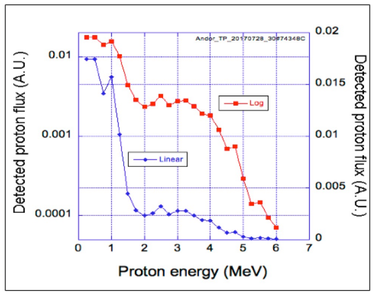

ELSEVIER

Nuclear Instruments and Methods in Physics Research Section A: Accelerators, Spectrometers, Detectors and Associated Equipment

Volume 909, 12 November 2018, Pages 160-163

Light Ion Accelerating Line (L3IA): Test experiment at ILIL-PW

L.A. Gizzi [a b], F. Baffigi [a], F. Brandi [a], G. Bussolino [a b], G. Cristoforetti [a], A. Fazzi [c], L. Fulgentini [a], D. Giove [d], P. Koester [a], L. Labate [a b], G. Maero [e], D. Palla [a], M. Romé [e], P. Tomassini [a]

Facility II: ILIL Pisa (I)

Intense Laser Irradiation Laboratory, CNR (I)
https://ilil.ino.cnr.it/
400 mJ/30 fs/14 TW Ti:Sa Laser
7-8*10^{19} W/cm^2
cut-off energy of up to ~3.5 MeV.

applied sciences
MDPI

Article

A Few MeV Laser-Plasma Accelerated Proton Beam in Air Collimated Using Compact Permanent Quadrupole Magnets

Fernando Brandi [1,*], Luca Labate [1,2,*], Daniele Palla [1,†], Sanjeev Kumar [1,†,‡], Lorenzo Fulgentini [1], Petra Koester [1], Federica Baffigi [1], Massimo Chiari [3], Daniele Panetta [4] and Leonida Antonio Gizzi [1,2]

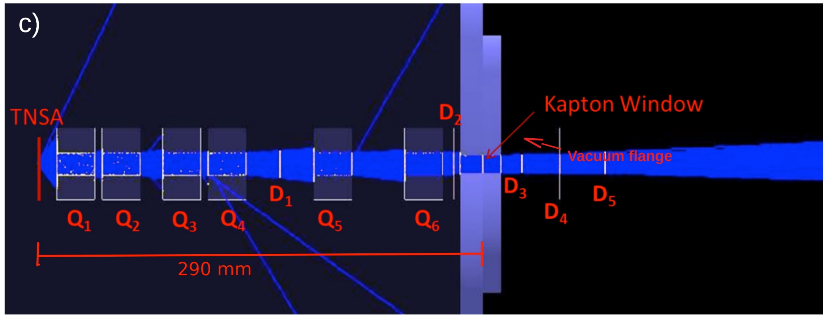

Six permanent magnets quadrupoles

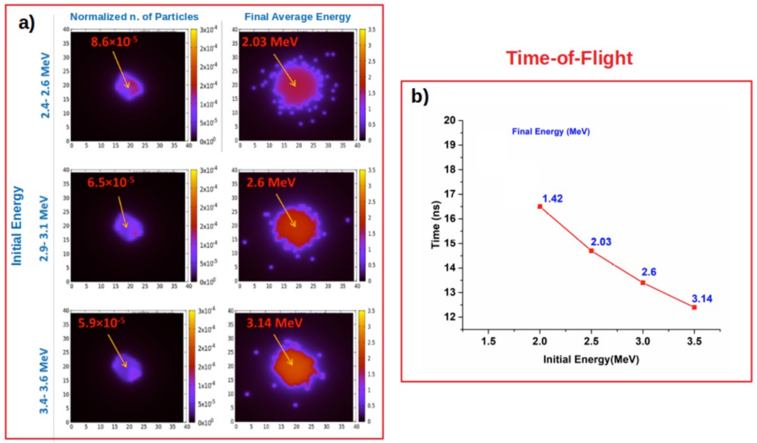

Figure 2. Proton beam characteristics at 1 cm after Kapton windows. (**a**) Proton particles distribution and final energy at various initial energy ranges calculated over an area of 40 mm × 40 mm centred on the MBL axis at position (20 mm, 20 mm); the highlighted numbers represents the values on the MBL axis; (**b**) graph of the ToF as function of the initial proton energy, with final energy also indicated.

Facility III: ELIMED at ELI-Beamlines, Dolnì Brezanì (CZ)

D Margarone, GAP Cirrone,
"ELIMAIA: A Laser-Driven Ion Accelerator for Multidisciplinary Applications", Quantum Beam Sci. 2 (2018) 8

ELIMAIA experimental area
30J / 30fs
Protons are emitted from metallic/plastic foils um thickness
cut-off energy of up to ~40 MeV.

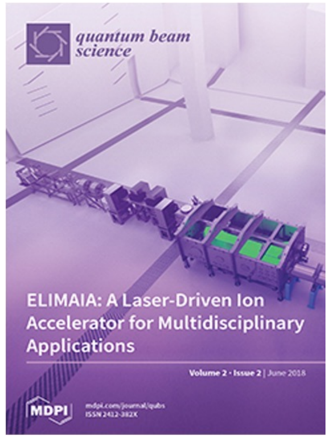

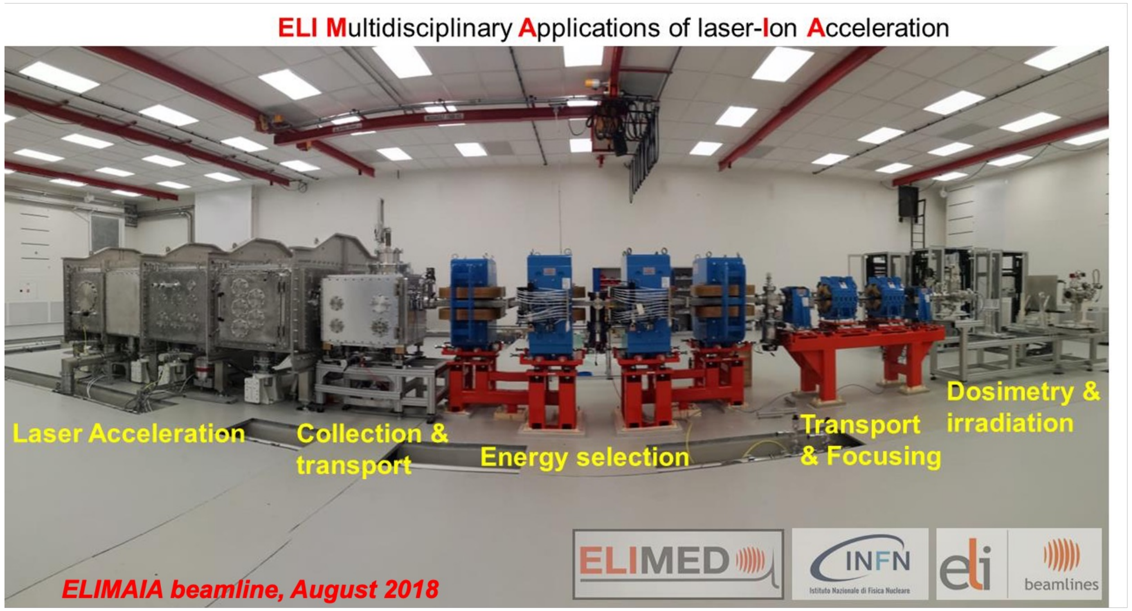

Curtesy of Dr Daniele Margarone and Lorenzo Giuffrida (ELI-Beamlines (CZ)

Facility III: ELIMED at ELI-Beamlines, Dolnì Brezanì (CZ)

Curtesy of Dr Daniele Margarone and Lorenzo Giuffrida (ELI-Beamlines (CZ)

ELIMAIA commissioning started!

L3-HAPLS laser system @ ELIMAIA	
Energy	10 J
Laser spot	~2*2 μm
Pulse duration	<30 fs
Laser intensity	>>2e21 W/cm^2

Pointing stability

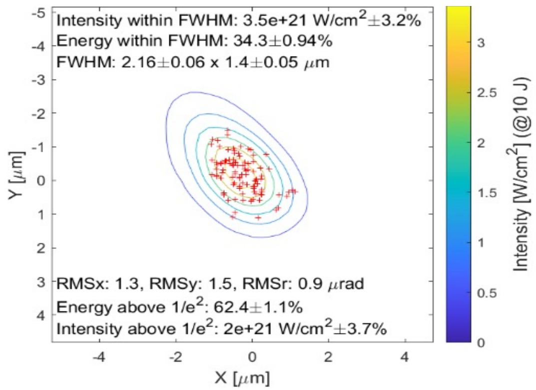

TP raw data

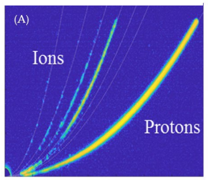

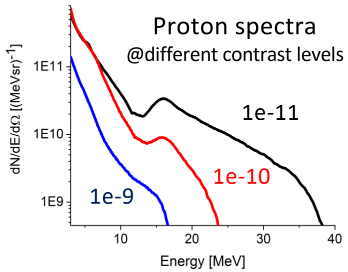

TOF spectrum

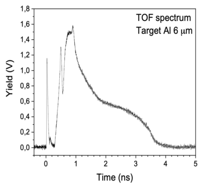

Main proton beam features

- Max proton energy ~40 MeV
- Flux above 3 MeV: 8.5e11 /sr
- Flux at 15 MeV (+/- 5%): 2.7e10 /sr
- Flux at 25 MeV (+/- 5%): 9.3e9 /sr

Basic commissioning	Fluctuation of the main experimental parameters	
Fluctuations	Single shot series	
Laser energy	0.3%	9.95±0.025 J
Laser intensity @FWHM	0.8%	(1.39±0.01)*10^{21} W/cm^2
Thot	3.96%	3.057±0.121 MeV
Photon flux	1%	
EpMAX	1.2%	14.48±0.17 MeV
Proton flux >3 MeV	5.3%	6.0710^{10}±0.3210^{9} sr-1
Pointing Stability	<<2,7 μrad	(RMS

Facility III: ELIMED at ELI-Beamlines, Dolnì Brezanì (CZ)

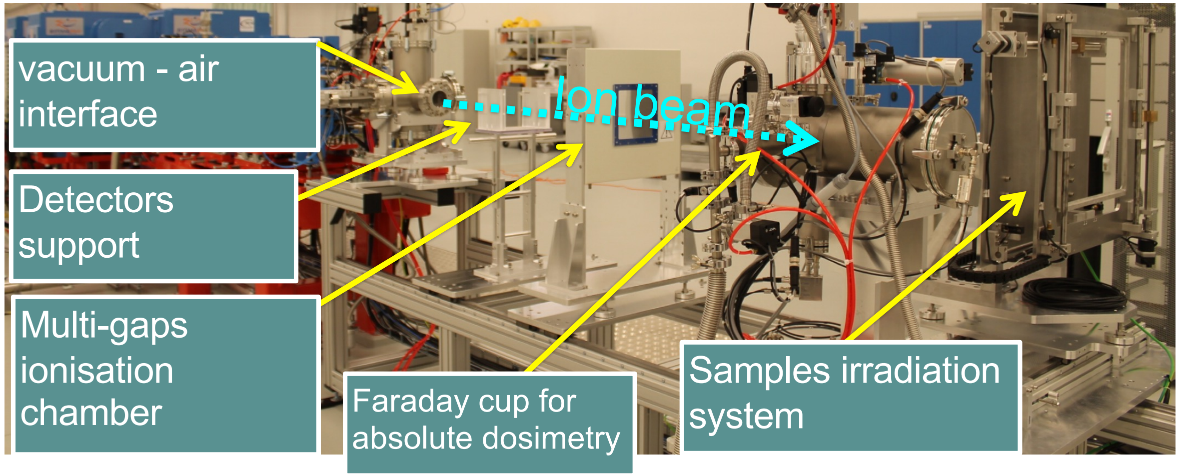

NOTE: the beam have to be transported in air for the majority of the applications !

Curtesy of Dr Daniele Margarone and Lorenzo Giuffrida (ELI-Beamlines (CZ)

Facility IV: I-LUCE, Catania (I)

Two laser lines

45 TW, >1J/<24fs/10Hz $7*10^{19}$ W/cm^2

320 TW, >7J/<24fs/1Hz $1*10^{21}$ W/cm^2

Protons, Ions, electron accelerations

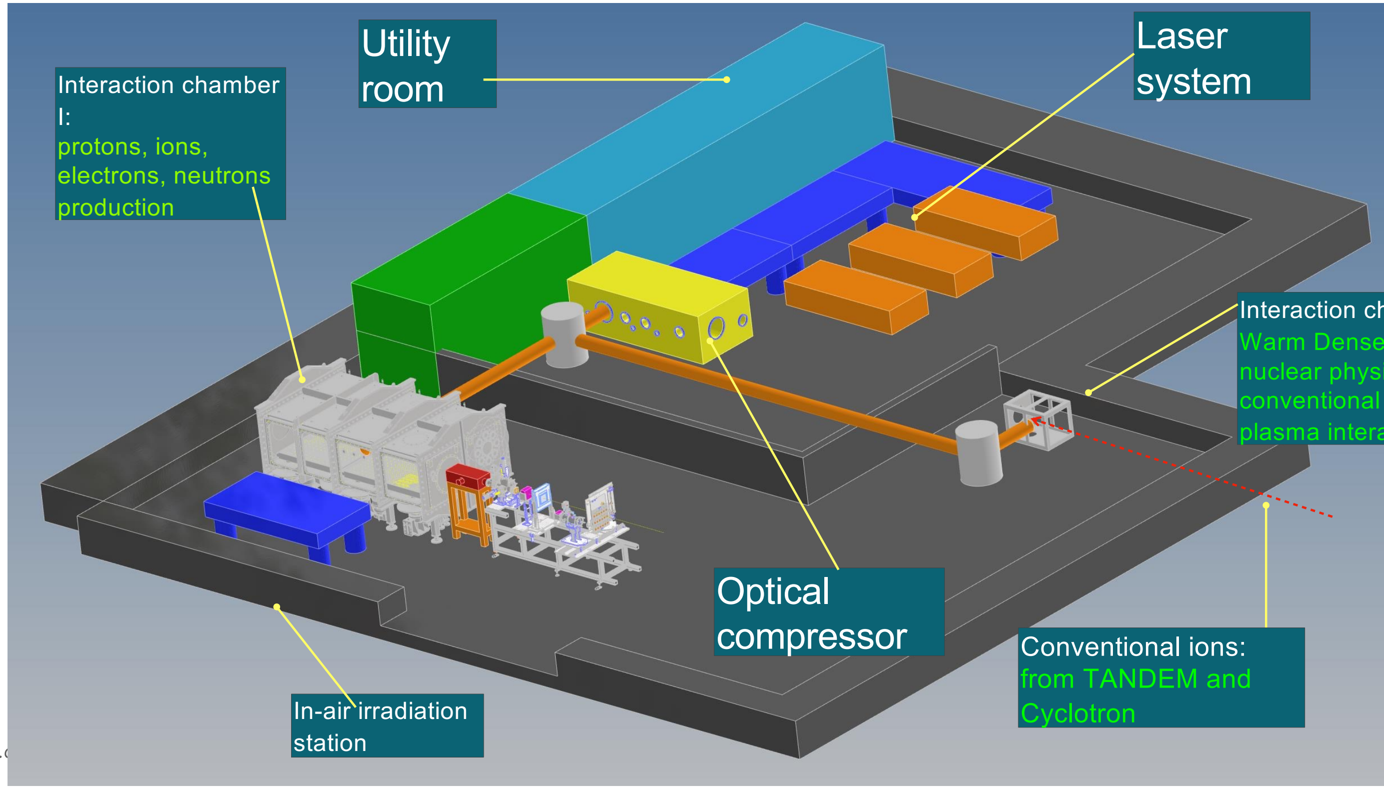

Laserlab

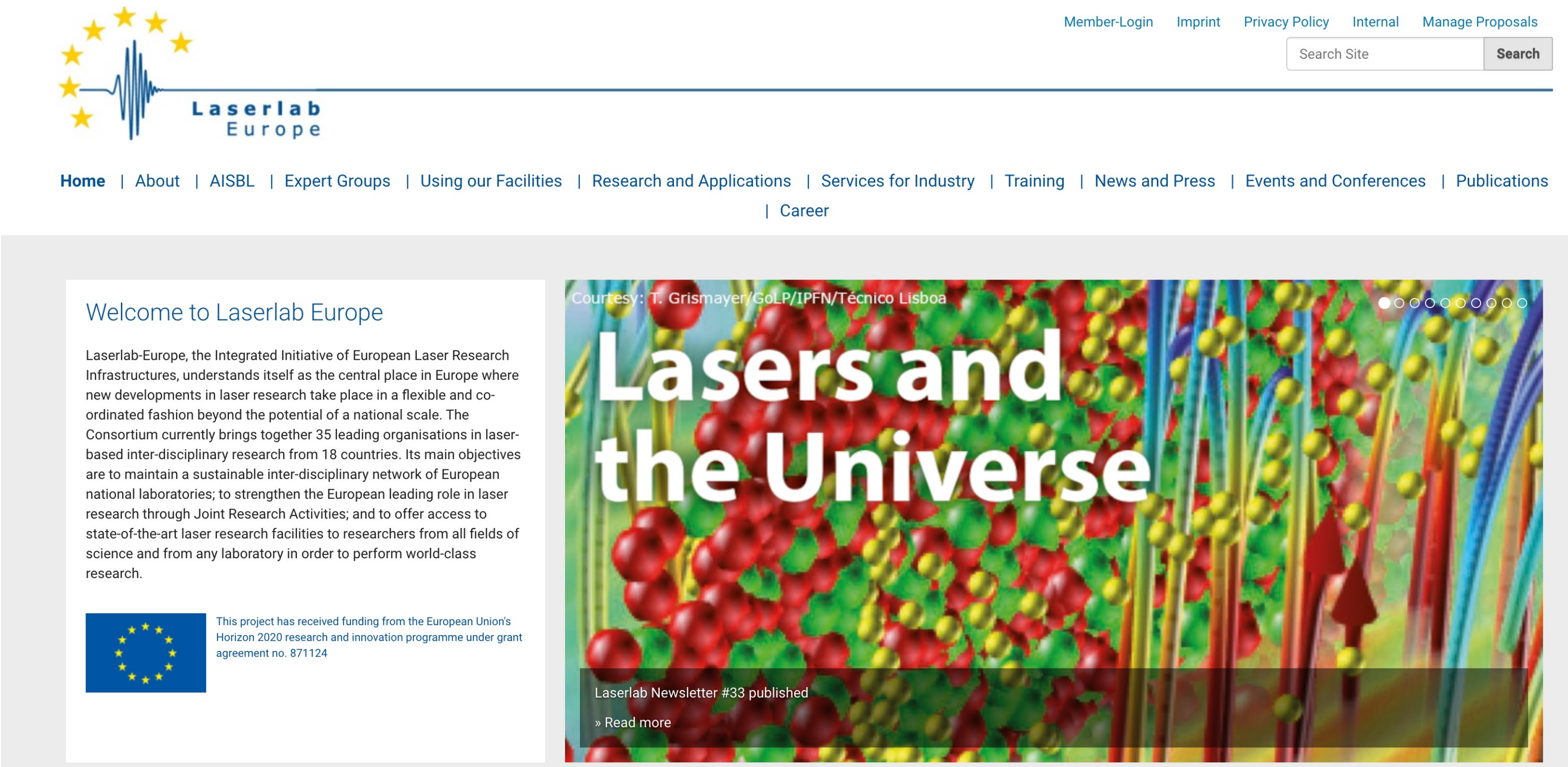

Open access beam in different facilities around the world

Thanks for listening

The role of the target thickness

The laser penetration depends also on the **target thickness**

when it becomes close or small then one wavelength

It exist a relation between the target thickness and the laser amplitude **for which we can reach the transparency** threshold:

$$a_0 = \pi \frac{n_e}{n_l} \frac{l}{\lambda} \equiv \xi$$

l is the target thickness

The hot electrons: heating models

The most famous is the **capacitor model**

In this model, electrons are dragged out of the surface of a perfect conductor by an oscillating ''capacitor field,'' **extending on the vacuum side**

Electrons are considered to be ''absorbed'' when after having performed about half of an oscillation on the vacuum side, they reenter the target, there delivering their energy, which is of the order of the oscillation energy in the external field.

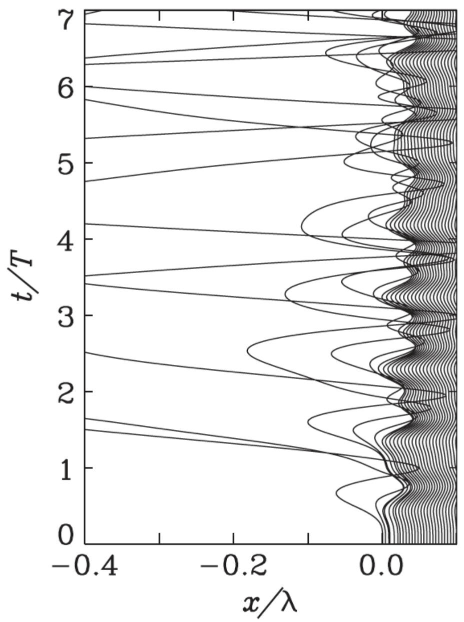

$$\frac{d^2\xi}{dt^2} = \begin{cases} -\omega_p^2\xi - eE_d/m_e & (x_0 + \xi > 0), \\ +\omega_p^2 x_0 - eE_d/m_e & (x_0 + \xi < 0). \end{cases}$$

Hot electrons transport in solid matter

Different effects occurs:

The large current generated is locally neutralised by a **return current**

This return current comes from both the free conduction electrons in the metals or produced by field and collisional ionization in insulators

Filamentation instabilities and **dependence on the target material** have also been extensively studied

Finally, it is noticeable that at least a fraction of hot electrons propagates coherently through the target **conserving the temporal periodicity of the driving force**

Ion acceleration mechanisms

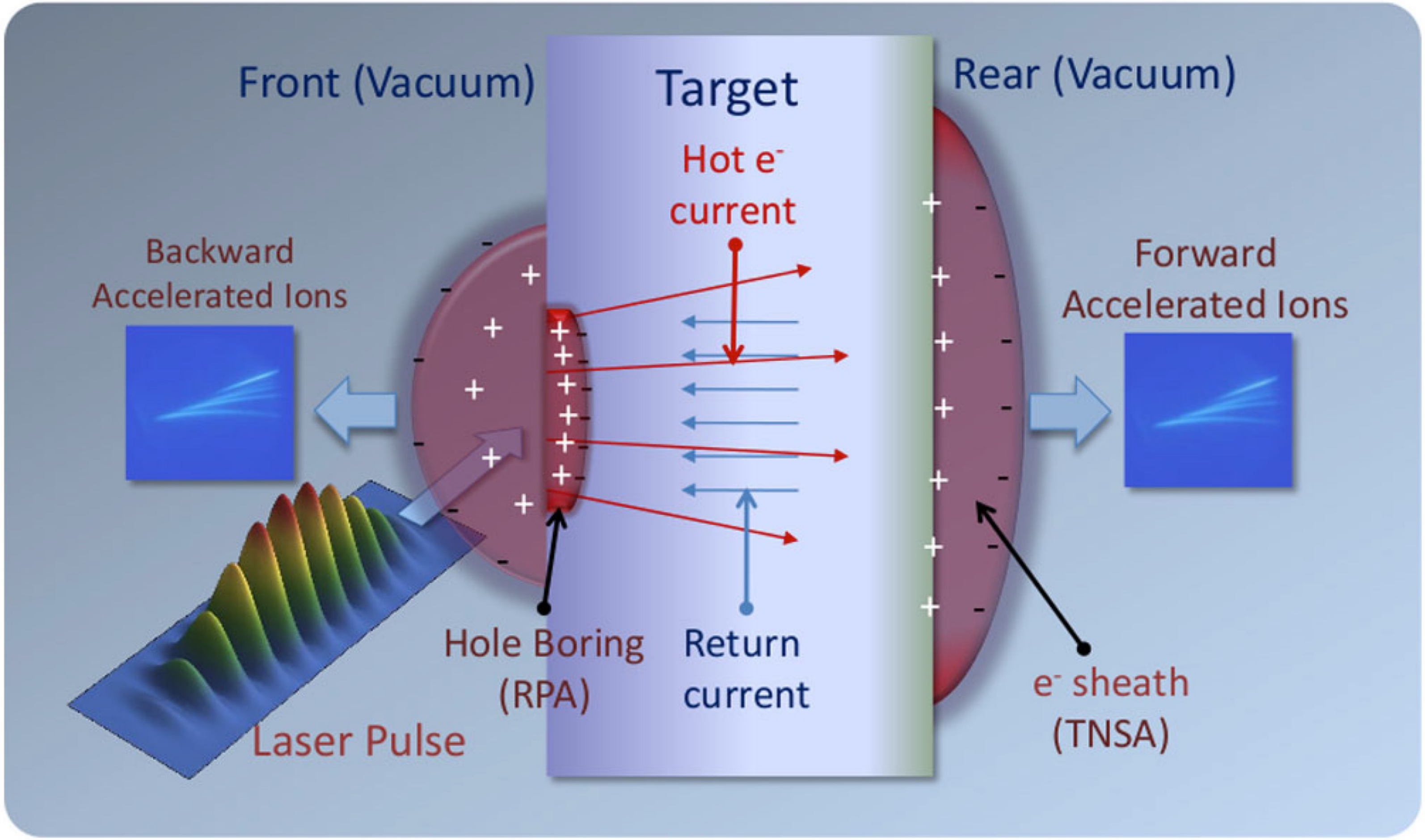

Ion acceleration mechanisms

There are different acceleration mechanisms

They can occur in different target regions

Rear surface acceleration

Front surface acceleration

TNSA (Target Normal Sheet Acceleration) and RPA (Radiation Pressure Acceleration)

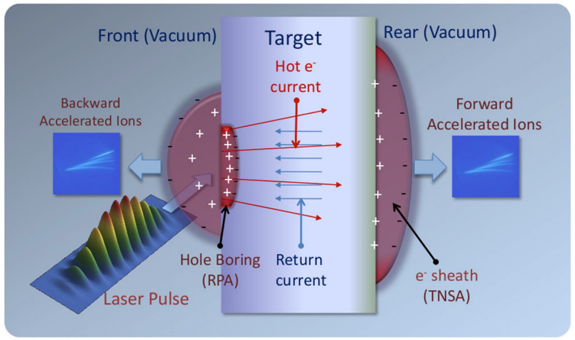

Rear surface acceleration

Hot electrons generated on the front side reaches the rear side

These hot electrons attempt to escape in vacuum and the charge unbalance create a sheath field Es normal to the rear surface

$$eE_s \sim \frac{T_h}{L_s}$$

Higher is the electron temperature higher is the electric field

Higher is the sheath distance lower is the electric field

Ls is may be roughy estimated as the Debye length of the hot electrons

Debye length and acceleration effects

You already know what a Debye length is?

Electric fields cannot penetrate a magnetic one in a charged "solution" (a plasma) as …

charges produce a screening ==> this screening length is the Debye distance

Typical values

$I \cdot \lambda^2 = 10^{20} W/cm^{-2} \mu m^2$

T_h = 2.6 MeV

n_h = 8 10^{20} cm^{-3}

$\lambda_D = 4.2 \cdot 10^{-5} cm$

$E_s \sim 6 \cdot 10^{10} V cm^{-1}$

This large field will backhold most of the escaping electrons, ionize atoms at the rear surface, and start to accelerate ions.

Debye length and acceleration effects

The energy acquired by a test-ion crossing the sheath is

$$\epsilon_i = ZeE_sL_s = ZT_h$$

==> ions reach MeV scale energy

TNSA modelling

Is described by a relatively simple system of equations that can be investigated analytically and numerically

We alway assume an **electrostatic approximation**, so that the electric field is

$E = -\nabla\phi;$

$\nabla^2\phi = 4\pi e(n_e - \sum_j Z_j n_j)$

with the sum running over each species of ions, having density n_j and charge Z_j.

As a consequence of the laser-solid interaction, the electron density n_e may be described as composed of at least two qualitatively distinct populations, which will be labeled **cold and hot**

TNSA modelling

The electron density in the interaction is then divided in:

$n_e = n_c + n_h$

Thermal moments are neglected for the cold population

while density for the hot component is given by a one-temperature Boltzmann distribution

$n_h = n_0 e^{e\phi/T_h}$

This formulation is good when we have only to take into account the presence of self-consistent sheath field

In more complex scenarios, the electron dynamics shall be included via either **fluid** or **kinetic** equations.

TNSA modelling

Considering this two main categories of TNSA models are developed

The **static (or quasi-static) models** in which it is assumed that the light ions, or at least the most energetic ones, are accelerated in the early stage of the formation of the sheath, so that the latter may be assumed as stationary.

The **dynamic model** where the system is described as a neutral plasma in which the ions acquire kinetic energy in the course of the sheath evolution

The last case is connected to the classical problem of the plasma expansion in vacuum

Multi MeV ions acceleration from the "rear" of thin foils was studied from 2000

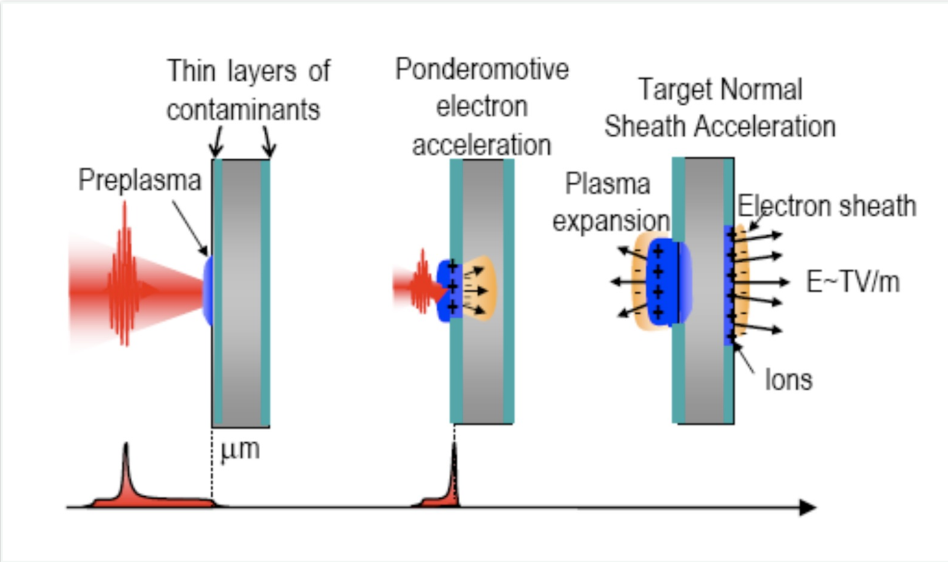

Intensities rising above E19 W/cm^2 – **electron acceleration to MeV energies**

Thin foils allow electrons to reach the rear of the target and **establish a field**.

Protons (from contaminants) **have beam features** contrary to lower energy, isotropic emission previously observed from the front.

Clark et al, "***Measurements of Energetic Proton Transport through Magnetized Plasma from Intense Laser Interactions with Solids***" PRL, 84 ,670 (2000)

Snavely et al, "***Intense High-Energy Proton Beams from Petawatt-Laser Irradiation of Solids***" PRL, 85,2945 (2000)

Maksimchuk et al, "***Forward Ion Acceleration in Thin Films Driven by a High-Intensity Laser***" PRL, 84, 4108 (2000)

Complex acceleration scenario

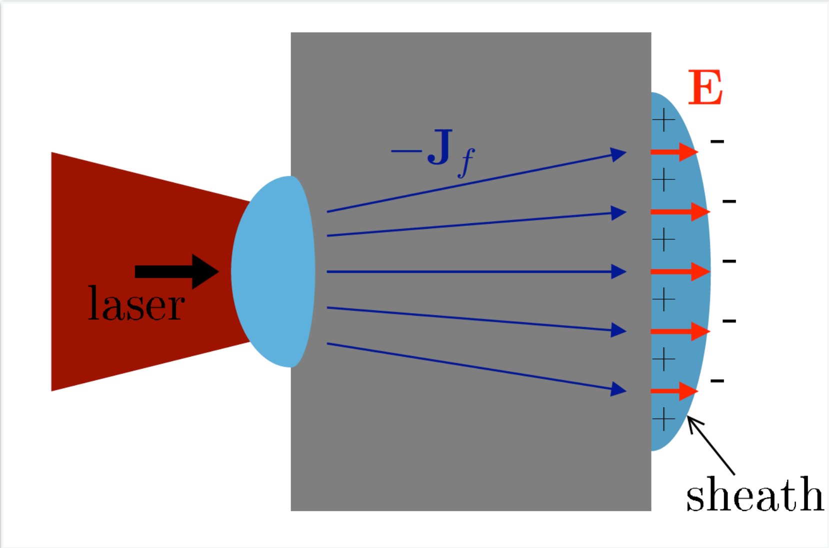

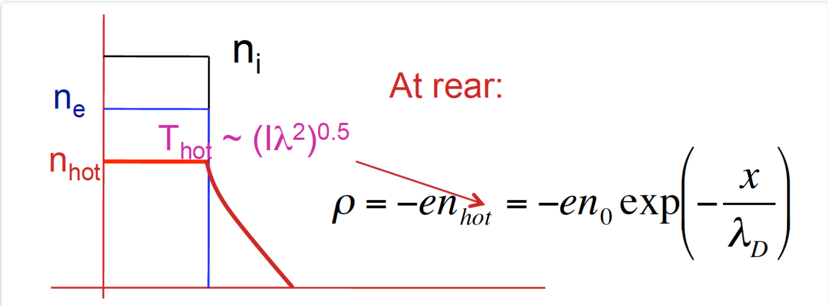

Laser pulse intense enough to ionise matter and couples with the fare electrons which **absorb energy** and **momentum**

1. **Heating of electrons** ==> "sheath" region where electrons and ions are accelerated
2. **Momentum absorption due to the ponderomotive force** (is the local flow of the electromagnetic momentum) ==> radiation pressure on plasma

Target transparency for the e.m. wave occurs when plasma density becomes lower the critical density

$$n_c = n_c(\omega_L) = \frac{m_e \omega_L^2}{4\pi e^2}$$

$n_e > n_c$ ==> Plasma opacity (or overdense)

$n_e < n_c$ ==> Plasma transparence

Complex acceleration scenario

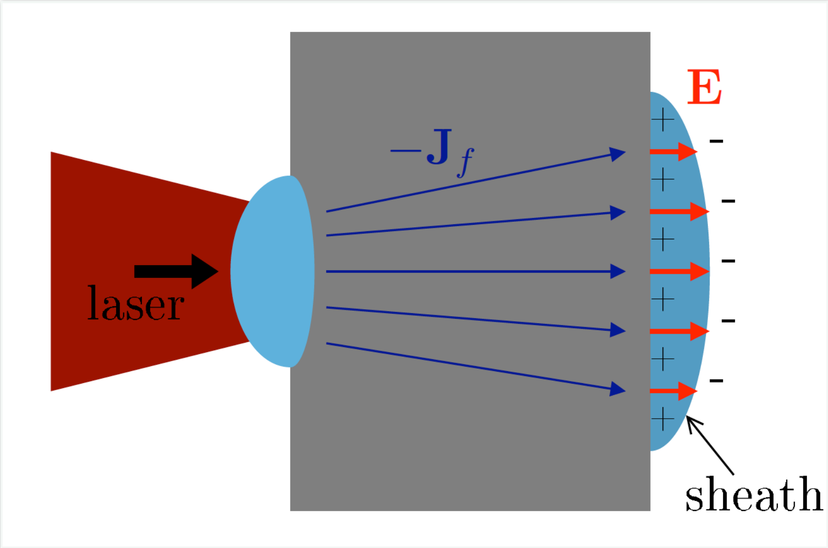

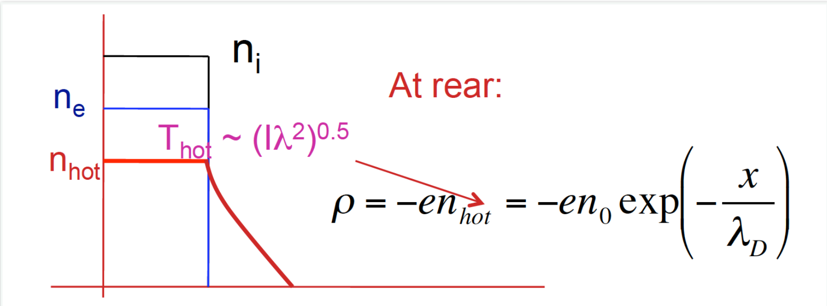

$$E(0) = \frac{KT_h}{e\lambda_D} = \sqrt{\frac{n_h KT_h}{\varepsilon_0}}$$

Typical values are:

$\lambda_D \sim 1\ \mu m$

$T_h \sim$ MeV

$$E(0) = \frac{10^6 V}{10^{-6} m} \sim TV/m$$

Complex acceleration scenario: role of the hot electrons

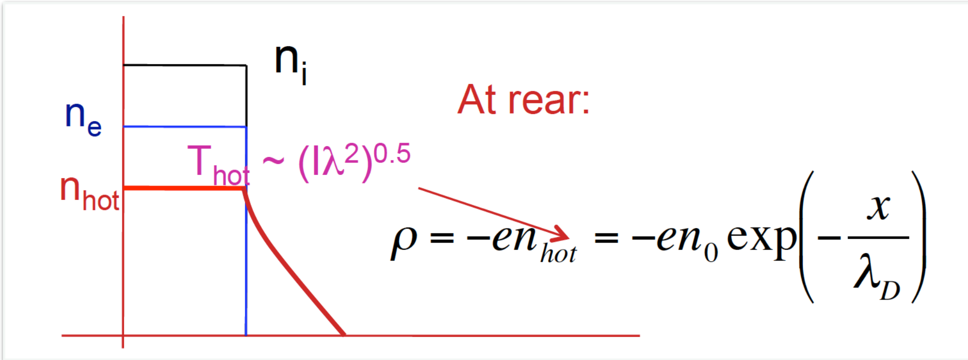

Hot electron temperature as a function of irradiance from experiments of sub-ps laser-solid interaction.

The lines give scaling laws derived from different models

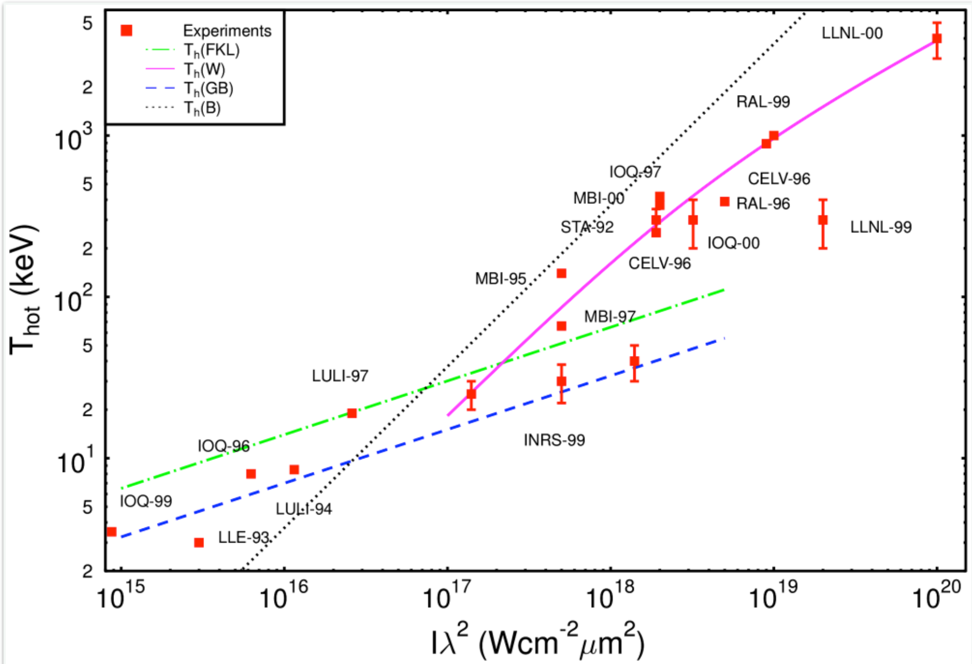

Gibbon, P., 2005b
Short Pulse Laser Interaction with Matter
(Imperial College Press, London)

On the theoretical side

The interpretation of experiments has revitalized classic and often controversial problems of plasma physics:

- plasma expansion into vacuum
- formation of collisionless sheaths
- motion of relativistic moving mirrors, a concept already discussed in the original work on special relativity by Einstein (1905) (used for the RPA description)

Einstein, A., 1905, Ann. Phys. (Berlin) 322, 891.

Even if we try to develop simple models a rich and complex dynamics of laser-plasma interaction and ion acceleration, involving **collective and self-organization effects**, is evident.

Unfolding such dynamics requires the use of self-consistent electromagnetic (EM), kinetic simulations. To this aim, the particle-in-cell (PIC) method.

Ion acceleration

Relativistic effects produce an **increase of the cutoff density** ==> the critical density is closer to that of a solid:

Relativistic self-induced transparency reduces the plasma mirroring effects

However laser-plasma interaction mechanisms are complicated by many phenomena:

— nonlinearity in the wave equations

— modification of the plasma density profile due to the **radiation pressure** that are described via the **ponderometive force**

The basic ingredients

An high power (TW)

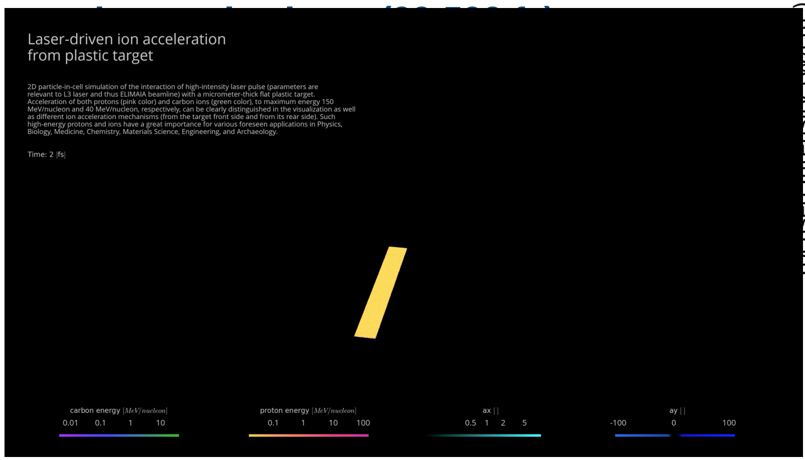

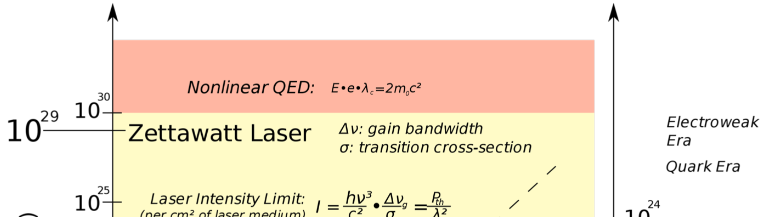

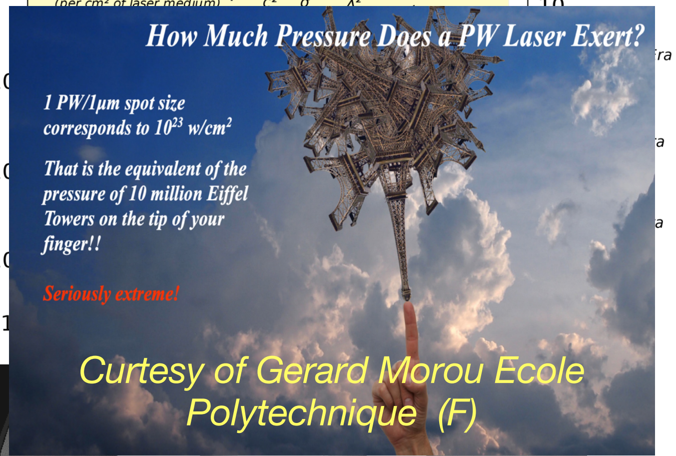

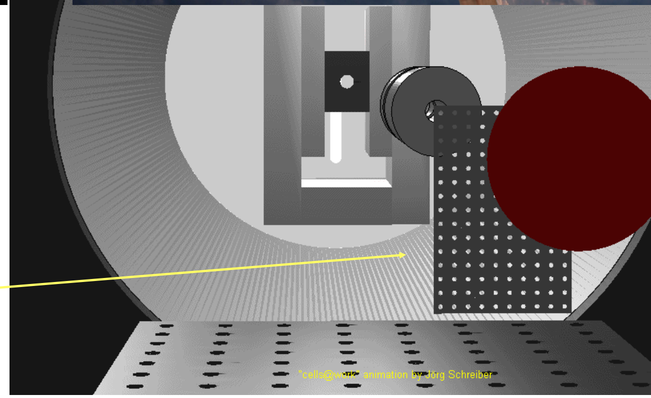

A target (usually a solid target)
um - nm range

Ingredients

TW/PW class lasers

- Usually Ti:sa
- mJ - tens of J
- 20 fs to 30 fs
- Good profile
- Good contrast

Focused on a target

- Usually solid/

The process occurs in vacuum

Brutal forces and less elegant then laser Wakefield

Based on "charge separation"

$$T_{\mathrm{hot}} \approx U_{\mathrm{pond}} \approx 1\ \mathrm{MeV} \times (I\lambda^2/10^{19}\ \mathrm{W}\cdot\ \mu\mathrm{m}^2/\mathrm{cm}^2)^{1/2}$$

Laser-plama Ion acceleration: a compact solution

Conventional ion acceleration

LHC @ CERN
- circular tunnel (27 km long!!!)
- superconductive electromagnets
- proton energy (per beam): 6.5 TeV

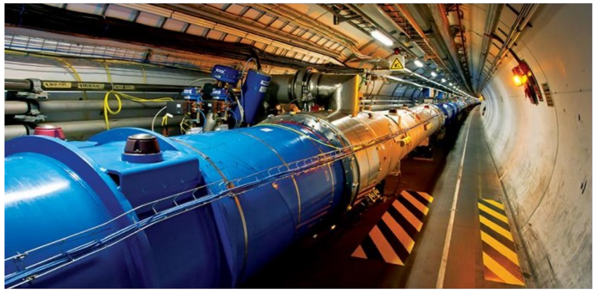

E-field $_{max}$ ≈ few 10 M V /meter (Breakdown)

Laser-plasma acceleration

No breakdown limit
10 - 100 GV/m

0.1-10 υm

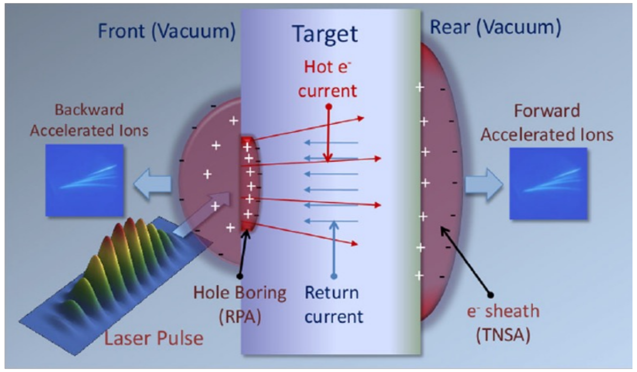

The energy gain for ions in a laser-plasma accelerator is of several tens of MeV/mm (just few tens of MeV/m in conventional accelerators due to breakdown effects)

Financial support

EuAPS

Roma TV, LNF, Pisa CNR, LNS
15 M€

EuPRAXIA

7.9 M€ WP3 High-Power lasers

Infrastructure

Laser system and interaction chambers

Electrons and ion acceleration

GAP Cirrone

S Tudisco

0.8 M€

Demonstration of a micro-acceleration system for laser-driven proton beams

Anthem

Advanced technologies for Human Centred Medicine

23 Istituti; Spoke 4: Caserta, Pavia, INFN

1.3 M€

GAP Cirrone, G Cuttone

Electron acceleration for conventional and ultra high dose rate beams nell'accelerazione di elettroni e UHDR

BCT

Breast Cancer Therapy

2.0 M€

G Cuttone, GAP Cirrone

Ottimizzazione nella selezione di fasci di protoni per applicazioni mediche

See talks by Giacomo Cuttone

I-LUCE layout

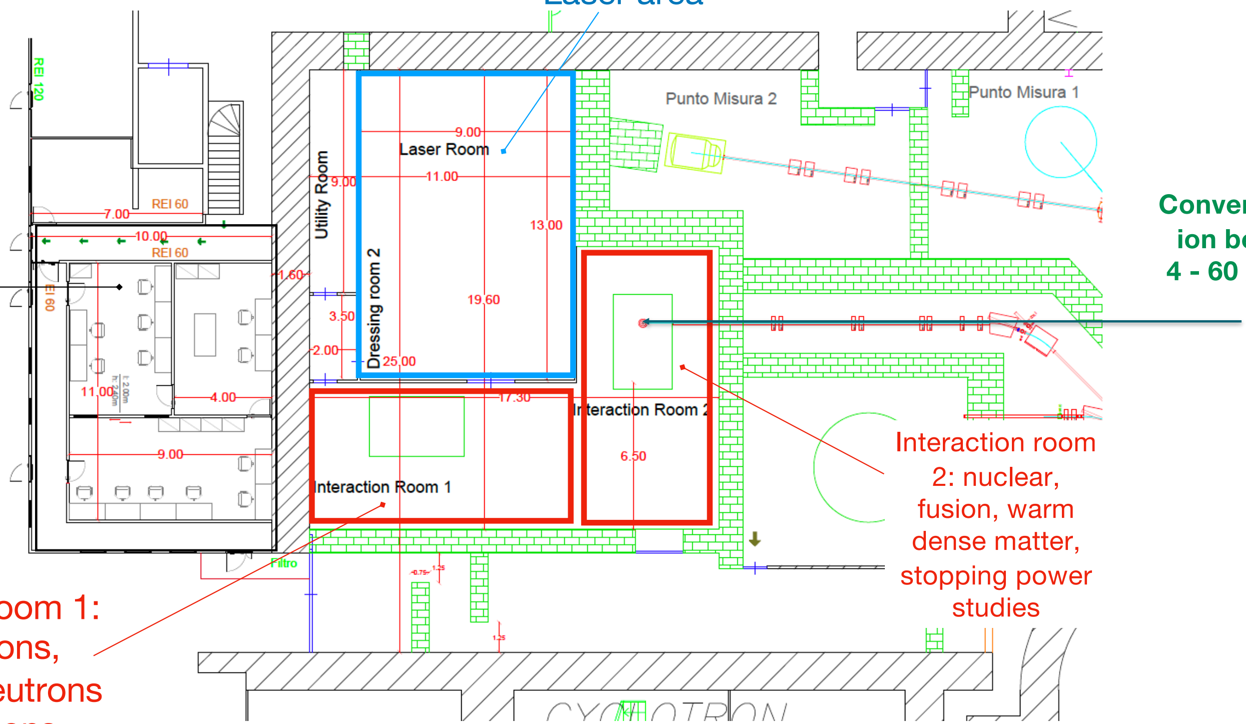

Control and Users' area

Conventional ion beams 4 - 60 AMeV

Interaction room 2: nuclear, fusion, warm dense matter, stopping power studies

Interaction room 1: protons, ions, electrons, neutrons accelerations

I-LUCE

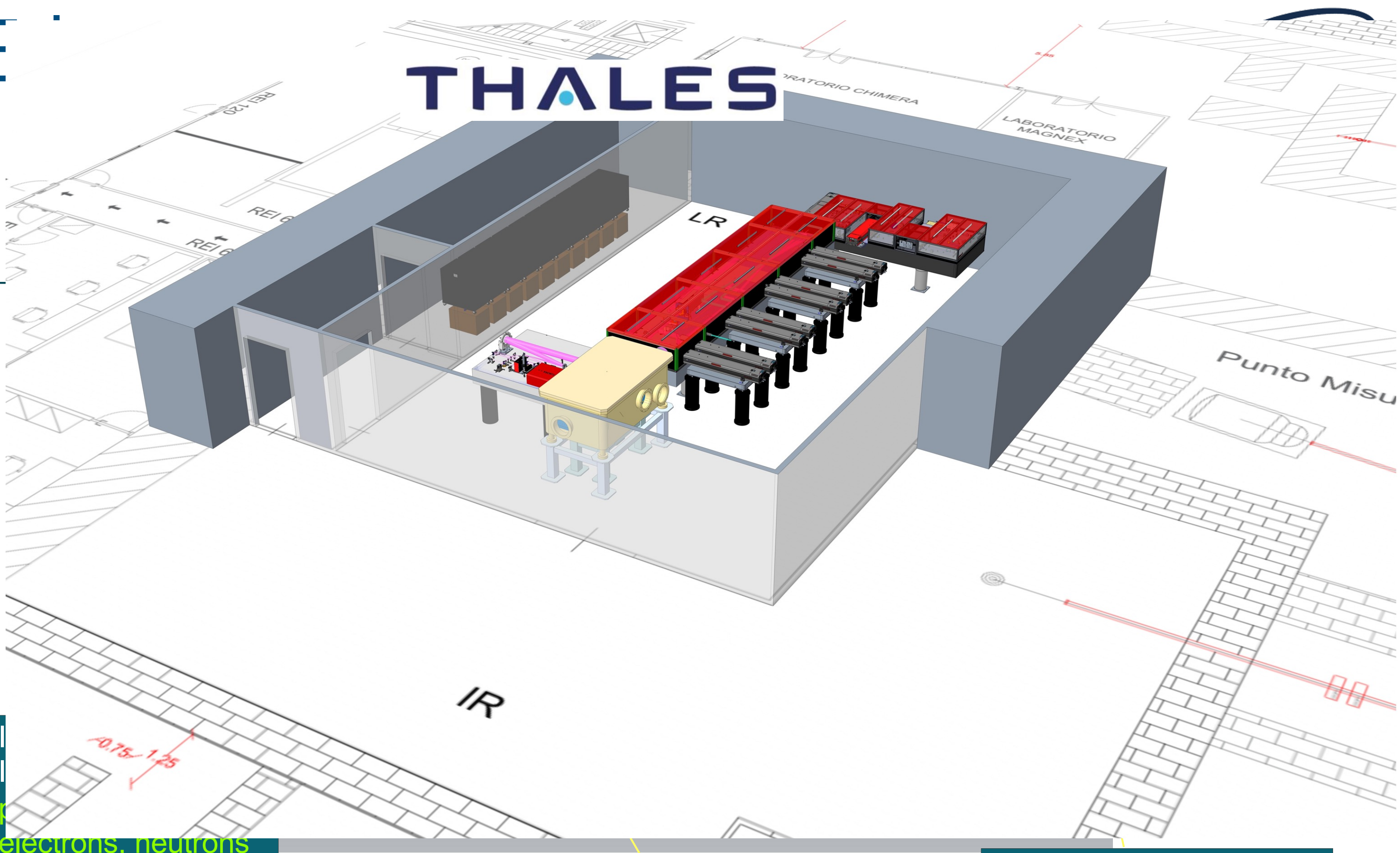

electrons, neutrons production

In-air irradiation station

Conventional ions: from TANDEM and Cyclotron

The main ingredients for radiation productions

A laser
- High power (TW - PW)
- Short pulse duration (ps - fs)
- Intensity > 10^{16} W/cm^2

A Target:
- Thin/thick solid/liquid/gassous

…

Other useful things
- High contrast laser
- High quality target fabrication
- High quality wave front-end
- …..

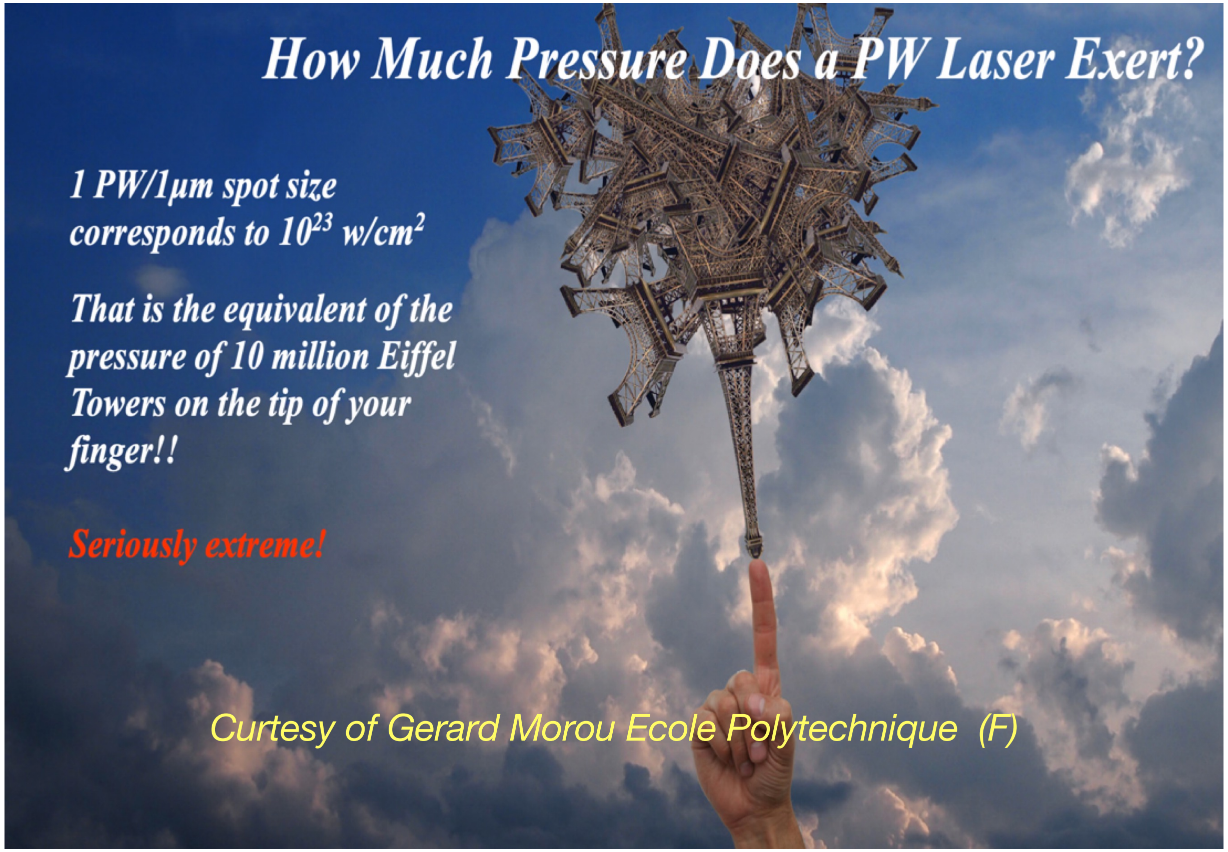

The main ingredients for radiation productions

A laser

- High power (TW - PW)
- Short pulse duration (ps - fs)
- Intensity > 10^{16} W/cm^2

A Target:
thin/thick solid/liquid/gassous …

Other useful things

- High contrast laser
- High quality target fabrication
- High quality wave front-end
- …. [many other laser and target parameters]

Laser-solid target interaction for protons, ions acceleration

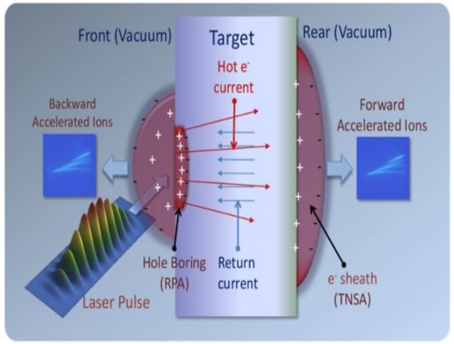

- •Multi species production: g, e-, p, ions
- • Emax ~ 10 TV/m
- •Short distance (~μm)

Proton characteristics

High energy: up to ~ 100 MeV
Pulse duration ≈ 10s fs - 100s ps
ppb ≈ 108-1011
Broad energy spectra (100%)
Wide angular divergence (≈ 10°-20°)

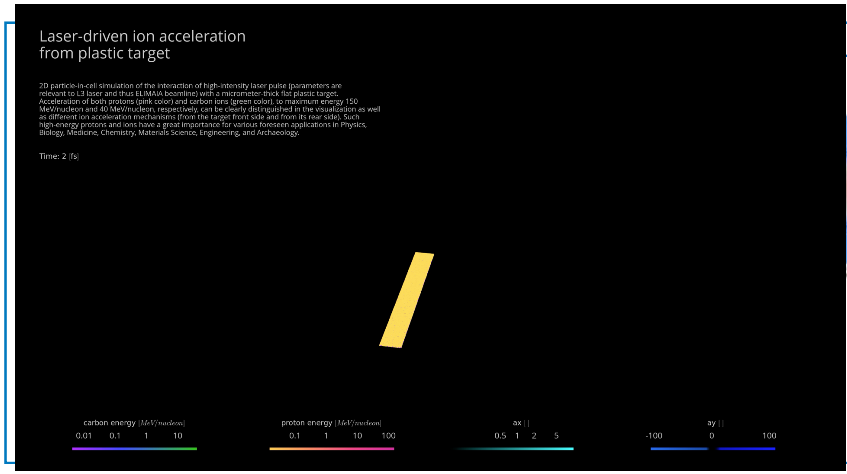

rons

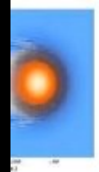

Laser plasma ion-acceleration

physical picture

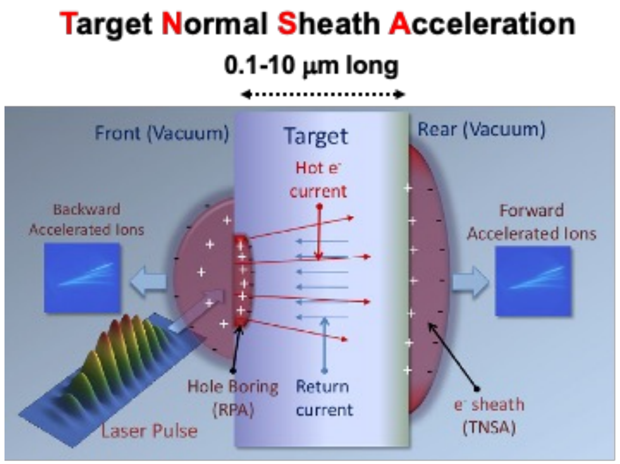

REVIEW PAPERS:

- *Macchi, Borghesi, Passoni, Rev. Mod. Phys. 85 (2013) 751*
- *Borghesi et al, Springer Proc. Phys. 231 (2019) 143*

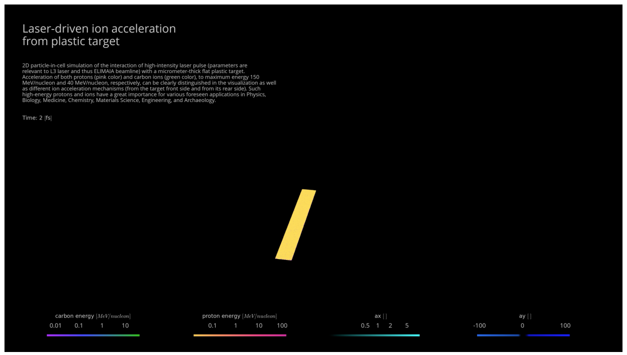

Role of the ponderomotive force on electrons energy gain

In an oscillating, quasi-monochromatic electromagnetic field described by a vector potential **a**(**r**,t), the relativistic ponderomotive force is given by:

$$f_p = -m_e c^2 \nabla \sqrt{(1 + < a >^2)}$$

$$f_p = \frac{dp^s}{dt} = -mc^2 \nabla \gamma$$

Energy Gain: 100 MeV/um (in a plasma medium)!!!

Pablo Cirrone, PhD - pablo.cirrone@lns.infn.it